Year : 2015

Role of Munc18c in SNARE-mediated exocytosis

Morey Czuee

UNIL | Université de Lausanne
Faculté de biologie
et de médecine

Département des neurosciences fondamentales

Role of Munc18c in SNARE-mediated exocytosis

Thèse de doctorat ès sciences de la vie (PhD)
Integrated Experimental and Computational Biology program

présentée à la

Faculté de biologie et de médecine
de l'Université de Lausanne

par

Czuee Morey

Master in Biotechnology, Indian Institute of Technology Bombay

Jury

Prof. Kim Quang Do Cuenod , président du jury
Prof. Dirk Fasshauer , directeur de thèse
Prof. Andreas Mayer, rapporteur
Prof. Ralf Schneggenburger, rapporteur
Prof. Romano Regazzi, rapporteur

Lausanne, UNIL, 2015

UNIL | Université de Lausanne
Faculté de biologie
et de médecine

Ecole Doctorale

Doctorat ès sciences de la vie

Imprimatur

Vu le rapport présenté par le jury d'examen, composé de

Président·e	Madame	Prof. Kim **Do Cuénod**
Directeur·rice de thèse	Monsieur	Prof. Dirk **Fasshauer**
Experts	Monsieur	Prof. Andreas **Mayer**
	Monsieur	Prof. Romano **Regazzi**
	Monsieur	Prof. Ralf **Schneggenburger**

le Conseil de Faculté autorise l'impression de la thèse de

Madame Czuee Morey

Master en biotechnology Indian Institute of Technology Bombay, Inde

intitulée

Role of Munc18c in SNARE-mediated exocytosis

Lausanne, le 27 novembre 2015

pour le Doyen
de la Faculté de biologie et de médecine

Prof. Kim Do Cuénod

Growth is a matter of curious exploration plus integration.
We increase chaos and then reduce it through organization. We tack new experiences onto our old organizing principles until we find it too cumbersome. Then we search for a new organizing principle that makes the chaos manageable again.
These are our “eureka" moments.
— Anonymous

To my parents...

Acknowledgements

I am greatly thankful to Prof. Dirk Fasshauer for giving me the opportunity to work on this project. He was always available for valuable advice, suggestions and critiques that helped me progress in this project. He not only provided expert guidance on the project, but also maintained a warm working atmosphere in the laboratory.

I am thankful to my thesis committee, Prof. Kim Quang Do Cuenod, Prof. Andreas Mayer, Prof. Ralf Schneggenburger, Dr. Karine Lapouge and Prof. Romani Regazzi for providing me valuable insights, advice and support during the course of my project.

I am grateful to the bioinformaticians in the lab, Dr. Tobias Kloepper, Dr. Nickias Kienle and Nicee Srivastava, for maintaining a well-curated database that proved useful to me in my project work, and for being available for questions and discussions.

I would also like to thank Dr. Iaroslav Savtchouk, Dr. Daniela Sahlender and Dr. Samia Habaas from Prof. Volterra's laboratory for our collaboration on testing the function of Syx4 and Munc18c in astrocytes. We had some interesting discussions together that helped me to better understand the role of SNARE and SM proteins *in vivo*.

My Ph.D. experience would not have been complete without the fun and warm atmosphere in our small group. I would like to thank my colleagues Janeta Iordanova, Dr. Xiong Chen, Yves Mingard, Dr. Nickias Kienle, Nicee Srivastava, Dr. Emilio Iraheta, Dany Khalifeh, Dr. Frédérique Varoqueaux, Jules Duruz and Lamia Quaresma for the camaraderie.

I would also like to thank my friends in Lausanne and Switzerland who were there for me in the toughest times, and without whom it would have been difficult to integrate in a new country.

Finally, I am indebted to my parents, sister and my close friends in India who were always a call away, despite the distance!

Lausanne, 22 Sept 2015 Czuee Morey

Abstract

Background: The SNARE (Soluble N-ethylmaleimide-sensitive factor Attachment protein Receptors) and SM (Sec1/Munc18) family of proteins form the core machinery that drives the fusion of vesicles in different membrane trafficking steps. They are highly conserved, implying a similar mode of binding and function. In vertebrates, Munc18a is essential for neuronal exocytosis. It binds to its partner syntaxin1a (Syx1a) at both its N-peptide and closed conformation, and thereby inhibits SNARE complex formation *in vitro*. By contrast, its close homolog Munc18c is thought to interact with only the N-peptide of its partner Syx4. Moreover, different effects of Munc18c on SNARE complex formation have been reported, suggesting that the two Munc18/Syx pairs act differently.

Objective: The aim of the present study was to investigate whether the mechanism of action of Munc18c indeed deviates from that of Munc18a by using sensitive biochemical and biophysical methods.

Results: I found that Munc18c does have a similar binding mode as Munc18a and interacts tightly with Syx4 at both the N-peptide and closed conformation. Moreover, I established, through a novel assay, that Munc18c inhibits SNARE complex assembly, with both the binding sites contributing to inhibition, similar to Munc18a. However, there were several subtle differences between the two Munc18/Syx pairs. Munc18a exerted stronger inhibition than Munc18c. Also their respective Syx partners were found to differ in the rate of binding to SNAP25, suggesting that the equilibrium of their open and closed conformations is different. Moreover, Munc18a was found to interact with Syx 1, 2, 3 but not 4, while Munc18c bound to Syx 2, 4 and 1 but not 3. By comparing the kinetics of interaction of Syx with either Munc18 or SNAP25, I found that the block of SNARE complex assembly by Munc18 is effective on a shorter time scale, but SNAP25 eventually binds to Syx resulting in SNARE complex formation. Nevertheless, these findings do not explain how Syx can escape the tight grip of Munc18, suggesting that other proteins or mechanisms are needed for this step. I also discovered that Munc18 is able to bind on the surface of the SNARE core complex; however, this observation needs to be tested more rigorously.

Conclusion: Munc18c was found to be similar to Munc18a in its mode of binding to Syx and inhibition of SNARE complex assembly. However, differences in kinetics and interaction specificities were observed between the different Munc18/Syx pairs.

Résumé

Contexte : Les familles des protéines SNARE (Soluble N-ethylmaleimide-sensitive factor Attachment protein Receptors) et SM (Sec1/Munc18) forment le coeur de la machinerie chargée de la fusion vésiculaire au cours des différentes étapes du trafic intracellulaire. Elles sont très conservées, suggérant un mode d'interaction et des fonctions semblables. Chez les Vertébrés, Munc18a est essentielle à l'exocytose neuronale. Elle se lie à sa partenaire d'interaction syntaxin1a (Syx1a) à la fois via un peptide N-terminal et la conformation fermée de celle-ci, inhibant ainsi la formation du complexe SNARE in vitro. Son homologue proche Munc18c au contraire, est supposée interagir seulement avec le peptide N-terminal de sa partenaire Syx4. En outre, différents effets de Munc18c sur la formation du complexe SNARE ont été décrits, suggérant que les deux paires Munc18/Syx fonctionnent différemment.
Objectif : Le but de cette étude est de tester si les mécanismes de fonctionnement de Munc18c diffèrent vraiment de ceux de Munc18a par le biais de méthodes biochimiques et biophysiques très précises.
Résultats : J'ai pu démontrer que Munc18c se comporte en effet de façon semblable à Munc18a, et interagit étroitement avec Syx4 à ses deux sites de liaison. J'ai pu de surcroît montrer par une nouvelle méthode que Munc18c inhibe l'assemblage du complexe SNARE en impliquant ces deux sites de liaison, comme le fait Munc18a. il existe cependant de subtiles différences entre les deux paires Munc18/Syx : Munc18a exerce une inhibition plus forte que Munc18c ; leurs Syx partenaires diffèrent également dans leur degré de liaison à SNAP25, ce qui suggère un équilibre different de leurs conformations ouverte et fermée. De plus, Munc18a interagit avec Syx 1, 2 et 3 mais pas Syx 4, alors que Munc18c se lie à Syx 2, 4 et 1 mais pas Syx 3. En comparant les cinétiques d'interaction de Syx avec Munc18 ou SNAP25, j'ai découvert que le blocage par Munc18 de l'assemblage du complexe SNARE est effectif de façon brève, bien que SNAP25 finisse par se lier à Syx et aboutir ainsi à la formation du complexe SNARE. Ces découvertes n'expliquent cependant pas comment Syx parvient à échapper à la solide emprise de Munc18, et suggèrent ainsi l'intervention nécessaire d'autres protéines ou mécanismes à cette étape. J'ai également découvert que Munc18 peut se lier à la surface de la partie centrale du complexe SNARE - cette observation reste à être testée de façon plus stringente.
Conclusion : Il a pu être établi que Munc18c est semblable à Munc18a quant à son mode de liaison à Syx et d'inhibition de l'assemblage du complexe SNARE. Des différences de cinétique et de spécificité d'interaction entre les diverses paires Munc18/Syx ont cependant été identifiées.

Contents

List of Figures

List of Tables

List of Abbreviations

E.coli	Escherichia coli
ER	Endoplasmic reticulum
FRET	Fluorescence Resonance Energy Transfer
GLUT4	Glucose transporter 4
GSVs	GLUT4 storage vesicles
H3	SNARE domain of syntaxins
Habc domain	regulatory domain of syntaxins
HOPS	HOmotypic fusion and vacuole Protein Sorting
IR	Insulin receptor
ITC	Isothermal titration calorimetry
K_d	Dissociation constant
LE	Mutant of Syx1a (L165A/E166A) or Syx4 (L173A/E174A)
Munc18	Mammalian uncoordinated protein 18
NMR	Nuclear Magnetic Resonance
NSF	N-ethylmaleimide Sensitive Factor
PM	Plasma membrane
SM	Sec1/Munc18 protein family
SNAP	Soluble NSF Association Proteins
SNAP25^{130OG}	SNAP25 labeled at Cys130 with Oregon Green
SNAREs	Soluble N-ethylmaleimide-sensitive factor Attachment protein Receptors
Syb	Synaptobrevin2, R SNARE
Syb 1-96^{28OG}	Syb (1-96) labeled at Cys28 with Oregon Green dye
Syb 1-96^{61OG}	Syb (1-96) labeled at Cys61 with Oregon Green dye
Syb 1-96^{79Ax}	Syb (1-96) labeled at Cys79 with Alexa488 dye
Syx	Syntaxin, Qa-SNAREs
Syx1 1-262^{1OG}	Syx1a (1-262) labeled at Cys1 with Oregon Green dye
Syx4 1-270^{1OG}	Syx4 (1-270) labeled at Cys1 with Oregon Green dye
Syx4RL	Syx4 mutant (R4A L8A)
TGN	trans-Golgi network
wt	wild-type

1 Introduction

1.1 Vesicular transport

The defining feature that distinguishes eukaryotic cells from prokaryotic cells is the presence of membrane-bound organelles. The presence of membranes organizes the cell into compartments that can have specialized functions, thus increasing the complexity of the cell. However, compartmentalization creates energetic and physical barriers for the transport of cellular material between the organelles or to the cell exterior. A trafficking machinery has evolved in eukaryotic cells to take care of intracellular transport. This trafficking machinery mediates transport through vesicles – membrane bound tiny sacs that shuttle cargo across the interior of the cell along cytoskeletal elements (Ferro-Novick and Jahn, 1994; Jahn and Scheller, 2006; Südhof and Rothman, 2009). A vesicle is formed when a membrane bulges out and is pinched off from the 'donor' compartment. The vesicle is then targeted to its 'acceptor' compartment where it fuses with the membrane and releases its cargo. In this way, soluble molecules and membrane components can be transported across the cell without the need to ever cross a membrane. Thus, vesicular transport forms a central and essential theme in the functioning of the eukaryotic cell.

When a vesicle is targeted to the plasma membrane, it releases its contents to the extracellular space and its membrane components integrate with the plasma membrane. This process is called secretion or exocytosis. Exocytosis is important in a number of bodily processes such as signaling, immune responses, insulin secretion by the pancreas, secretion of neurotransmitters, etc. Constitutive exocytosis takes place in all cells continuously and helps to transport molecules such as newly-synthesized membrane proteins to be incorporated in the plasma membrane. Some specialized cells have a second secretory pathway in which the cargo is stored in secretory vesicles inside the cell awaiting a stimulus for exocytosis. In presence of the stimulus, these vesicles can readily fuse with the plasma membrane. For example, a rise in the intracellular Ca^{2+} concentration elicited by an arriving action potential in neurons causes fusion of vesicles at the plasma membrane. The stimulus could also be in the form of a hormone binding to its receptor on the cell surface that transmits the signal for exocytosis

inside the cell. Following exocytosis, vesicular membrane and proteins are retrieved from the plasma membrane through endocytosis.

The central players of vesicle fusion belong to several structurally conserved protein families such as Soluble N-ethylmaleimide-sensitive factor Attachment protein Receptors (SNAREs), Sec1/Munc18 (SM) proteins, Rab proteins and a group of tethering proteins termed CATCHR (complex associated with tethering containing helical rods) (See reviews by Jahn and Fasshauer (2012); Jahn and Scheller (2006); Rizo and Xu (2015); Südhof and Rothman (2009) and '2013 Nobel prize in Physiology or Medicine' lectures by Rothman et al. (2013)). These proteins are conserved not only in different eukaryotic species but also at different trafficking steps. This suggests that the repertoire of protein machinery functioning at various trafficking steps arose from duplication and diversification events from a primordial set of proteins involved in trafficking (Kloepper et al., 2007; Klöpper et al., 2012; Koumandou et al., 2007). The duplication events probably occurred early in eukaryotic evolution, and the last common eukaryotic ancestor (LCEA) was already equipped with the vesicle trafficking machinery necessary for transport between various compartments (Dacks and Field, 2007; Gurkan et al., 2000).

The molecular machinery involved in neuronal exocytosis has been extensively studied. Synaptic vesicles filled with neurotransmitter are localized to the synaptic plasma membrane by tethering factors and cytoskeletal elements. The vesicles are then docked at the active site of the plasma membrane. Priming factors render the vesicles in release-ready state. In the final step on arrival of the action potential, the core fusion machinery drives fusion of vesicles with the plasma membrane, secreting the neurotransmitter into the synaptic cleft. After release, the neurotransmitter binds to its receptors on the post-synaptic cell membrane, thus transmitting the signal to the neighbouring cell. The core machinery involved in synaptic fusion consists of the SNARE proteins Syntaxin 1a (Syx1a), SNAP25 and Synaptobrevin2 (Syb) and the SM protein Munc18a.

1.2 The SNARE protein family

SNARE proteins are the major drivers of vesicle fusion and are identified as the minimal fusion machinery required to fuse artificial membranes in the absence of other factors (Weber et al., 1998). SNARE proteins anchored on vesicle and target membranes associate to form a four helical SNARE complex that leads to vesicle fusion. In the synaptic system, for example, SNAP25 and Syx1 on the plasma membrane form a complex with Syb embedded in the vesicle membrane. Essentially, the alpha-helices of these proteins "zip up" to form a tight helical bundle that snaps the two membranes together (Jahn and Scheller, 2006). The free energy released on complex formation is thought to overcome the energetic barrier to membrane fusion. A characteristic feature of all SNARE proteins that participate in SNARE complex formation is the SNARE motif – a highly conserved stretch of 60-70 amino acids arranged in heptad repeats.

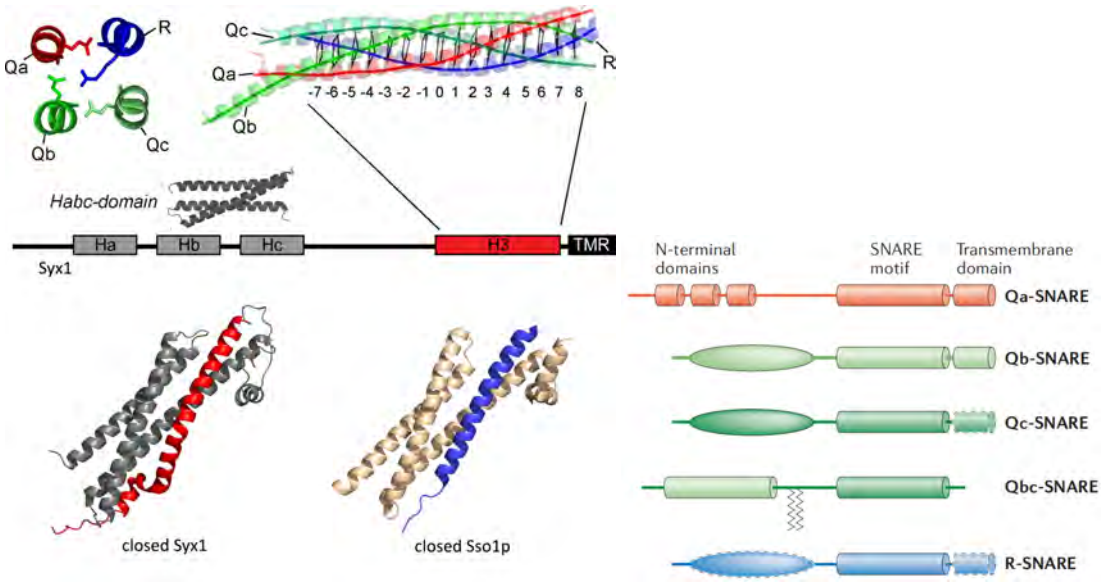

(a) (b)

Figure 1.1 – **The structure of SNARE proteins.**
(a) The structure of the neuronal SNARE core complex is shown on the top right (Qa-SNARE, red; Qb-SNARE, light green; Qc-SNARE, dark green; and R-SNARE, blue). The layers (−7 until +8) in the core of the bundle are indicated by virtual bonds between the corresponding Cα positions.The structure of the central '0' layer is shown in detail on the top left. Below, the domain architecture of the Qa-SNARE Syx 1a is shown along with the structure of the N-terminal Habc domain. The closed conformation adopted by the Qa-SNAREs Syx1a (Misura et al., 2001) and Sso1p (Munson et al., 2000) show the Habc domain interacting with the SNARE (H3) domain. Adapted from Kloepper et al. (2007) (b) The domain structure for the SNARE subfamilies shows the SNARE domain flanked by the N-terminal domain and the C-terminal transmembrane domain. Dashed domain borders highlight domains that are missing in some subfamily members. Qa-SNAREs have an N-terminal domain formed by antiparallel three-helix bundles. Qbc-SNAREs represent a small subfamily of SNAREs — the SNAP-25 (25-kDa synaptosome-associated protein) subfamily — that contain one Qb-SNARE motif and one Qc-SNARE motif. These motifs are connected by a linker that is frequently palmitoylated (zig-zag lines in the figure), and function in exocytosis. Adapted from Jahn and Scheller (2006).

1.2.1 The SNARE domain

In monomeric SNARE proteins, the individual SNARE domains are largely unstructured in solution. These disordered peptides undergo major structural rearrangements to form a highly stable, hetero-oligomeric four helical complex. The protease-resistant minimal portion of this complex was termed as "SNARE core complex" and consists of the SNARE motifs of the participating proteins (Fasshauer et al., 1998a). The structure of the SNARE core complex (Figure 1.1a) revealed four parallel α-helices that form 16 stacked layers of interacting side chains (Sutton et al., 1998). These layers are mainly hydrophobic except for the '0'-layer

at the center, that contains three highly conserved glutamine (Q) residues and one highly conserved arginine (R) residue. In the neuronal SNARE core complex, for example, the three Q residues are contributed by Syx1a and SNAP25 and the R residue by Syb. Since the sequence conservation is exceptionally high across SNAREs of different pathways and species, the interacting SNAREs were grouped as Qa, Qb, Qc and R SNAREs on the basis of the '0'-layer residue (Fasshauer et al., 1998b). Later, an elaborate phylogenetic analysis of SNARE domains of proteins participating in various trafficking steps from 145 species confirmed that SNAREs can be grouped into four major classes based on their sequences (Kloepper et al., 2007) (Figure 1.1b). Functional SNARE complexes are thought to be composed of a SNARE domain from each major class (QabcR complex). The SNARE proteins from each major class can be further divided into four subclasses based on the transport step at which it functions – endoplasmic reticulum (ER; I), Golgi apparatus (II), trans-Golgi network (TGN; III.a), digestive endosomal compartments (III.b), and plasma membrane (IV). A subfamily of SNAREs called Qbc-SNAREs, represented by the neuronal SNAP25 protein, are thought to have arisen from the merger of independent Qb- and Qc-SNARE genes. SNAP25 contains two SNARE domains joined by a linker region that is palmitoylated for membrane attachment.

1.2.2 Structure of Syntaxin N-terminal domain

The Qa SNAREs, syntaxins (Syx), have an additional regulatory domain at the N-terminus of the SNARE domain (Figure 1.1a). In most syntaxins, this domain consists of a short conserved peptide sequence called 'N-peptide' followed by three α-helices that form the 'Habc domain'. This is followed by a short linker region that connects the Habc domain to the SNARE (H3) domain. The Habc domain in exocytotic syntaxins can interact with the H3 domain to form a helical bundle called the 'closed conformation'. This closed conformation renders the H3 domain inaccessible for SNARE complex formation. In solution, syntaxin is thought to be in a dynamic equilibrium between such an auto-inhibitory 'closed conformation' and an extended (open) state.

1.2.3 SNARE complex assembly

The SNARE assembly reaction is thought to start with the formation of an acceptor complex. In exocytosis, for example, the Qbc and Qa SNAREs form a Qabc-SNARE complex that serves as an acceptor. The R-SNARE can then bind to this acceptor complex to form a ternary SNARE complex as seen for the synaptic and yeast exocytosis machineries (Fasshauer et al., 2002; Nicholson et al., 1998). The SNARE motifs 'zip up' from the N-terminal end towards the C-terminal membrane anchors (Figure 1.2). The directionality of SNARE complex formation was deduced from truncation experiments (Fasshauer and Margittai, 2004) which suggested that the N-termini (but not the C-termini) of Q-SNAREs affect the rate of SNARE assembly *in vitro*. Thus, the N-termini of the three Q-SNARE helices must come together to nucleate the SNARE assembly reaction. The formation of the acceptor complex is supposed to be the rate-limiting step in the SNARE assembly reaction. The interaction of the R-SNARE on the

vesicle and acceptor complex on the target membrane takes place in the trans-configuration *in vivo*. On fusion, this trans-SNARE complex is converted to a cis-configuration as the SNARE proteins reside on the same membrane. The cis-SNARE complexes cannot function in fusion anymore, and are disassembled by the ATPase protein N-ethylmaleimide Sensitive Factor (NSF) and its co-factor, the Soluble NSF Association Protein (SNAP).

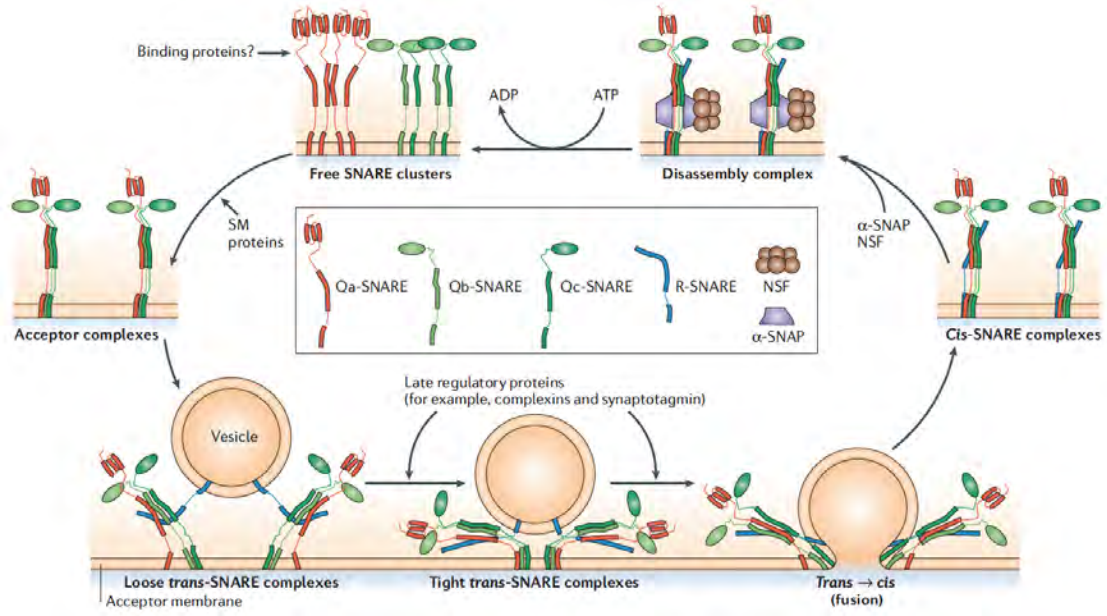

Figure 1.2 – **Model for the SNARE conformational cycle in vesicle fusion.**
SNARE proteins (Q-SNAREs in this case) present in clusters on the acceptor membrane (top left) assemble into acceptor complexes. The vesicle SNARE (R-SNARE here) interacts with the acceptor complex and nucleates the SNARE complex. SNARE complex formation proceeds by zippering of the SNARE domains from the N-terminal to the C-terminal end, forming a tight helical bundle. SNARE complex formation leads to opening up of the fusion pore and fusion of the vesicle. As a result of fusion, the trans-SNARE complexes relax into the cis configuration. Cis-complexes are disassembled with ATP hydrolysis by NSF (N-ethylmaleimide-sensitive factor) protein together with SNAPs (soluble NSF attachment proteins) that function as cofactors. Adapted from Jahn and Scheller (2006).

Acceptor complexes are thought to be formed by participation of one SNARE helix of each SNARE type. However, the *in vitro* assembly of the synaptic Qa and Qbc-SNAREs (Syx1 and SNAP25), also shows the formation of a 2:1 complex (Qaabc). The 2:1 complex is similar to the ternary QabcR-SNARE complex with Syb but with Syx1 substituting the Syb binding site (Margittai, 2001). Since, the site for Syb is occupied by Syx1, the 2:1 complex is a dead-end complex that cannot lead to ternary SNARE complex formation and forms an off-pathway. The 1:1 complex is found to be favored in the presence of excess SNAP25. Binding of Syb to the 1:1 complex is enhanced compared to the 2:1 complex, indicating that it is an on-pathway intermediate (Fasshauer and Margittai, 2004). However, it is difficult to isolate only the 1:1 complex to study its interactions with Syb. Pobbati et al. (2006) tried to stabilize the 1:1

Syx/SNAP25 complex with a C-terminal fragment of Syb. Addition of the intact Syb SNARE domain lead to replacement of the Syb fragment and rapid assembly of the ternary SNARE complex. Also, the stabilized acceptor complex lead to fast liposome fusion ($t_{1/2} \approx 1$ min), which is manifold faster than the assembly kinetics in absence of stabilization ($t_{1/2} \approx 20$ min). Thus, SNAREs have the ability to execute fast exocytosis required for the milli-second timescale kinetics of neuronal fusion, probably by a mechanism that stabilizes the acceptor complex.

1.3 Sec1/Munc18 protein family

The Sec-1/Munc18 (SM) family of proteins along with the SNARE proteins form the core machinery for vesicle fusion. Most SM proteins are known to function by binding to the Qa SNARE proteins, syntaxin. As mentioned before, the SM protein family probably evolved through duplication and diversification along with the repertoire of vesicle trafficking proteins functioning at different compartments. Thus, it is possible that the SM proteins evolved together with their cognate Qa-SNAREs and became specialized for functioning at a certain trafficking step. Accordingly, there are four sub-groups of SM proteins characterized till now – Munc18 involved in exocytosis, Sly1 involved in ER-Golgi transport, Vps33 involved in Golgi-vacuole transport and Vps45 involved in Golgi-endosome transport (Table 1.1, Appendix A.2). Two homologs of Vps33 (Vps33a, Vps33b) arose during animal evolution, and three homologs of Munc18 (Munc18a, Mun18b and Munc18c) arose during vertebrate evolution, probably from different rounds of duplication. The SM proteins are found to have high sequence similarity along the entire sequence, indicating that they are paralogs that arose from duplication and divergence. The SM proteins from the different sub-groups are also structurally conserved possessing an arch-shaped structure with three domains (Baker et al., 2013; Bracher and Weissenhorn, 2002; Burkhardt et al., 2008, 2011; Hackmann et al., 2013; Hu et al., 2007; Misura et al., 2000).

The knockdown or loss-of-function mutations of SM proteins result in a severe impairment of vesicle fusion, and in some cases also prove lethal (see review Toonen and Verhage, 2003). The earliest SM genes to be studied, Unc-18 in *Caenorhabditis elegans* and Sec1p in *Saccharomyces cerevisiae*, were both found to be critical for functioning. The Unc18 protein was identified in genetic screens to be required for coordinated movement and was later found to be essential for acetylcholine secretion (Brenner, 1974; Gengyo-Ando et al., 1993). A temperature-sensitive mutant of Sec1p caused accumulation of vesicles near the plasma membrane, indicating that it is essential for secretion (Novick and Schekman, 1979). A decade later, Sly1p gene was discovered in yeast and was found to be essential for trafficking between the ER and Golgi apparatus (Dascher et al., 1991; Ossig et al., 1991). Also, the mammalian homologues of Unc18 were identified in brain homegenates (Munc18a) and non-neuronal tissues (Munc18b and Munc18c) (Garcia et al., 1994; Hata et al., 1993; Pevsner et al., 1994b; Tellam et al., 1997). The essential role of Munc18a in synaptic fusion was established when Munc18a knockout mice were found to be deficient in neurotransmitter release (Verhage et al., 2000). Later, Munc18b and Munc18c were found to be essential for survival as knockdown of these genes

Table 1.1 – **SM protein interactions and functions.**
The table shows the information for SM proteins from various sub-groups that have been studied in different organisms. The names given to individual proteins are mentioned in brackets. The table is adapted from (Toonen and Verhage, 2003).

SM sub-group	Species	Syntaxin interaction	Null-mutant phenotype	Subcellular localization	Proposed function
Sly1	*S. cerevisiae* (Sly1p)	Sed5p, Ufe1p	Lethal	ER/ Golgi membrane	ER to Golgi
	M. musculus	Syx5, 18	N.D.	ER/ Golgi membrane	ER to Golgi
Vps45	*S. cerevisiae* (Vps45p)	Tgl2p, Pep12p	Viable	TGN/early & late endosome	Golgi to vacuole/ late endosome
	M. musculus	Syx16	N.D.	Golgi/ endosome	N.D.
Vps33	*S. cerevisiae* (Vps33p)	Vam3p	Viable	Vacuolar membrane	Endosome to vacuole
	D. melanogaster	N.D.	Eye color	Cytosol & membrane	Transport to lysosomes & pigment granules
Munc18	*S. cerevisiae* (Sec1p)	Sso1p, Sso2p	Lethal	PM (exocytosis)	Secretion
	D. melanogaster (ROP)	Syx	Lethal	Cytosol & membrane	General & synaptic exocytosis
	C.elegans (Unc18)	Unc-64	Lethal	N.D.	Synaptic exocytosis
	*M. brevicollis**	Syx 1	N.D.	Apical pole	N.D.
	M. musculus (Munc18a)	Syx1, 2, 3, 11[#]	Lethal	Neuronal cytosol & membrane	Synaptic exocytosis
	M. musculus (Munc18b)	Syx1, 2, 3, 11[#]	Lethal[#]	Cytosol & membrane	Apical trafficking in epithelial cells
	M. musculus (Munc18c)	Syx2, 4	Lethal	Cytosol & membrane	GLUT4 vesicle fusion with PM

N.D.: Not determined; PM: Plasma membrane; * from Burkhardt et al. (2008); [#] from Kim et al. (2012)
S. cerevisiae: *Saccharomyces cerevisiae, M. musculus*: *Mus musculus, D. melanogaster*: *Drosphila melanogaster, C.elegans*: *Caenorhabditis elegans, M. brevicollis*: *Monosiga brevicollis*

had a lethal phenotype (Kanda et al., 2005; Kim et al., 2012). Recently, it was found that Munc18a mutations in humans are linked with the epileptic conditions Ohtahara syndrome (Early infantile epileptic encephalopathy) and West syndrome (Otsuka et al., 2010; Saitsu et al., 2008). Mutations in Munc18b have been linked with a type of familial hemophagocytic lymphohistiocytosis (FHL5) (Côte et al., 2009). Munc18c and Syx4 are implicated in diabetes

and the development of insulin resistance. Several studies have observed a notable decrease in Munc18c and Syx4 mRNA and/or protein levels in obese and type 2 diabetic human subjects as well as rodent obese and diabetic models (Bakke et al., 2013; Bergman et al., 2008; Garrido-Sanchez et al., 2013; Yechoor, 2004). It can be deduced from these studies on SM proteins involved at different trafficking steps in different species that SM proteins play a vital role in vesicle fusion events and hence, the functioning of the organism.

1.3.1 SM-SNARE interactions

Interaction with syntaxins

It was discovered early on that SM proteins interact with syntaxins. However, different modes of binding were proposed for the various SM proteins (see review Toonen and Verhage, 2003). The mode of binding for the vertebrate SM protein Munc18a with Syx1 was one of the first binding modes to be studied. Biochemical analysis revealed that tight binding of Munc18a to Syx1 prevents the formation of the ternary SNARE complex (Pevsner et al., 1994a; Yang et al., 2000), indicating that Munc18a might bind to the closed conformation of Syx1. Later, the crystal structure of Munc18a in complex with Syx1 demonstrated that the arch-shaped Munc18a indeed envelops Syx1 in the closed conformation (Misura et al., 2001). This high-affinity interaction of Munc18a with Syx1 was thought to inhibit the participation of Syx1 in SNARE complex assembly.

The studies on Sly1 and Vps45, however, suggested that these SM proteins interact with their cognate syntaxins at another binding site. The yeast and mammalian Sly1 proteins were seen to interact with their cognate syntaxins through a short conserved N-terminal peptide, using pulldowns and yeast two-hybrid assays (Yamaguchi et al., 2002). In the same year, Sly1p was crystallized in complex with the short N-terminal peptide of Sed5p that bound on the surface of Sly1 at a site opposite to the Munc18a/Syx1 binding site (Bracher and Weissenhorn, 2002). These interacting regions were found to be conserved in other Sly1 and Vps45 homologs and their cognate syntaxins, pointing towards a conserved mode of binding. Indeed, the Vps45 homologs from yeast and mammals were found to interact with the the N-peptide of Tlg2p and Syx16 similar to the binding mode of Sly1 (Dulubova et al., 2002). Hence, the general consensus in the field a decade ago was that SM proteins function by binding to the N-terminal peptide of their partner syntaxins, in accordance with the essential role of SMs. The binding mode of Munc18a was thought to be an exception and a specially evolved function for neuronal exocytosis. Munc18c, a close homolog of Munc18a involved in exocytosis in vertebrates, was crystallized with the N-peptide of Syx4 and was also proposed to interact only through the N-peptide binding mode (Christie et al., 2012; Hu et al., 2007). However, some low-resolution pull-down assays suggested binding to the closed conformation as well (Aran et al., 2009; Beest et al., 2005) (See Section 1.4.2 for details).

However, the view that most SM proteins interact only with the Syx N-peptide is gradually changing. Biochemical studies from our laboratory showed that Munc18a can also bind to

the N-peptide of Syx1 and the x-ray diffraction data was re-examined to include this binding mode (Burkhardt et al., 2008). The dissociation constant (K_d) for Munc18a/Syx1 interaction was observed to reduce from ≈1.4nM to ≈8nM in the absence of the N-peptide, indicating that the N-peptide contributes to the binding affinity. Moreover, binding to both the N-peptide and closed conformation was also observed in the crystal structure of Munc18/Syx from the choanoflagellate *Monosiga brevicollis* (Burkhardt et al., 2011). Choanoflagellates are a group of single-celled eukaryotes that are thought to be the closest living relatives of metazoans, thus suggesting that the binding mode of Munc18a could be conserved for all metazoan Munc18 proteins involved in exocytosis. Moreover, recent studies show that yeast Tlg2p can interact with Vps45p in absence of the N-peptide (K_d ≈280nM), although the interaction of the isolated N-peptide with Vps45p has higher affinity (K_d ≈35nM) (Furgason et al., 2009). Similar results were also obtained by Burkhardt et al. (2008) for the vertebrate homologue Vps45/Syx16 that suggested binding through the closed conformation (K_d for Vps45/Syx16: ≈ 2nM, K_d for Vps45/Syx16(1-27): 27nM). Similarly, Sly1p was found to bind to the closed conformation of Sed5p in addition to its high-affinity N-peptide interaction (Demircioglu et al., 2014) (K_d for Sly1p/Sed5p: ≈ 0.25nM, K_d for Sly1p/Sed5p(1-21): 1.47nM). Thus, it is possible that a general interaction mechanism exists between SM proteins and syntaxins which involves both the N-peptide and the closed conformation of syntaxin with differing contributions to the binding affinity in various SM-syntaxin pairs. However, the interaction mode of Munc18c with Syx4 is still debated as the binding of Munc18c with the closed conformation of Syx4 has not yet been analyzed rigorously.

Interaction with SNARE complex

Another mode of binding has been proposed for the yeast SM protein involved in exocytosis, Sec1p. Sec1p was found to co-precipitate not only with the Qa-SNARE but also the Qbc and R-SNAREs, indicating that it interacts with the SNARE complex (Carr et al., 1999). Also Sec1 was proposed to play a role after SNARE complex assembly was complete (Grote et al., 2000). The partner syntaxin, Sso1p was found to adopt a closed conformation (Munson et al., 2000), but no interaction with Sec1p has been observed. However, these findings have not yet been corroborated by quantitative approaches and should be considered with caution. The interaction of SM proteins with the pre-assembled SNARE complex has also been observed for Sly1p, Vps45 and the vertebrate Munc18 homologs (Burkhardt et al., 2008; Carpp et al., 2006; Dulubova et al., 2007; Latham et al., 2006; Peng, 2002; Peng et al., 2010; Xu et al., 2010; Yu et al., 2013). However, all these studies describe the affinity of the SM protein with SNARE complex containing the full-length Syx which still carries an N-peptide and Habc domain. Hence, it is possible that the SM-SNARE interaction observed is because of binding to the Syx N-peptide and Habc domain rather than the SNARE core complex. The interaction between Munc18a and the SNARE core complex was found to be either very weak (FRET assay) or absent (ITC) (Burkhardt et al., 2008; Xu et al., 2010).

1.3.2 How do SM proteins function during SNARE complex formation?

Although it is becoming clear that most SM proteins have a common mechanism of binding to their cognate syntaxin, their exact mechanism of action and role in SNARE complex assembly is still shrouded in mystery. Given their essential role in vesicle fusion, it is possible that SM proteins are required to orchestrate SNARE assembly. However, the various SM proteins seem to act through different mechanisms and no consensus has been reached on a universal function.

As described earlier, Munc18a binds tightly to the closed conformation of Syx1 and inhibits SNARE complex formation *in vitro* (Dulubova et al., 1999; Misura et al., 2000; Pevsner et al., 1994a; Yang et al., 2000). However, loss of Munc18a blocks neurosecretion *in vivo*, suggesting that its presence is essential rather than inhibitory for secretion (Verhage et al., 2000). Hence, it is puzzling how Syx1a can escape the tight grip of Munc18a to facilitate fast synaptic exocytosis. The inhibitory activity of Munc18a *in vitro* seems to require binding at both the N-peptide and the closed conformation (Burkhardt et al., 2008). When the Syx1a N-peptide is deleted, Munc18a can still bind to it but it can no longer inhibit SNARE complex formation. Similarly, a Syx1a LE mutant has a similar effect. The LE mutant has a double mutation in the linker region (L165A/E166A) of Syx1a and is supposed to shift the equilibrium towards a more open state, thus rendering the SNARE domain accessible for SNARE complex formation. Thus, any mechanism that could detach the N-terminal peptide or open up the syntaxin, could help to relieve the inhibitory effect of Munc18a. Additional factors such as Munc13 or Rabs have been implicated in the release of Syx1 from Munc18a (Ma et al., 2013; Yang et al., 2015).

On the other hand, the SM proteins Vps45 and Sly1 have been found to have a stimulatory function in SNARE complex assembly. The effect of Vps45p on SNARE complex assembly was studied by following SNARE complex formation with time using pull-down assays (Struthers et al., 2009). Vps45p was found to stimulate SNARE complex formation in a manner similar to the deletion of the Tlg2p Habc domain that binds to the H3 domain. A recent study using several sensitive methods also found that Sly1 accelerates the rate of SNARE assembly by re-arranging and loosening the tight closed conformation of Sed5 (Demircioglu et al., 2014). Thus, Sly1 and Vps45 seem to function by destabilizing the closed conformation of their partner syntaxins.

SM proteins are thought to play a secondary role in vesicle fusion by binding to the assembled SNARE complex (Toonen and Verhage, 2007). As described earlier, the studies on SM binding to assembled SNARE complexes are not conclusive. Nonetheless, what could be the relevance of SM protein interaction with the fully assembled SNARE complexes that have already performed vesicle fusion? One possibility is that SM proteins might facilitate the correct assembly of the SNARE complex by stabilizing the acceptor SNARE complex or not allowing the formation of off-pathway intermediates. Hence, it would be interesting to observe if SM proteins can interact with SNARE complexes that are partially assembled. Such a breakthrough has been recently published for the crystal structures of Vps33 with Qa (Vam3) and R-SNAREs (Nyv1),

which suggests that Vps33 could aid the zipping up of the SNARE complex by interacting with SNAREs on opposing membranes (Baker et al., 2015). However, it remains to be seen if this mechanism is true for all SM proteins. Vps33 is different from the other SM sub-groups since it functions as a part of a tethering complex 'Homotypic fusion and vacuole Protein Sorting' (HOPS), that binds to trans-SNARE complexes (Collins and Wickner, 2007). Vps33 has also been shown to interact with the monomeric Qa SNARE Vam3p (Dulubova et al., 2001; Price et al., 2000) and Qc SNARE Vam7p (Stroupe et al., 2006). Interestingly, Vam3p does not form a closed conformation, and its N-teminal peptide is not required for binding to Vps33p (Dulubova et al., 2001). Therefore, it is possible that Vps33 bypasses the requirement to open the closed conformation of Vam3p, and the secondary role of aiding SNARE complex formation is easier to study.

1.4 SM proteins in exocytosis

The SM proteins involved in secretion are usually referred to as Sec1 (in fungi and plants) or Munc18 (in animals). These proteins were named as Unc18 (Uncoordinated protein 18) when discovered in *C.elegans* genetic screens. The homologous proteins found subsequently in mammals were named as 'Mammalian Unc18' or Munc18.

1.4.1 Munc18 and syntaxin homologs in vertebrates

As mentioned earlier, the Munc18 proteins probably evolved with their syntaxin counterparts (Qa.IV class) during evolution. Generally, most invertebrates have a single copy of the Munc18 and syntaxin genes. However, duplication in vertebrates has resulted in three homologs of Munc18 (Munc18 a, b, c also referred to as Munc18-1, 2, 3) and seven homologs of syntaxin (Syx1(a,b), 2, 3, 4, 11, 19, 21) (Appendix A.2 and A.3). The nomenclature for the Munc18s is distinct from the Munc18a splice variants Munc18a-1 and Munc18a-2 expressed in different brain regions (Meijer et al., 2015). Syntaxin 1a and 1b are very similar and most publications do not distinguish between the two isoforms. In the following text, I will therefore refer to both isoforms as Syx1. The Munc18 homologs in vertebrates have high sequence identity and similar secondary and tertiary structures (Figure 1.4 and 1.3). The different Munc18 homologs were found to have specific tissue expression profiles (Table 1.2), suggesting that the different vertebrate homologs have specialized for different secretion processes in different tissues. Note that most of these studies were performed in the 1990s and early 2000s. Munc18a and Syx1 are primarily found in neuronal cells and neuroendocrine tissues, and are known to be involved in synaptic exocytosis and the first phase of insulin release in pancreas (Hata et al., 1993; Jewell et al., 2010; Tomas et al., 2008). Munc18b has around 62% amino acid identity with Munc18a, and is studied in exocytosis along with Syx3 and Syx11 in epithelial cells, platelets and recently, in pancreas (Al Hawas et al., 2012; Kim et al., 2012; Lam et al., 2013; Riento, 2000). Munc18c has 51% amino acid identity with Munc18a and is found in almost all tissues, but is mainly studied in the exocytosis of glucose transporter 4 (GLUT4) in adipocytes and

skeletal muscle cells and in insulin exocytosis in pancreas, both processes in association with Syx4 (Jewell et al., 2010; Oh and Thurmond, 2009; Tellam et al., 1995; Thurmond et al., 2000). Although, the Munc18 homologs in vertebrates are associated with a certain Syx homolog, *in vitro* studies show that they can interact with other Syx homologs as well. Munc18a as well as Munc18b are found to interact with Syx 1, 2, 3 and 11, while Munc18c binds to Syx 2 and 4 (Hackmann et al., 2013; Hata and Südhof, 1995; Tamori et al., 1998; Tellam et al., 1995). These interactions could be functional in other tissues where the Munc18-Syx interactions have not yet been explored thoroughly. Also, some tissues express more than one Munc18 and Syx isoform. An open question then is how does the cell recruit the correct Munc18/Syx pair for a particular exocytosis event.

Table 1.2 – **Tissue localization of Munc18 and Syx isoforms in vertebrates.**

	Tissue localization	Reference
Munc18a	brain, pancreas	Pevsner et al. (1994b); Tellam et al. (1995); Zhang et al. (2000)
Munc18b	kidney, intestine, testis	Tellam et al. (1995)
Munc18c	All tissues tested	Khan et al. (2000); Tellam et al. (1995); Yang et al. (2001)
Syx1a/b	brain, pancreas	Bennett et al. (1993)
Syx2	heart, spleen, liver, testis, kidney, lung	Bennett et al. (1993)
Syx3	spleen, lung, kidney	Bennett et al. (1993)
Syx4	All tissues tested, expression levels differ	Bennett et al. (1993); Tellam et al. (1997); Yang et al. (2001)
Syx11	lung, thymus, spleen, lymphnode	Prekeris et al. (2000)

1.4.2 Role of Munc18s in exocytosis

The vertebrate Munc18a and its partner syntaxin1 involved in neuronal exocytosis have been extensively studied, as presented in the last section. Munc18a is known to bind Syx1 at the N-terminal peptide and the closed conformation (Figure 1.4), and inhibits SNARE complex assembly *in vitro* (Burkhardt et al., 2008). However, it is indispensable for neurosecretion that is thought to be driven by SNARE complex assembly between fusing membranes (Verhage et al., 2000). There are also studies on Munc18 proteins from invertebrates that posses a single copy – ROP (*D. melanogaster*) and Unc-18 (*C.elegans*). The ROP protein has been shown to be indispensable for synaptic transmission and normal embryonic development in Drosophila (Harrison et al., 1994). However, studies using electrophysiology and pulldown assays indicated that ROP binds to the Syx SNARE domain, and that the ROP-syntaxin interaction inhibits synaptic transmission (Wu et al., 1999, 2001). The Unc18 protein from *C.elegans* was found to interact with both the N-peptide and the closed conformation of its partner syntaxin, Unc-64 (Johnson et al., 2009). Moreover, a Unc18 construct defective in closed conformation binding

was able to rescue Unc18 null mutant worms, but a Unc18 mutation in the N-peptide binding site was not able to rescue the phenotype, suggesting that the N-peptide interaction is necessary for Unc18 function in vesicle fusion. Similar to the studies in *C.elegans, in vivo* studies in Munc18a are inconclusive about the role of binding at the two sites in vesicle fusion (Deàk et al., 2009; Meijer et al., 2012; Zhou et al., 2013). Although some aspects are yet to be clarified, the secretory SM proteins studied in invertebrates seem to have a common mechanism of action similar to that of Munc18a.

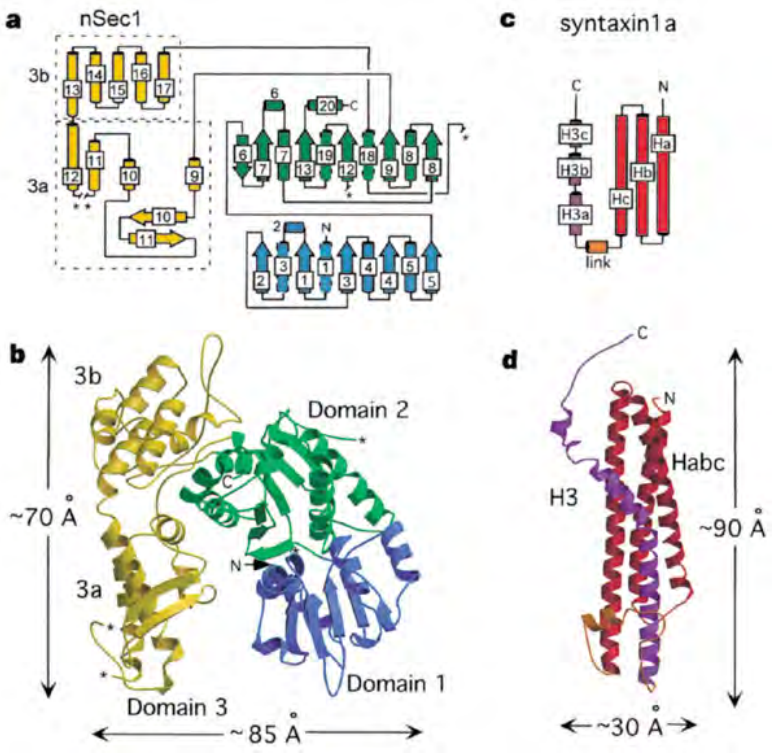

Figure 1.3 – **Structure of Munc18a and Syx1a.**
(a, b) Topology and ribbon diagrams of Munc18a (nSec1). Domain 1 is shown in blue, domain 2 in green and domain 3 in yellow. Helices are denoted by cylinders and strands by arrows. Breaks in the structure are indicated with asterisks. Dashed outlines denote domains 3a and 3b. Note that domain 3 is an insertion within domain 2. (c, d) Topology and ribbon diagrams of Syx1a. The Habc domain is shown in red, the Habc/H3 linker in orange and the H3 region in purple. The Munc18a and Syx1a structures are represented as they appear in the crystal structure. The Munc18a arch binds to Syx1a closed conformation, and the Syx1a N-peptide interacts with another site on the surface of Munc18a domain 1 (Figure 1.4a). Adapted from (Misura et al., 2000)

In addition to Munc18a, vertebrates possess two other homologs - Munc18b and Munc18c. Munc18b has a vital function since Munc18b knockout mice do not survive (Kim et al., 2012). Qualitative and quantitative assays demonstrate that Munc18b has a high binding affinity for both Syx3 and Syx11 ($K_d \approx 30$nM measured by surface plasmon resonance) and interacts with both the N-peptide and closed conformation (Hackmann et al., 2013; Peng, 2005). A mutation

(a) Munc18a/Syx1 structure

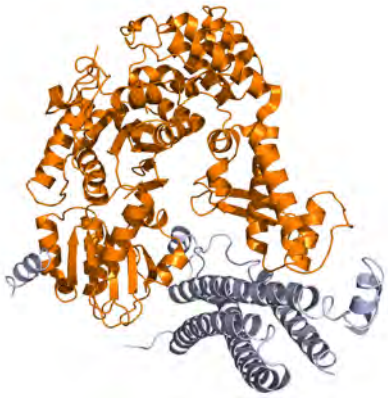

(b) Munc18/Syx from M.brevicollis

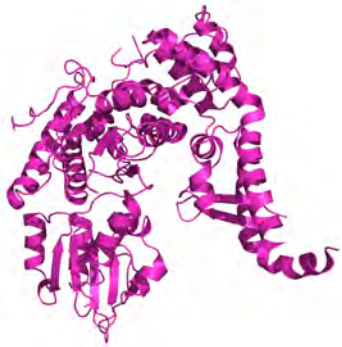

(c) Munc18b structure

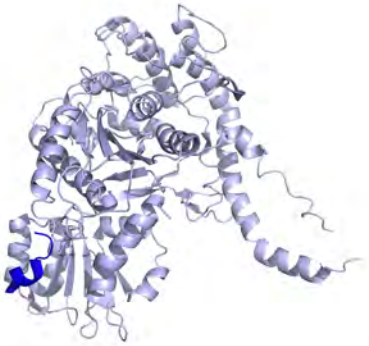

(d) Munc18c/Syx4 N-peptide structure

Figure 1.4 – **Structures of Munc18 proteins involved in exocytosis.**
(a) The structure of Munc18a (gray) in complex with Syx1 (red) shows interaction at both the closed conformation and the N-peptide on the outer surface (Burkhardt et al., 2008). (b) The structure of the choanoflagellate Munc18(orange)/Syx(gray) complex has a similar mode of binding as Munc18a-Syx1 (Burkhardt et al., 2011). (c) The structure of Munc18b (pink) was not solved in complex with a syntaxin (Hackmann et al., 2013). (d) Munc18c (light blue) interacts with the N-peptide of Syx4 (dark blue) in the crystal structure (Hu et al., 2007).

in the N-peptide binding site of Munc18b was observed to cause a 1000-fold reduction in its interaction with Syx3 and no interaction was detected with Syx11 (Hackmann et al., 2013). Although Munc18b has been shown to play an essential role in many types of epithelial cells (Al Hawas et al., 2012; Houng et al., 2003; Kim et al., 2012; Riento, 2000), the effect of Munc18b on SNARE complex assembly has not yet been analyzed directly.

As described earlier, the studies on Munc18c suggest contradictory evidence for the mode of Munc18c binding to Syx4, which I will elaborate here. J. Martin and colleagues claim through several publications that Munc18c interacts with only the N-peptide of Syx4. They solved the structure of Munc18c in association with a 19 residue N-terminal peptide of Syx4 (Hu et al., 2007, Figure 1.4) and also showed that the loss of this N-peptide disrupts binding of Syx4 to Munc18c through Isothermal titration calorimetry (ITC) and pull-down assays (Christie et al., 2012). Moreover, they suggested from low-resolution solution structure models that Munc18c/Syx4 (and also Munc18a/Syx1a) interact in an extended (open) conformation, only through its N-peptide (Christie et al., 2012). However, the interaction of Munc18c with the Syx4 N-peptide was 15-fold lower ($K_d \approx 1.5\mu M$) (Hu et al., 2011) than that reported for full-length Syx4 ($K_d \approx 95nM$). Therefore, binding of the isolated Syx4 N-peptide to Munc18c seems inadequate to describe the Munc18c/Syx4 interaction. Moreover, studies by other groups using pull-down assays with Syx4 N-peptide deletion mutants indicate that Munc18c is able to bind to the rest of the Syx4 molecule as well (Aran et al., 2009; Beest et al., 2005).

The physiological role of Munc18c has been investigated by several *in vivo* and *ex vivo* studies. Munc18c probably plays an essential role, since Munc18c knockout mice ($Munc18c^{-/-}$) die in the embryonic stage. Adipocytes cultured from these $Munc18c^{-/-}$ embryos required 100-fold lower insulin levels for exocytosis of GLUT4 storage vesicles (GSVs), indicating an inhibitory role for Munc18c (Kanda et al., 2005). Similarly, several studies found that over-expression of Munc18c in adipocytes inhibits insulin-stimulated GLUT4 translocation to the plasma membrane (Khan et al., 2000; Macaulay et al., 2002; Tamori et al., 1998; Thurmond et al., 1998). However, Munc18c or Syx4 heterozygous knockout mice show reduced insulin sensitivity in clearing blood glucose, indicating that Munc18c stimulates vesicle fusion (Jain et al., 2012; Oh et al., 2005). A recent review by (Ramalingam et al., 2014) suggests that glucose homeostasis is linked with a delicate balance of Munc18c, i.e. the glucose control topples if Munc18c levels are either higher or lower than optimal. The direct effect of Munc18c on SNARE complex assembly has been studied through liposome fusion assays, although with contradictory results. Yu et al. (2013) found that Munc18c accelerates liposome fusion, while (Brandie et al., 2008) found that it inhibits fusion.

The major players that act in insulin-stimulated vesicle fusion have also not been characterized in detail. Binding of insulin to the insulin receptor (IR) activates the IR tyrosine kinase. The IR activates a signal cascade of phosphorylation and de-phosphorylation of various substrates that cause various intracellular changes. One of the results of the insulin signal is the translocation and exocytosis of GSVs at the plasma membrane. GLUT4 allows entry of glucose from the blood into the cells. However, the molecular details of how the insulin-signaling cascades transmit the signal for SNARE-mediated GLUT4 vesicle fusion are not resolved. This is one of the missing links in understanding how insulin mediates glucose uptake. The existing experimental evidence suggests few plausible mechanisms. It is thought that Rab proteins might serve as a direct link between insulin signaling and GSV SNARE-fusion regulated by Munc18c, however no concrete evidence is available (James, 2005). Also, qualitative pull-down assays found that Munc18c can be directly phosphorylated by the IR

kinase at the residue Tyr521 (Aran et al., 2011; Jewell et al., 2011).

Comparison of synaptic and GSV exocytosis

Munc18a and Munc18c are involved in synaptic and GLUT4 vesicle exocytosis respectively, both of which are regulated events. However, there are major differences between the two processes. Synaptic vesicle fusion is stimulated by rise in Ca^{2+} levels, while GLUT4 vesicle exocytosis in insulin-responsive cells is regulated by binding of insulin to the insulin receptors on the cell surface. (See reviews Jahn and Fasshauer, 2012; Leto and Saltiel, 2012; Stockli et al., 2012).

Synaptic secretion is a fast process that takes place on a millisecond timescale. Insulin-stimulated GLUT4 vesicle fusion is slower and takes place with a half time of 2-5 minutes. In synaptic fusion, vesicles are docked and primed in the form of a readily releasable pool that undergoes fast exocytosis on Ca^{2+} influx (Figure 1.5). GLUT4, a transmembrane glucose transporter, is usually stored intracellularly in GSVs. In the absence of insulin, GLUT4 is excluded from the plasma membrane, and only ≈5% of the total GLUT4 pool is found on the cell surface that is involved in a basal level of exocytosis. After insulin stimulation, the plasma membrane GLUT4 levels escalate 10-40 fold. There is an initial rapid burst of GLUT4 on the surface, followed by endocytosis and recycling of GLUT4 on prolonged stimulation. These different phases are related to exocytosis from different pools of GLUT4 in the cell. GLUT4 vesicle fusion is targeted to a large area of the plasma membrane while synaptic fusion is restricted to the synaptic active zone.

The level of GLUT4 on the cell surface is regulated by the net rate of exocytosis and endocytosis. The increase in surface GLUT4 levels after stimulation, might be a result of an increased exocytosis rate, a decreased endocytosis rate or a combination of both. It is generally accepted that insulin increases the rate of exocytosis, but its effect on endocytosis is not clear. GLUT4 is endocytosed through clathrin-mediated and cholesterol-dependent endocytic pathways, both of which recycle GLUT4 through the endosome, and might be further passed for recycling to TGN. After synaptic fusion, the vesicles are recycled locally through clathrin-mediated endocytosis, but the presence of endosomal intermediate is not clear.

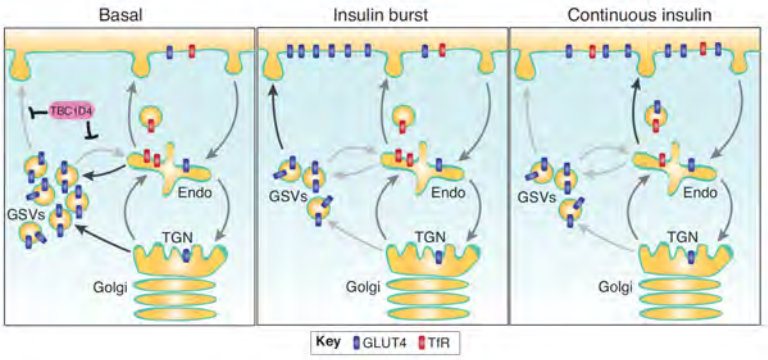

(a) GLUT4 storage vesicle (GSV) exocytosis

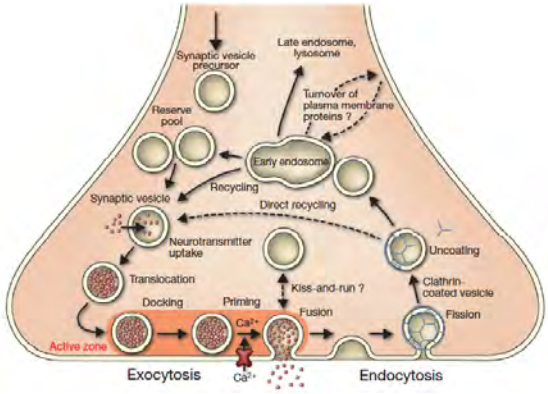

(b) Synaptic exocytosis

Figure 1.5 – **Synaptic and GLUT4 vesicle exocytosis.**
(a) There is a constant cycling of GLUT4 between the plasma membrane and intracellular GLUT4 containing compartments - the endosome (Endo), the trans-Golgi network (TGN) and GLUT4 storage vesicles (GSVs). In the absence of insulin (basal), GSVs are derived from endosomes and/or TGN. In the presence of insulin, there is rapid translocation and fusion of the insulin-sensitive GSVs at the plasma membrane (insulin burst). However, on prolonged stimulation with insulin (continuous insulin) the GLUT4 from endosomes is mobilized to the plasma membrane instead of reformation of GSVs. Transferrin receptor (TfR) is a protein that is absent in GSVs and is used to differentiate between the different pools of GLUT4. Adapted from Stockli et al. (2012) (b) Synaptic vesicles filled with neurotransmitter are stored in the cytoplasm. Active vesicles are translocated and docked to release sites in the active zone. Fusion occurs rapidly on the arrival of an action potential. After exocytosis, the vesicle proteins probably remain clustered and are then retrieved by endocytosis. Adapted from Jahn and Fasshauer (2012)

2 Aim of the project

The highly conserved Sec1/Munc18 (SM) and SNARE family of proteins form the core machinery for vesicle fusion. The SM proteins are known to function through a high-affinity interaction with the SNARE protein Syntaxin (Syx). In vertebrates, there are three SM (Munc18) homologs (Munc18a, Munc18b, Munc18c) and six Syx homologs (Syx 1, 2, 3, 4, 11, 21) involved in exocytosis. Of these, Munc18a and Syx1 play an essential role in synaptic vesicle fusion and have been extensively studied. Munc18a binds to Syx at its N-peptide and closed conformation *in vitro* and inhibits SNARE complex formation. Recent studies on several SM/Syx interactions suggest that SM proteins regulate SNARE complex assembly by binding to both the N-peptide and closed conformation of Syx. Munc18b and Munc18c are also found to play an essential physiological role, however, their mode of binding to Syx and mechanism of action are not well studied. Interestingly, recent publications on Munc18c infer that it can bind to its partner Syx4 only through the N-peptide and not the rest of the protein (Christie et al., 2012; Hu et al., 2007). This is contradictory to the close homology of Munc18c to Munc18a and the universal mode of binding emerging for several SM-Syx pairs studied. The effect of Munc18c on SNARE complex assembly and its role in vesicle fusion is also not rigorously studied.

The major aim of my project was therefore to find out if Munc18c/Syx4 indeed has a different mode of binding than Munc18a/Syx1a, and what differences cause this divergence, if any. I used various deletion/mutation constructs to determine the binding of Munc18c to the closed conformation of Syx4 using various sensitive biochemical and biophysical methods such as isothermal titration calorimetry (ITC).

Previous studies on the role of Munc18c in SNARE complex formation based on liposome fusion studies show contradictory results (Brandie et al., 2008; Yu et al., 2013). Another important objective of my project was to study the effect of Munc18c on the SNARE complex assembly, using quantitative methods. Since the SNARE complex assembly with Syx4 was not studied previously, I initially developed assays to understand the assembly pathways of the SNAREs and the dynamics of their interactions. I further investigated the role of Munc18c in the SNARE complex assembly with Syx4. The kinetics of interactions were studied using sensitive fluorescence anisotropy assays with labeled proteins.

The secretory Munc18 proteins in vertebrates are specific for certain syntaxins, although interactions with other syntaxins have also been observed (Hata and Südhof, 1995; Tamori et al., 1998; Tellam et al., 1995). I explored the interaction specificities of homologs Munc18a and Munc18c with Syx 1, 2, 3 and 4 and also studied their effects on SNARE complex formation. Since vertebrates express several Munc18 and Syx proteins, sometimes in the same cell type, how do the different Munc18/Syx pairs function at their respective secretion processes? In order to investigate the differences between the vertebrate Munc18 homologs, available sequences were collected and phylogenetic analyses were performed. The sequence differences observed between different homologs were mapped onto the available structures to find possible deviations that might explain the Munc18 specificities.

3 Materials & Methods

3.1 Chemicals & enzymes

All chemicals, reagents and enzymes used in the study were purchased from BioRad, Roth, MP Biomedicals and Sigma. Thiol-reactive fluorescent probes were purchased from Life Technologies.

3.2 DNA constructs

The protein constructs used in the experiments are given in Figure 3.1. All Syx4, Syx2, Syx3 and Munc18c protein constructs were derived from mouse (*Mus musculus*), while the Syx1a, SNAP25, Synaptobrevin and Munc18a constructs were derived from rat (*Rattus norvegicus*). The full-length Munc18c and Syx4 contructs with the cytoplasmic domain - Syx4 (1-270), Syx4 (25-270), Syx4 L173A/E174A (Syx4LE), Syx4 R4A L8A (Syx4RL) cloned in pET28a vector were ordered from GenScript. The bacterial expression constructs for full length Munc18a, cysteine-free SNAP25 (1-206), Synaptobrevin 2 cytoplasmic domain [Syb (1-96)], Syx1a cytoplasmic domain [Syx1a (1-262)] have been described previously (Burkhardt et al., 2008). The cytoplasmic domains of Syx1a, Syx2, Syx3 and Syx4 cloned in pGEX-4T2 plasmid were used for GST-pulldown assay.

Syx1a (1-262) is referred to as Syx1a in this text. Syx4 (1-270) is referred to as 'Syx4'. It should be noted that the syntaxin 4 sequence does not contain the thrombin cleavage site found in Syx1a, and we were able to cleave the His-tag from Syx4.

3.3 Protein expression and purification

Plasmid transformation

The recombinant plasmid DNA (10-100ng) was transformed into 50-80μl *Escherichia coli (E.coli)* BL21(DE3) competent cells using heat shock at 42°C for 45 seconds. The cells were

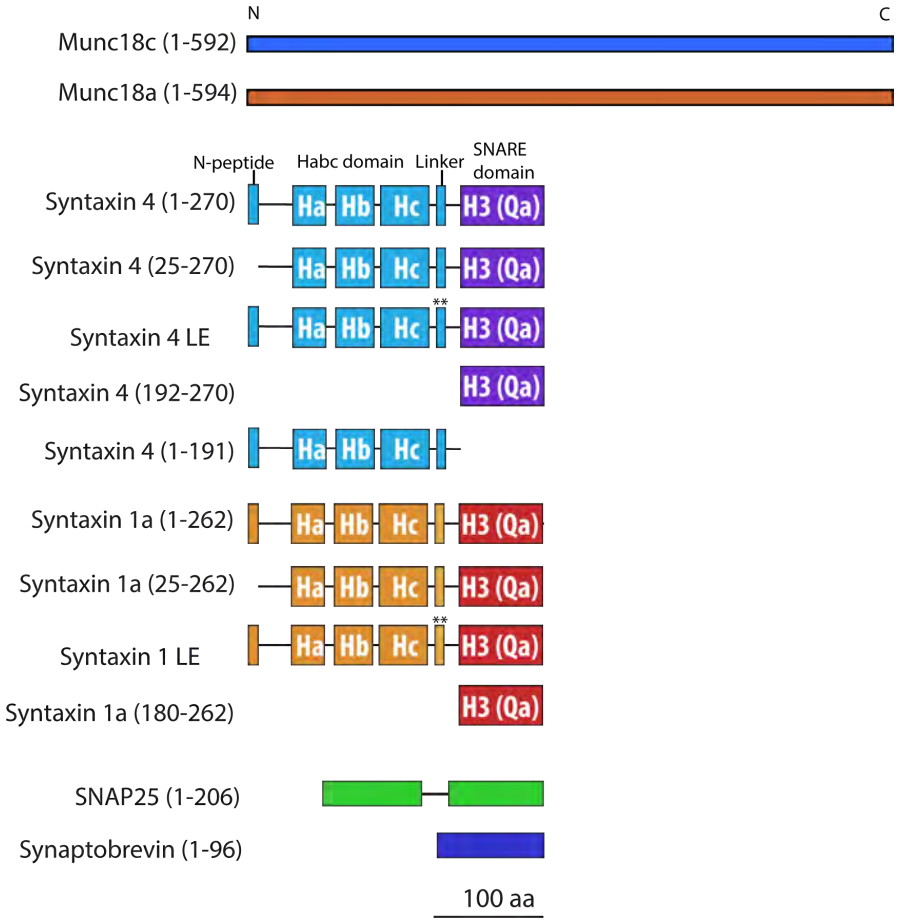

Figure 3.1 – **Protein constructs used in experiments.**
The constructs used in experiments represented here are the full-length Munc18a and Munc18c, cysteine-free SNAP25 (1-206), Synaptobrevin 2 cytoplasmic domain [Syb (1-96)] and cytoplasmic domains and deletion constructs of syntaxins (Syx). The deletion mutants and domains used for Syx4 and Syx1 are shown. Similar constructs were also used for Syx2 and Syx3. The protein lengths are represented to scale.

mixed with 200μl Luria Bertani (LB) medium (1% (w/v) tryptone, 0.5% (w/v) yeast extract, 1% (w/v) NaCl, pH: 7.0) containing 100 mM glucose and were grown in a shaker for 1 hour at 37°C. The transformed cells were grown on LB agar plates (containing 100 μg/ml of Ampicillin or 50 μg/ml of Kanamycin depending on the antibiotic resistance gene on the plasmid vector).

Protein expression

For expression, a single colony was picked to produce an overnight starter culture with required antibiotic. The cells (except those with Munc18c construct) were transferred to 2L Erlenmeyer flasks containing 500ml LB medium with the required antibiotic. Each flask was inoculated with 5ml of starter culture and incubated at 37°C with constant shaking till an O.D of 0.4-0.6

was reached. Protein expression was induced by adding 1mM IPTG. The SNARE proteins were expressed at 37°C for 4 hours with constant shaking. Munc18a was expressed at 25°C, overnight with constant shaking.

Munc18c plasmid containing cells were grown in Terrific Broth (TB) medium (1.2% (w/v) tryptone, 2.4% (w/v) yeast extract, 0.4% (w/v) glycerin) with 10% (v/v) TB salt (0.17M KH2PO4, 0.72M K2HPO4) and kanamycin until high optical density was reached (≈ 1.8-2.0). The cells were cooled to 20°C before inducing with 0.3mM IPTG. Munc18c was expressed at 20°C, overnight with constant shaking.

After protein expression, the cells were harvested by centrifugation at 3000rpm for 20 mins. The cells were resuspended in Ni^{2+}-NTA beads washing buffer (20 mM Tris pH 8.0, 500 mM NaCl, 8 mM imidazole) or in Glutathione beads washing buffer (20 mM Tris pH 8.0, 500 mM NaCl) depending on the affinity-purification method to be used after lysis. The resuspended cells were stored at −20°C or lyzed immediately.

Protein purification

The resuspended cells were thawed, and the following lysis reagents were added: 0.5% (v/v) Triton-X 100, 1mM $MgCl^2$, 1mM PMSF, 0.25 mg/ml lysozyme, 1mg/ml DNase. 6M urea was added for purification of SNARE proteins. The bacterial cells were lysed by sonication (Branson Sonifier) with 4×30 sec pulses with 1 minute intervals. The lysate was centrifuged at 14000rpm for 1 hour and filtered to remove bacterial debris.

The supernatent was allowed to bind to Ni^{2+}-NTA or GSH beads (≈1ml beads/liter culture, pre-equilibrated with respective binding buffers) for 2 hours at 4 °C with end-to-end rotation. The protein-bound beads were collected and washed with 10x bead volume of Ni^{2+}-NTA or 3×5ml GSH washing buffer to remove unspecifically bound proteins. The GST-tagged proteins bound to GSH beads were stored for GST-pulldown assay as a 50% slurry at 4 °C. The His_6-tagged proteins were eluted from the beads in 2-3 fractions using 2–3× bead volume of Ni^{2+}-NTA elution buffer with 500mM Imidazole for SNARE proteins and 200mM Imidazole for Munc18a.

For Munc18c, stringent conditions were used to specifically select the protein of interest from a large background of bacterial proteins. 1.5ml Ni^{2+}-NTA beads (pre-equilibrated with Ni wash buffer containing 20mM Imidazole) were allowed to bind to ≈200ml supernatant. The beads were washed with 2×15ml Ni wash buffer containing 20mM Imidazole, and the protein was eluted into 3×3ml fractions with elution buffer containing 200mM Imidazole.

The eluates were dialyzed into ion exchange buffer - Buffer A (20mM Tris pH 7.4, 100mM NaCl, 1mM EDTA, 1mM DTT) and thrombin was added at this step for cleaving the His_6 tag, except for Syx1 and Munc18c. The proteins were further purified using ion exchange chromatography. Depending on the pI of the proteins, either MonoQ HR 10/10 or MonoS HR 10/10 columns (Pharmacia Biotech) were used. The ÄKTA explorer purification system was

used for controlling the gradient and carrying out all the steps of the purification. The protein was loaded on the column that had been pre-equilibrated with buffer A. The protein was washed with 2 column volumes of buffer A and eluted by applying a linear gradient from buffer A to buffer B (20mM Tris pH 7.4, 1M NaCl, 1mM EDTA, 1mM DTT). A linear NaCl gradient from 100mM NaCl to 500mM NaCl was generally sufficient to elute most proteins. For Munc18c, an alternate buffer was used for dialysis and ion exchange buffer A (HEPES pH 7.0, 150mM NaCl, 1mM DTT, 1mM EDTA). For elution of Munc18c from the Mono S column, a linear gradient up to 800mM to 1M NaCl was used.

3.4 GST-pulldown assay

The GST-Syx proteins were expressed and bound to GSH beads as mentioned in the previous section. The GST-pulldown assays were performed for binding of Munc18a or Munc18c to each of GST-tagged Syx 1, 2, 3 and 4. Munc18a/Munc18c in 1:1 molar amount was added to 10μl of GSH beads bound to GST-Syx. The mix were incubated for 1 hour at 4°C with end-to-end rotation. Two control reactions were also setup in parallel. In the first control, the same amount of pure Munc18 protein was added to GSH beads without tagged Syx to check for unspecific binding. In the second control, equivalent amount of buffer was added to GSH proteins bound to GST-Syx instead of Munc18 to check the bands arising from only the beads.

The beads were centrifuged after incubation at 500g for 5 min at 4°C in a tabletop centrifuge and the supernatant was aspirated, minimizing bead loss. The beads were washed thrice with 50μl of GSH wash buffer, the supernantant was removed. The protein was eluted from the beads to avoid unspecifically bound proteins, by adding 30μl of GSH elution buffer (20 mM Tris pH 8.0, 500 mM NaCl, 10mM glutathione). The elutions from the experiments and controls were run on an SDS-PAGE gel for comparison.

3.5 Isothermal titration calorimetry (ITC)

All ITC experiments were done using a VP-ITC instrument (MicroCal, GE Healthcare). The ITC instrument is a sensitive instrument used to study the thermodynamics of interactions. It measures the heat released on binding of two macromolecules in solution as a function of the electrical energy required to keep the solution at a constant temperature. The thermodynamic parameters of the interaction such as the enthalpy (ΔH), dissociation constant (k_d:), stoichiometry (n) can be calculated from the binding curve.

The ITC system consists of two twin coin-shaped cells, i.e., the sample and the reference cell, mounted in an adiabatic jacket and that are maintained at equal temperatures. The reference cell is usually filled with degassed water or buffer and the sample cell with one of the binding partners. In an ITC experiment, a ligand is titrated into a macromolecule in the sample cell at constant temperature. Upon each injection a heat change (ΔH) occurs proportional to the number of contacts between the two molecules. The feedback power applied to maintain a

constant temperature between the two cells gives a peak. The binding curve obtained by an ITC experiment is an integrated area of each peak as a function of time. The binding curve is analyzed to determine the thermodynamic parameters of the interaction (n, ΔH and K_d).

For ITC experiments, all proteins were dialysed in the same HEPES buffer (60 mM HEPES pH 7.0, 150mM NaCl, 1mM DTT). Protein concentrations were determined by absorption at 280 nm. Protein samples were pre-incubated at 22 °C and degassed prior to experiments. Experiments were performed at 25 °C with 20-28 injections of 10 μl each. The raw data was analyzed with MicroCal Origin 7.0 and the binding curves were fitted by using a non-linear least squares fit for a single-site binding model.

3.6 Fluorescence spectroscopy

Protein labeling with fluorescent dyes

The single cysteine variants of proteins were labeled with thiol-reactive fluorescent dyes such as Oregon green 488 iodoacetamide, Alexa 488 C5 maleimide or Texas Red C2 maleimide. Prior to labeling, DTT was removed from the protein solution by dialysis overnight in PBS buffer (20mM NaH_2PO_4/Na_2HPO_4 pH 7.4, 150mM NaCl). The fluorescent dye was dissolved in an organic solvent (di-methyl sulphoxide) and added to 1ml of protein solution at ≈10x molar excess. The labeling reaction was carried out at room temperature with end-to-end rotation for 2 hours. The reaction was stopped with 5-10 mM DTT. The free dye was separated from the labeled protein using size-exclusion chromatography (Sephadex G-50 beads packed into a column). The labeled proteins were run on 10-15% SDS-PAGE gels and visualized with UV light. To determine the labeling efficiency, the concentration of the fluorophore was measured by absorption spectroscopy and the concentration of the protein was measured by Bradford assay (Bradford, 1976).

The fluorescence spectroscopy measurements were done using either a Cary Eclipse fluorescence spectrophotometer (Varian) with a L-configuration or fluorescence spectrophotometer with excitation and emission polarizers (Photon Technology International) with a T-configuration. All experiments were performed in 1cm quartz cuvettes in HEPES buffer (60 mM HEPES pH 7.0, 150mM NaCl). All proteins were dialyzed in this buffer prior to measurements.

Fluorescence anisotropy

Single-cysteine variants of Synaptobrevin (1-96) labeled at position Cys61 or Cys28, and SNAP25 labeled at position 130 with Oregon green dye (λ_{ex}: 496nm, λ_{em}: 524nm) were used for the anisotropy experiments. In some experiments, Synaptobrevin (1-96) labeled at Cys79 with Alexa488 (λ_{ex}: 495nm, λ_{em}: 520nm) was used.

When fluorescently labeled molecules are excited by linearly polarized light, only the dye

molecules with transition dipoles aligned parallel to the plane of polarization, will selectively absorb the light. The polarization of the emitted light will depend on the orientation of the emitting transition dipole with respect to the absorbing transition dipole and the molecular rotation in the fluorescence lifetime. The reduction in polarization of the fluorophore on complex formation is measured as the anisotropy. Fluorescence anisotropy, thus, measures the local flexibility of the labelled residue, that changes upon complex formation.

Experimentally, the degree of polarization is determined by measuring fluorescence intensities parallel and perpendicular relative to the plane of linearly polarized excitation light. The anisotropy (r) is determined as

$$r = (I_{vv} - GI_{vh})/(I_{vv} + 2GI_{vh})$$

where I_{vv} and I_{vh} are the intensities of the vertically and horizontally polarized fluorescence emission upon excitation with vertically polarized light. The G factor is a property of the instrument and measures the relative sensitivities of the two detecting systems. It is given as

$$G = I_{hv}/I_{hh}$$

where I_{hv} and I_{hh} are the intensities of the vertically and horizontally polarized fluorescence emission upon excitation with horizontally polarized light.

3.7 Other methods

Gel electrophoresis

The proteins were routinely resolved by electrophoresis separation by SDS-PAGE (Polyacrylamide gel electrophoresis with anionic detergent sodium dodecyl sulphate) (Laemmli, 1970). Gels containing 10–15% acrylamide/bisacrylamide were prepared according to standard method and reagents from BioRad. The electrophoretic device used was Mini-PROTEAN Tetra Cell from BioRad. For native gels, SDS was excluded from the gel, running buffer and loading solution.

After electrophoresis, the gels were stained using Coomassie blue dye (40% (v/v) ethanol, 10% (v/v) acetic acid and 0.5% (w/v) Coomassie Brilliant Blue R-250). The excess dye was removed from the gels using destaining solution (20% (v/v) ethanol and 10% acetic acid) until the background is transparent.

Protein concentration determination

Protein concentrations were determined by absorption spectroscopy at 280nm using Cary 50 Bio UV-Visible spectrophotometer (Varian). Since syntaxins do not contain any Trp residues, the absorption was measured at 276nm (λ_{max} for Tyr). The extinction co-efficients were calculated using the Edelhoch method (Grimsley and Pace, 2003). The protein concentrations were determined from the absorption, extinction coefficient and path-length using the Beer-Lambert's law.

4 Results

4.1 Purification of Munc18c

One of the biggest problems with studying Sec1/Munc18 (SM) proteins is that they are generally quite difficult to express and purify in sufficient quantities for structural and biophysical analyses. The first challenge in the project was thus, to purify Munc18c in milligram quantities and at high concentrations (about 10μM) in order to use it for quantitative (biophysical) experiments.

Munc18c has previously been expressed and purified by Hu et al. (2003) using recombinant baculovirus infected Sf9 insect cells. However, the expertise for baculoviral expression was not available in the lab. Also, the technique is expensive, time consuming and does not produce enough protein. Hence, I tried to express the protein using a traditional bacterial expression system.

The Munc18c full length construct inserted in pET28a (+) vector was transformed into BL21 *E.coli* cells. Protein expression from the native Munc18c gene was not successful, and the protein could not be identified in the bacterial supernatent or pellet after lysis. Heterologous protein production in *E.coli* can be problematic because of the differences in codon usage between bacterial and mammalian genes. Hence, a codon optimized Munc18c construct was used next to achieve high-level gene expression.

I optimized the expression and purification protocol for Munc18c using different conditions to obtain pure protein in large quantities (See Materials & Methods 3.3). Under standard expression conditions, the protein expression was low and majority of the protein was precipitating. Hence, I carried out the expression under mild conditions using lower temperature and lower IPTG concentration to keep the protein soluble. I used LB medium to grow the culture to higher optical density and thus obtain higher quantity of protein.

Stringent conditions were used in affinity purification by Ni^{2+}-NTA beads to specifically select the protein of interest from a large background of bacterial proteins. Mono S ion exchange

chromatography was used to further purify the protein. Figure. 4.1 shows the various fractions obtained at different steps of purification and the MonoS chromatography elution profile. An average yield of 1.5mg of pure protein per liter of induced culture, with a concentration of 10-12μM was obtained with this protocol.

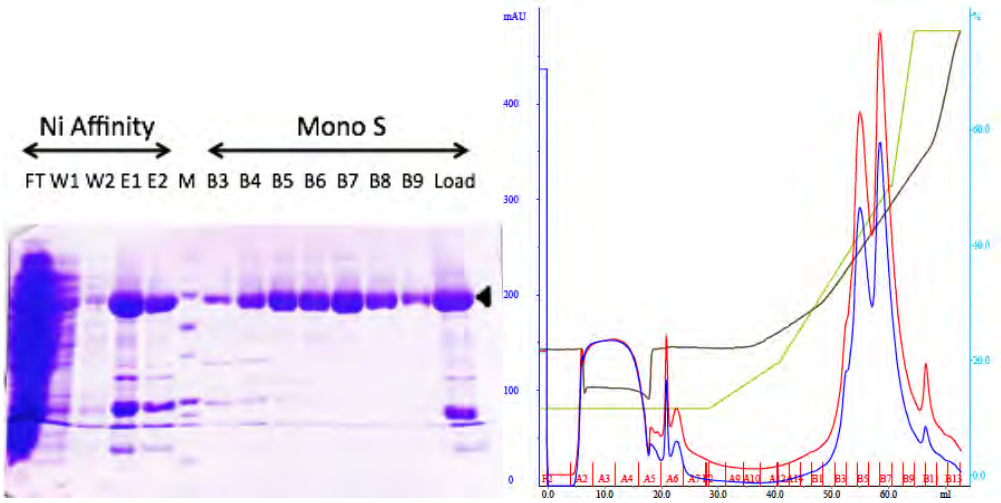

(a) (b)

Figure 4.1 – **Munc18c purification.** (a) The SDS-PAGE gel stained with Coomassie blue shows the protein enrichment at different stages of purification. The protein was first purified by Ni-NTA affinity chromatography from the bacterial supernatant. From this step, the flow-through (FT), washes (W1, W2) and elution from beads (E1, E2) were loaded on the gel. The eluates were pooled, dialysed and purified further by Mono S ion exchange chromatography. The sample after dialysis (load) and the eluted fractions from Mono S were loaded on the gel. 'M' refers to standard protein marker. (b) The Mono S elution profile. — Absorbance at 280nm (y1 axis), — Absorbance at 230nm, — Conductivity (y2 axis), — Salt gradient.

After I had established this protocol for Munc18c purification, Rehman et al. (2013) published a similar purification strategy for codon-optimized Munc18c in *E.coli* BL21 cultures. They used auto-induction media and co-expressed Munc18c with Gro EL/ES chaperones. The induction was carried out at 16°C to get a yield of 1mg of protein per liter culture. They stored Munc18c at −80°C after purification. Note that for my experiments I have used fresh Munc18c purified each time. I found early on through biophysical experiments that freezing and thawing reduced the activity of Munc18c.

4.2 Investigating the interaction of Syntaxin 4 (Syx4) with Munc18c

4.2.1 Syx4 binds to Munc18c with high affinity

The binding of Syx4 (1-270) to Munc18c was studied using analytical gel filtration to determine if the proteins can form a complex in solution. Analytical gel filtration is a method to

characterize proteins and their complexes on the basis of their size. Larger proteins or protein complexes elute before smaller proteins from the column helping to separate the complex from the individual proteins.

Syx4 (1-270) and Munc18c were incubated in a 1:1 ratio and loaded on the gel filtration column. Figure 4.2a shows the elution profiles for the complex and the individual proteins. The Syx4(1-270)/Munc18c complex was seen to elute before the individual proteins. The gels below the elution profiles showing the composition of each fraction clearly indicate the shift in elution of Munc18c and especially Syx4 when they are a part of the complex.

A more sensitive method of isothermal titration calorimetry (ITC) was then used to measure the binding affinity of Syx4 (1-270) and Munc18c. The ITC instrument measures the heat released on binding of two macromolecules in solution, from which the thermodynamic parameters can be calculated.

The titration of Syx4 (1-270) into Munc18c observed by ITC shows that the two proteins interact with a high binding affinity (K_d 10nM) (Figure 4.3 and Table 4.1). I observed a higher binding affinity than published previously by Christie et al. (2012, see Supp Fig.S1), who had reported a K_d of 95nM for Syx4 (1-275)/Munc18c interaction. It should be noted that the syntaxin 4 sequence does not contain the thrombin cleavage site found in Syx1a, and we were able to cleave the His-tag from Syx4 N-terminus. Hence there is no contribution from the His-tag towards binding.

4.2.2 Munc18c interacts with Syx4 at two binding sites

SM proteins are thought to interact with their partner syntaxins at two binding sites, although the contribution of both these sites to the binding affinity differs in various SM-syntaxin pairs. Vertebrate Munc18a has been crystallized in complex with syntaxin 1a (Syx1a) (Burkhardt et al., 2008). In this structure, it is seen that Munc18a binds to Syx1a in its closed conformation as well as to the N-peptide. Both these syntaxin binding sites contribute to the inhibitory activity of Munc18a on SNARE assembly. By contrast, the vertebrate homolog, Munc18c, has been crystallized only in the presence of the N-peptide of Syx4 (Hu et al., 2007). However, the binding of the rest of the Syx4 protein to Munc18c is debated.

Along with the binding of Syx4(1-270), Christie et al. (2012) had also reported that Syx4 (30-275) lacking the N-terminal peptide doesn't bind to Munc18c. Hence, they claimed that Munc18c binds to Syx4 only through the N-terminal peptide. Since I observed a higher binding affinity and enthalpy for Syx4 (1-270)/Munc18c, I also investigated the binding of Syx4(25-270) lacking N-terminal peptide with Munc18c.

The analytical gel filtration experiment was carried out as mentioned earlier. Similar to the elution of Syx4(1-270)/Munc18c complex, the Syx4 (25-270)/Munc18c complex elution profile is distinct from the elution profiles of the individual proteins (Figure. 4.2b). The gels below the elution profiles showing the composition of each fraction clearly indicate the shift in

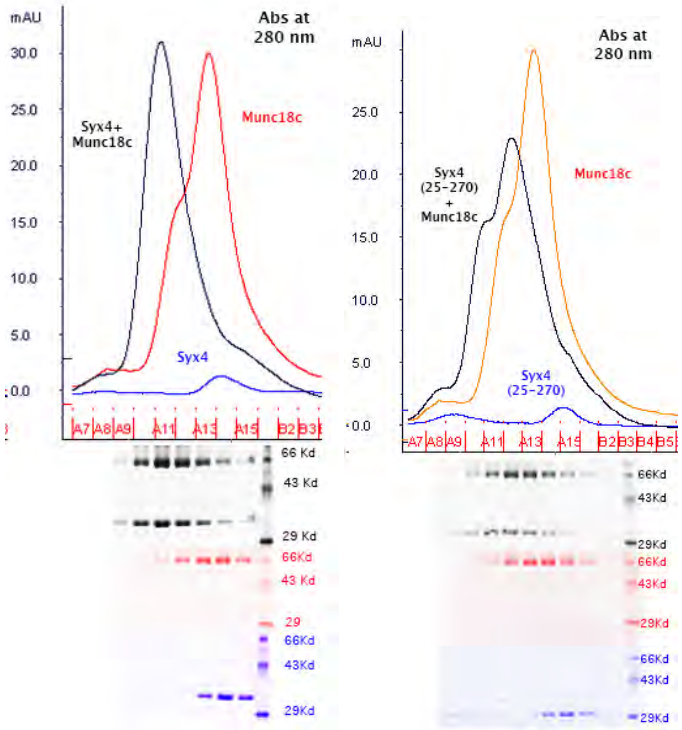

(a) (b)

Figure 4.2 – **Munc18c forms a complex with Syx4, with or without the N-peptide** (a) Analytical gel filtration profiles for Syx4(1-270), Munc18c and their complex show a shift in the elution profile of individual proteins when they are part of a complex. This indicates distinct complex formation. (b) Analytical gel filtration profiles for Syx4(25-270), Munc18c and their complex also indicate complex formation. The SDS-PAGE gels below the elution profiles show the composition of individual fractions from each elution. The gels are color coded according to the elution graphs. The gels also illustrate a shift in elution of individual proteins on complex formation.

elution of Munc18c and especially Syx4 (25-270) when they are a part of the complex. The complex formed between Syx4(25-270) and Munc18c shows a wider and shorter peak than that observed for Syx4-Munc18c complex. Possibly due to weaker binding of Syx4(25-270) to Munc18c, the complex could be falling apart while passing through the column resulting in a broader peak.

The titration of Syx4(25-270) into Munc18c was followed using ITC (Figure. 4.4a). In the absence of the N-peptide Syx4 still binds to Munc18c, although with a lower affinity (K_d 700nM) and enthalpy change ($\Delta H \approx -9.2$kcal/mol) than Syx4(1-270)/Munc18c interaction (Figure. 4.4a). This proves that Munc18c interacts with Syx4, even in the absence of the N-peptide.

Syx1a adopts a closed conformation where the SNARE domain binds to its own Habc domain. In the Munc18a/Syx1a complex, the biggest contribution to the binding affinity is from the

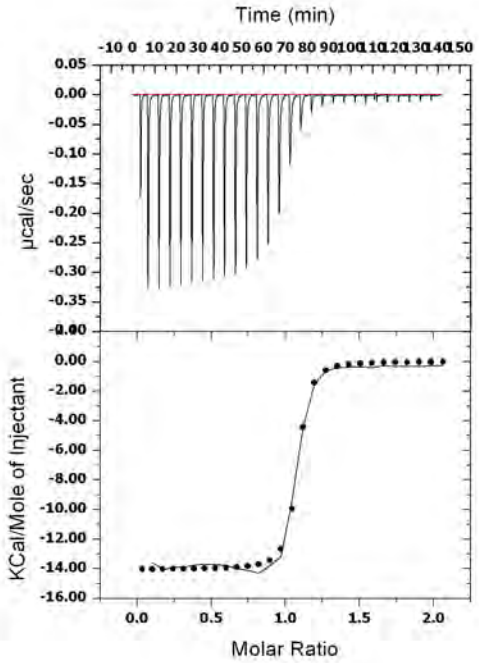

Figure 4.3 – **Munc18c binds to Syx4 (1-270) with high binding affinity.** The titration of Syx4 into Munc18c was followed by ITC. The upper panel shows the titration curve where each peak corresponds to the heat released on titrating a small quantity of Syx4 into Munc18c. The decrease in the peak height indicates the completion of titration. Integration of the area under each peak gives the binding curve in the lower panel (circles). The line in the lower panel shows the fit for the binding curve. The slope of the line gives the binding affinity ($1/K_d$) and the difference before and after titration denotes the enthalpy change (ΔH). The stoichiometry (n) is given by the mid-point of titration, and the entropy (ΔS) is calculated by the equation $-RTl_nK_d = \Delta G = \Delta H - T\Delta S$. The thermodynamic parameters K_d (10.6 nM), ΔH (−14.3 kcal/mol), ΔS (−11.3 cal/mol/deg), stoichiometry (1.05) calculated from the binding curve show that there is a strong interaction between Syx4 (1-270) and Munc18c.

SNARE domain as part of the closed conformation. My ITC results indicate that Syx4 adopts a similar closed conformation consisting of the Habc domain and the SNARE domain.

In order to evaluate the contribution of the Syx4 SNARE domain to binding, I used a deletion mutant lacking the SNARE domain i.e. Syx4 (1-191). The ITC experiment showed that Syx4(1-191)/Munc18c interaction has lower enthalpy change ($\Delta H \approx -3.5$kcal/mol) and affinity ($K_d \approx$ 550nM) compared to Syx4 (1-270) (Figure 4.4a and Table 4.1). Moreover, the reduction in enthalpy in absence of the SNARE domain is greater than when the N-peptide is deleted, indicating that a larger binding surface is involved. Hence, the SNARE motif contributes to the binding affinity between Syx4 and Munc18c, probably as a part of the closed conformation with the Habc domain.

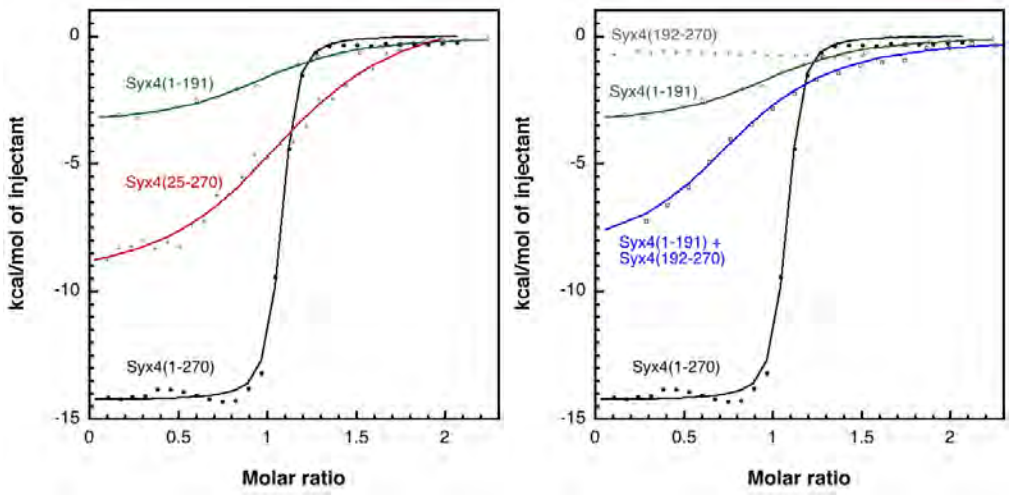

(a) (b)

Figure 4.4 – **Munc18c interacts with Syx4 through both its N-terminal peptide and the closed conformation.**
(a) Syx4 constructs lacking either the N-terminal peptide [Syx4 (25-270)] or the SNARE domain [Syx4 (1-191)] show a decrease in binding affinity compared to Syx4 (1-270) when measured by ITC. Hence, both the N-peptide and the SNARE domain contribute to the binding affinity. (b) When Syx4 fragments containing the N-peptide and Habc domain (1-191) and the SNARE domain (192-270) are mixed and titrated (using ITC) into Munc18c, the affinity and enthalpy is higher for the mixture than for each individual fragment. Hence, the SNARE domain and the Habc domain form a closed conformation that binds to Munc18c.

Two fragments of Syx4 – Syx4 lacking the SNARE domain [Syx4 (1-191)] and the Syx4 SNARE domain [Syx4 (192-270)] – were used to evaluate if the SNARE domain and the Habc domain interact with Munc18c together. The two fragments were then mixed in a 1:1 molar ratio and titrated into Munc18c. The binding affinity and enthalpy was higher when the two fragments were mixed as compared to titration of the individual fragments into Munc18c (Figure. 4.4b). This indicates that the fragments interact to form a closed conformation that is then bound by Munc18c.

A change in the Trp fluorescence intensity of Munc18a occurs when it forms a complex with Syx1a (Burkhardt et al., 2008, Supp Fig.1a). I found that although Munc18c shows intrinsic tryptophan fluorescence similar to Munc18a, the binding of either Syx4 or Syx1a did not result in a change in the fluorescence intensity. This might be due to structural differences between the Munc18 and Syx proteins (Section 4.8).

Table 4.1 – **Thermodynamic parameters for the interaction of syntaxin with Munc18 measured by ITC.**

	K_d (nM)	ΔH (kcal/mole)	n
Syx4 (1-270)/Munc18c	10	−14.3	0.90
Syx4(1-270)^{LE}/Munc18c	164	−11.0	0.92
Syx4(25-270)/Munc18c	714	−9.2	0.95
Syx4RL/Munc18c	386	−7.0	1.04
Syx4(1-191)/Munc18c	546	−3.5	0.99
Syx1a (1-262)/Munc18c	19.2	−8.3	0.93
Syx2 (1-262)/Munc18c	8.9	−8.9	0.92
Syx3 (1-263)/Munc18c	–	–	–
Syx4(1-270)/Munc18cY521E	21	−9.8	0.91
Syx2(1-262)/Munc18cY521E	29.6	−6.3	1.03
Syx1a (1-262)/Munc18a	2	−25	0.96
Syx2 (1-262)/Munc18a	1	−29.1	1.08
Syx3 (1- 263)/Munc18a	62	−12.2	1.02
Syx4 (1-270)/Munc18a	–	–	–

4.3 Effect of Munc18c on SNARE complex assembly of Syx4

In the previous section, I showed that Munc18c binds to Syx4 at both the N-peptide and its closed conformation, similar to the interaction of Munc18a with Syx1a. Hence, the next question was whether Munc18c has a similar inhibitory effect on SNARE complex formation as reported for Munc18a (Burkhardt et al., 2008).

During the process of SNARE complex formation in exocytosis, the Qa- and Qbc-SNAREs (Syx and SNAP25) form a binary complex, which then binds to the R-SNARE (synaptobrevin2) to form the ternary SNARE complex. Burkhardt et al. (2008) has shown for the neuronal SNARE complex containing Syx1a that Munc18a inhibits the rate of complex formation for both the binary and ternary SNARE complexes. In the absence of its N-peptide or when the Syx1 LE mutant (L165A/L166A) is used, Munc18a inhibition of the SNARE complex is relieved.

4.3.1 Munc18c slows down SNARE complex assembly with Syx4 (1-270)

In order to investigate the effect of Munc18c on SNARE complex formation, I first established a fluorescence anisotropy assay to follow the formation of the binary and ternary SNARE complexes containing Syx4 (1-270). *In vivo* Syx4 has been reported to form SNARE complexes with SNAP23 and synaptobrevin2 (Syb) (Araki et al., 1997; Volchuk et al., 1996). Initially, I studied the complex formation on mixing labeled Syb with Syx4 (1-270) and SNAP23. However, the SNARE complex formation with SNAP23 was observed to be much slower compared to that with SNAP25 (see Appendix A.2). Hence, for practical considerations, SNAP25 was used instead of SNAP23 for all the fluorescence anisotropy studies for ease of conducting

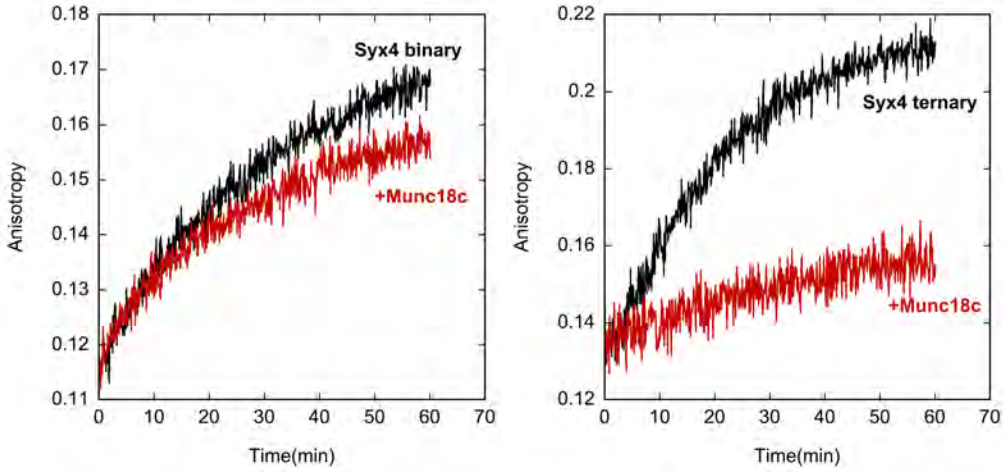

(a) (b)

Figure 4.5 – **Munc18c inhibits SNARE complex formation with Syx4.**
(a) The binary complex formation was studied by following fluorescence anisotropy increase of 100nM SNAP25^{130OG} on addition of 2μM Syx4 (1-270). When 3μM Munc18c is present in the reaction mixture, the anisotropy change is slower indicating that Munc18c interferes with binary complex formation. An excess of Munc18c was used to ensure that all the Syx4 is bound by Munc18c (b) The ternary complex formation was studied by following fluorescence anisotropy increase of 40nM Syb 1-96^{61OG} on addition of 1μM Syx4 (1-270) and 1.5μM SNAP25. In the presence of 1.5μM Munc18c, the ternary complex formation was inhibited. The effect of Munc18c in slowing down SNARE complex formation was more pronounced for formation of the ternary complex.

experiments and to better identify any perturbations.

The binary complex formation was studied by following the change in fluorescence anisotropy of SNAP25 (full-length construct) labeled at Cys130 with Oregon Green (SNAP25^{130OG}), when Syx4 (1-270) is added. The ternary complex formation was studied by following the change in fluorescence anisotropy of Syb (1-96) labeled at Cys61 with Oregon Green (Syb 1-96^{61OG}), on binding of Syx4 (1-270) and SNAP25. Note that Syb (1-96) does not form a complex with individual SNAP25 or Syx4.

The change in the fluorescence anisotropy with time indicates the rate at which complex formation takes place. When Munc18c was included in the reaction mixture, the rate of complex formation was reduced for both the binary and ternary complexes (Figure 4.5). This effect was more pronounced in the case of ternary complex formation.

4.3.2 Munc18c does not inhibit SNARE complex assembly in the absence of Syx4 N-peptide interaction

The N-peptide plays a role in the inhibitory effect of Munc18a on SNARE complex formation. To test if the inhibition by Munc18c is also affected by the Syx4 N-peptide interaction, I used a N-peptide deletion mutant Syx4 (25-270). This construct showed precipitation during experiments which caused problems during fluorescence anisotropy measurements. To overcome this problem, I used another construct with a double mutation in the N-peptide region, R4A L8A (Syx4RL). These positions were selected for mutation, because these residues are conserved in all syntaxins and primarily contribute to the N-peptide interaction. The titration of Syx4RL into Munc18c using ITC showed a similar binding affinity and enthalpy as the Syx4 (25-270)/Munc18c interaction (Table 4.1). Hence, the ITC data confirm that the N-peptide interaction is mostly eliminated in the Syx4RL mutant.

The binary and ternary SNARE complex formation with Syx4RL was carried out in the absence or presence of Munc18c and the rates were found to be comparable to SNARE complex formation with Syx4 wt. The rate of SNARE complex formation with Syx4RL was not affected by the presence of Munc18c, indicating that Munc18c cannot inhibit SNARE complex formation in the absence of the N-peptide interaction (Figure 4.6). These results are similar to those obtained for Syx1a-Munc18a complex in absence of the N-peptide interaction (Burkhardt et al., 2008).

4.3.3 Munc18c slows down the SNARE assembly of the Syx4LE mutant

The effect of Munc18c on the SNARE complex assembly was found to be similar to Munc18a, for SNARE assembly containing Syx4 or Syx4RL. When the LE mutant of Syx4 was used, some differences were seen.

The Syx4LE mutant was constructed similar to the Syx1a LE mutant, where the corresponding 'LE' residues in the linker region are mutated to Ala (L173A E174A). In the LE mutant, the equilibrium between closed and open states is shifted towards the open configuration, thus increasing the availability of the SNARE domain for binding. I observed through ITC experiments that Syx4LE binds to Munc18c (k_d 160 nM), although with $\approx 1/10^{th}$ the affinity of the wild-type (Table 4.1). A similar interaction pattern has been observed by Burkhardt et al. (2008) for Syx1a LE mutant binding to Munc18a, where Syx1a LE interaction (k_d 8 nM) is weaker than for the full length protein ($K_d \approx$ 1.4nM).

Using the fluorescence anisotropy approach, I observed that the rate of binary and ternary SNARE complex formation was faster for Syx4LE than Syx4 (1-270), when identical concentrations were used. This was expected, since Syx4LE equilibrium is supposed to be shifted towards the more open configuration.

When the experiments were carried out in the presence of Munc18c, I observed that Munc18c slows down the rate of SNARE complex formation for Syx4LE (Figure 4.7). Note that no

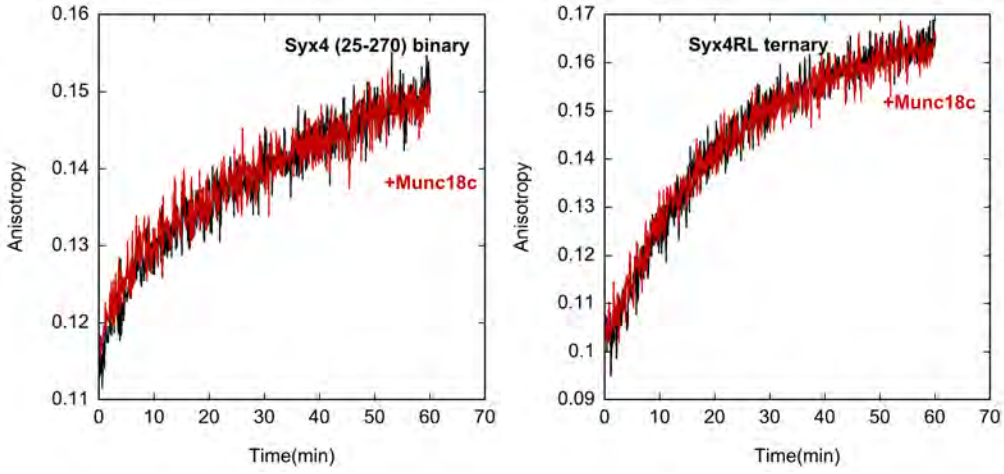

(a) (b)

Figure 4.6 – **Munc18c does not affect SNARE complex formation in the absence of N-peptide interaction.**
(a) The binary complex formation was studied by following fluorescence anisotropy increase of 100nM SNAP25^{130OG} on addition of 2μM Syx4 (25-270). The presence of 3μM Munc18c in the reaction mixture did not change the rate of complex formation. (b) The ternary complex formation was studied by following fluorescence anisotropy increase of 40nM Syb 1-96^{61OG} on addition of 1μM Syx4RL and 1.5μM SNAP25. The presence of Munc18c did not affect the SNARE complex formation rate. The N-peptide interaction is disrupted in the Syx4RL mutant (R4A, L8A) similar to the Syx4 (25-270) deletion mutant.

detectable decrease in the ternary SNARE assembly rate had been reported for the Syx1a LE mutant in the presence of Munc18a (Burkhardt et al., 2008). A possible reason for this observation is that the Syx4LE mutant has a slower rate of binding to SNAP25 compared to Syx1a LE mutant (See Section 4.6).

4.4 Interaction between mammalian Munc18 and Syx homologs

4.4.1 Munc18a and Munc18c interact with multiple syntaxin homologs

Most vertebrates have three homologs of Munc18, and six homologs of syntaxin with different tissue distributions. The specificity of the Munc18-syntaxin interactions are probably important, because many tissues express multiple Munc18 and syntaxin homologs. Previous studies have shown that different Munc18 homologs are specific for certain syntaxin homologs (Hackmann et al., 2013; Tamori et al., 1998; Tellam et al., 1997). Most of these studies have been carried out using qualitative pull-down assays that can only indicate if a specific Syx-Munc18 pair binds or not. Since I had purified Munc18c in enough quantity for biophysical analyses, I could measure the interactions between the Syx-Munc18 pairs quantitatively by ITC. But before using ITC, I tested the interaction and binding affinities for neuron-specific Munc18a

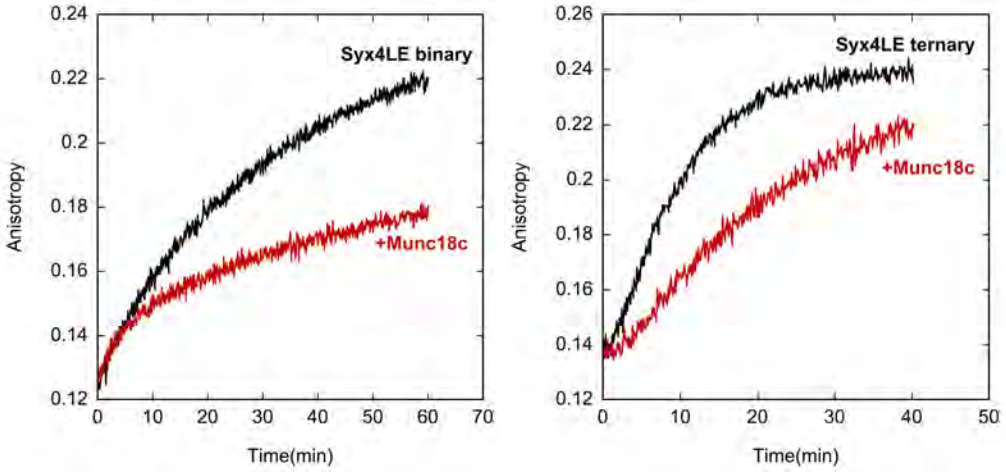

(a) (b)

Figure 4.7 – **Munc18c slows down SNARE complex formation for the Syx4LE mutant.** (a) The binary complex formation was studied by following fluorescence anisotropy increase of 100nM SNAP25^{130OG} on addition of 1μM Syx4LE. The presence of 1.5μM Munc18c in the reaction mixture reduced the rate of complex formation. (b) The ternary complex formation was studied by following fluorescence anisotropy increase of 40nM Syb 1-96^{61OG} on addition of 800 nM Syx1LE and 1.2μM SNAP25. The presence of 1.2μM Munc18c reduced the rate of SNARE complex formation.

and the more ubiquitously expressed Munc18c using GST-pulldown assay.

For GST-pulldown assay, Syx 1, 2, 3 and 4 were purified as GST-tagged proteins and were bound to reduced glutathione sepharose beads. The beads were incubated with Munc18a or Munc18c, the flow-through was collected, the beads were washed and the proteins eluted using buffer containing glutathione. The proteins in these fractions were visualized using SDS-PAGE. The detailed method for the GST-pulldown assay is given in Materials & Methods 3.4.

Figure 4.8 shows that Munc18a binds to Syxs 1a and 2, and to a lesser extent to Syx3 while Munc18c binds to Syxs 2 and 4, and to a lesser extent to Syx1a. Munc18a did not bind to Syx4 and Munc18c did not bind to Syx3. This is consistent with published experiments using a similar approach which show that Munc18a and Munc18b bind to Syx1, 2 and 3 while Munc18c binds to Syx2 and 4 (Tamori et al., 1998; Tellam et al., 1997).

Using the sensitive method of ITC, I found that Munc18c has a high affinity for both Syx4 and Syx2 ($K_d \approx$ 10nM). Munc18c also binds to Syx1a, although with a slightly lower affinity ($K_d \approx$ 20nM) (Figure 4.9a and Table 4.1). However, no interaction was observed between Munc18c and Syx3.

Munc18a bound tightly to Syx1a, confirming previously reported values from our group (Burkhardt et al., 2008). The enthalpy value probably varies from the earlier reported value,

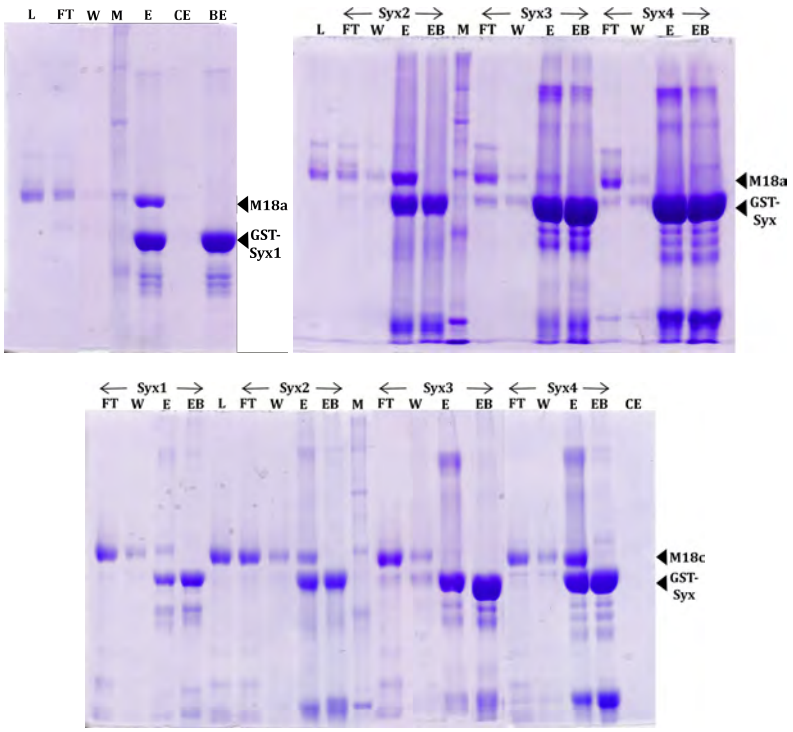

Figure 4.8 – **GST-pulldown assay of Munc18a (upper panels) and Munc18c (lower panel) with GST tagged Syx1a, 2, 3 and 4.**
The samples loaded on the gel are Munc18 (L), flow-through (FT), wash (W), elution (E), positive control of elution from beads incubated with GST-Syx (EB), negative control of elution from beads incubated with only Munc18 without GST-Syx (CE). The difference between the bands in E and EB columns shows the specificity of Munc18a or Munc18c for binding to the corresponding Syx.

because I used HEPES buffer instead of PBS for studying the interaction. I also found that Munc18a has a similar high affinity for Syx2 ($K_d \approx 1$nM) and also interacts with Syx3 (Figure 4.9b and Table 4.1). No detectable interaction was found for Syx4 with Munc18a.

Thus, the ITC approach confirms the results obtained by GST-pulldown assays. From the above experiments, it is evident that Munc18 proteins have a preference for a certain Syx, but can also interact with other secretory syntaxins. The third vertebrate Munc18 homolog, Munc18b has been shown previously to interact with Syx1, 2 and 3 but not with syntaxin 4. I was unable to express and purify Munc18b from the E.coli expression system in adequate quantity for biophysical experiments.

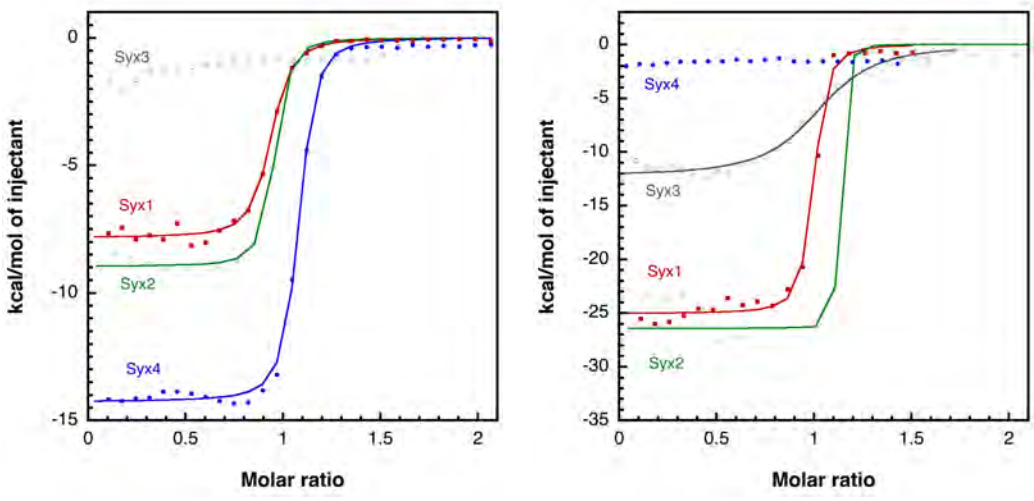

(a) (b)

Figure 4.9 – **Titration of secretory syntaxins into Munc18c and Munc18a by ITC.** The interaction of (a) Munc18c and (b) Munc18a with secretory syntaxins Syx1 (■), Syx2 (○), Syx3 (□) and Syx4 (●) was measured by ITC. The graphs show the overlay of the binding curves obtained in individual experiments.

4.4.2 Munc18a and Munc18c have an inhibitory effect on SNARE complex formation of secretory syntaxins

The previous sections demonstrated that Munc18 homologs can bind to multiple syntaxins. Each of Syx1 and Syx2 were found to interact with both Munc18a and Munc18c. However, no interaction was seen between Syx3/Munc18c and Syx4/Munc18a.

In the previous sections, I have described experiments that demonstrate that Munc18c inhibits the formation of the SNARE complex of Syx4. Moreover, it has been published that Munc18a inhibits the SNARE complex formation with Syx1 (Burkhardt et al., 2008; Pevsner et al., 1994b). Since Munc18a and Munc18c bind tightly to other Syx homologs, I tried to further investigate the effect of Munc18a and Munc18c on the SNARE complex assembly of Syx1 and Syx2. This approach allowed for a more direct comparison of the activity of the two Munc18 homologs. The fluorescence anisotropy assay mentioned in Section 4.3 was used to follow SNARE complex formation.

When Munc18c was added to the mix of Syx1, SNAP25 and Syb, the rate of SNARE complex formation was reduced similar to the inhibition exerted by Munc18a (Figure 4.10a). A similar result was obtained for the SNARE complex formation of Syx2 in the presence of Munc18a or Munc18c, where both Munc18 homologs slowed down the rate of SNARE complex formation (Figure 4.10b).

These results provide further proof for the inhibitory activity of Munc18a and Munc18c on SNARE complex assembly. However, Munc18a showed stronger inhibition of the SNARE com-

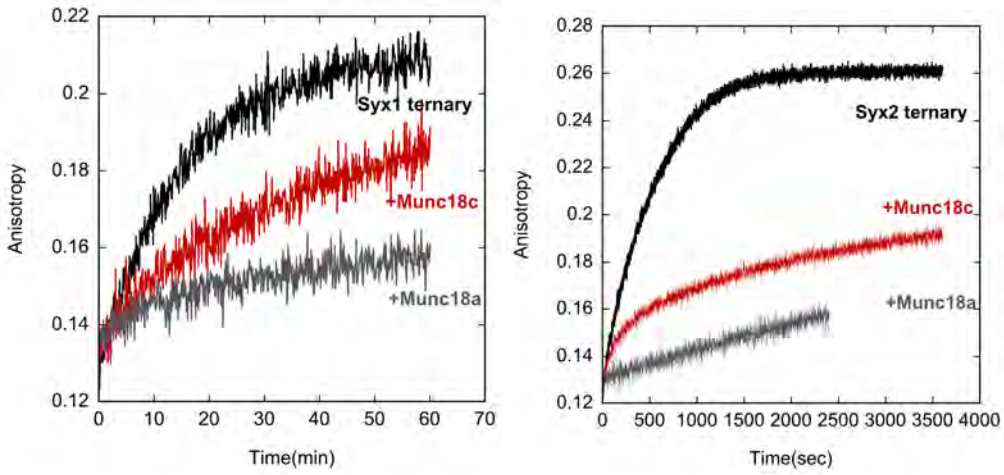

(a) Syx1a SNARE assembly

(b) Syx2 SNARE assembly

Figure 4.10 – **Munc18a and Munc18c inhibit the SNARE complex assembly of non-cognate syntaxins.**
(a) The formation of the Syx1a ternary complex was followed by fluorescence anisotropy increase of 40nM Syb 1-96^{61OG} on addition of 500nM Syx1a and 750nM SNAP25. The presence of 750nM Munc18a or Munc18c in the reaction mixture reduced the rate of SNARE complex formation. (b) The formation of the Syx2 ternary complex was followed by fluorescence anisotropy increase of 40nM Syb 1-96^{61OG} on addition of 2μM Syx2 and 3μM SNAP25. The presence of 3μM Munc18a or Munc18c in the reaction mixture reduced the rate of SNARE complex formation. Note that a higher concentration of Syx2 was required to see a change in the anisotropy on SNARE complex formation. This is because the rate of binary complex formation with SNAP25 was found to be slower for Syx2 (See Section 4.6).

plex assembly as compared to Munc18c. One reason for this could be that the binding affinity of Syx1a and Syx2 with Munc18a is stronger than with Munc18c (Table 4.1). In particular, the off-rates of the complexes of Syx1a and Syx2 with Munc18c are higher than those with Munc18a as elaborated in the next section (See Section 4.6).

4.4.3 Munc18c reduces the rate of SNARE complex formation with Syx1LE mutant.

As mentioned earlier, the rate of SNARE complex formation with Syx4LE was reduced in the presence of Munc18c. As Munc18c can interact with Syx1a, I was able to test the the effect of Munc18c on the binary and ternary SNARE complex formation of Syx1 in presence of the LE mutation (Syx1LE). Munc18a was used as a control, since it has been shown to not affect the ternary SNARE complex formation of Syx1LE (Burkhardt et al., 2008).

The presence of either Munc18a or Munc18c had little effect on rate of binary complex formation with Syx1LE (Figure 4.11a). However, Munc18a and Munc18c had differing effects on the ternary SNARE complex formation with Syx1LE (Figure 4.11b). The presence of Munc18a did

not have any effect on the rate of SNARE complex formation as shown earlier (Burkhardt et al., 2008). However, Munc18c reduced the rate of SNARE complex formation similar to its effect on Syx4LE SNARE assembly.

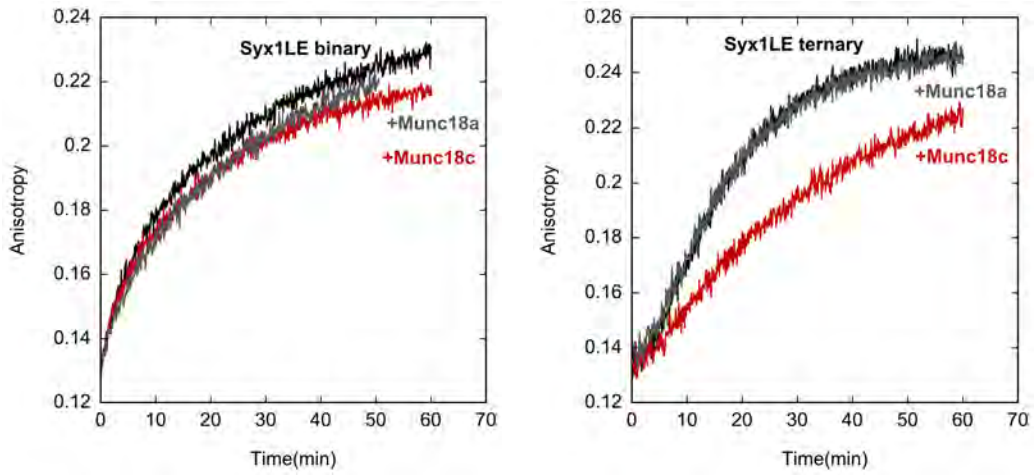

(a) (b)

Figure 4.11 – **Munc18c slows down ternary but not binary SNARE complex formation for the Syx1LE mutant.**
(a) The binary complex formation was studied by following fluorescence anisotropy increase of 100nM SNAP25^{130OG} on addition of 700nM Syx1LE. The presence of 1μM Munc18c or Munc18a in the reaction mixture did not have much effect on the rate of SNARE complex formation. (b) The ternary complex formation was studied by following fluorescence anisotropy increase of 40nM Syb 1-96^{61OG} on addition of 500 nM Syx1LE and 750nM SNAP25. The presence of 750nM Munc18c reduced the rate of SNARE complex formation, but Munc18a did not have any effect.

4.5 Effect of the Munc18c phospho-mimetic mutation Y521E

The phosphorylation of Munc18c at position Tyr521 has been reported to cause a change in its functionality and in insulin response. Either phosphorylation of this site or introduction of a negative charge at this position mimicking a phosphate group, has been shown to cause reduced Munc18c binding to Syx4, elevated GLUT4 externalization and increased glucose uptake (Aran et al., 2011; Bakke et al., 2013; Jewell et al., 2011; Umahara et al., 2007). The Tyr521 residue is present on a disordered region in domain 2 and is not conserved in other Munc18 homologs (Jewell et al., 2011). Also, Munc18c is thought to be phosphorylated at Tyr521 directly by the insulin receptor (IR) kinase, thus linking insulin signaling with the regulation of GLUT4 vesicle exocytosis.

I used a mutant of Munc18c, Y521E, where the glutamate residue introduces a negative charge that mimics tyrosine phosphorylation at this site. I then measured the affinity of Munc18c Y521E mutant with Syx4 and Syx2 using ITC, and compared the results with binding of wild-

type Munc18c. I observed that the binding affinity and enthalpy for the titration of Syx4 or Syx2 into Munc18c Y521E was lower than that observed for Munc18c wt (Figure 4.12).

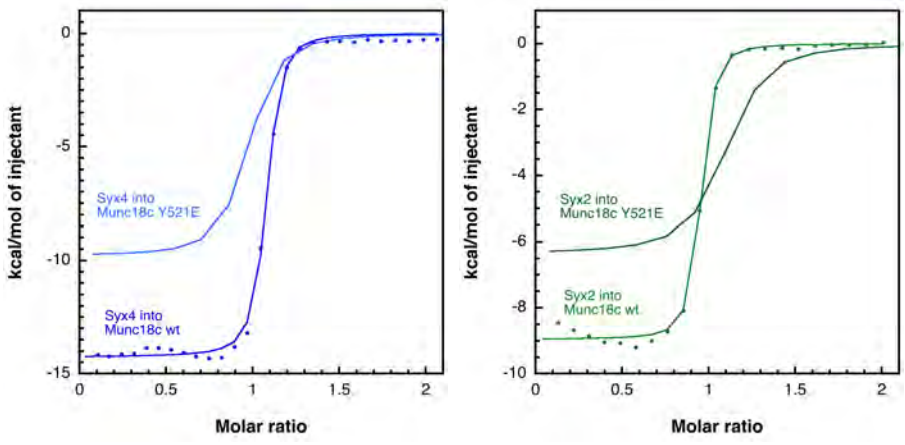

(a) (b)

Figure 4.12 – **Munc18cY521E had weaker interaction with syntaxin compared to Munc18c wild-type.**
(a) The interaction of Syx4 (1-262) with Munc18c Y521E (void circles) had lower binding affinity and enthalpy than that with wild-type Munc18c (filled circles). (b) The interaction of Syx2 (1-270) with Munc18c Y521E (void circles) had lower binding affinity and enthalpy than that with wild-type Munc18c (filled circles).

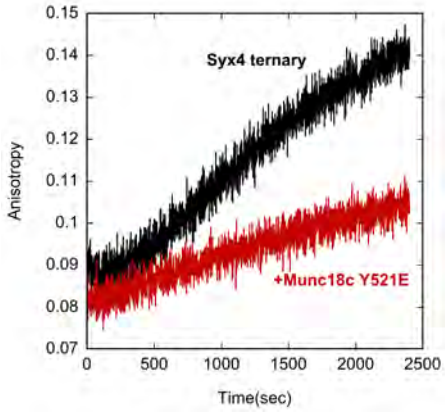

Figure 4.13 – **Munc18cY521E reduces the rate of SNARE complex formation.**
The SNARE complex formation was followed by studying the change in anisotropy of 40nM Syb 1-96^{61OG} on addition of 1μM Syx4 (1-270) and 1.5μM SNAP25. The presence of 1.2μM Munc18c Y521E in the reaction mixture reduced the rate of SNARE complex formation.

The effect of the Munc18c Y521E mutation on the rate of SNARE complex formation was also assayed. The SNARE complex formation was studied by following the fluorescence anisotropy of Syb 1-96^{61OG} on addition of Syx4 (1-270) and SNP25 as described earlier. The presence of Munc18c Y521E caused a reduction in the rate of SNARE complex formation (Figure 4.13). The

inhibition of the SNARE complex formation with the mutant was similar to that observed for Munc18c wt. Thus, the mutation probably did not alter the activity of Munc18c during SNARE complex formation.

4.6 Binding equilibria dictate the rate and direction of reaction

4.6.1 Binary complex formation is regulated by the syntaxin Habc domain

Recapitulating the process of SNARE complex formation discussed in the introduction, the t-SNAREs form an intermediate binary complex which then reacts with the v-SNARE to form the ternary SNARE complex. The syntaxin regulatory Habc domain can fold over its SNARE domain to form an auto-inhibitory 'closed configuration' that does not allow its binding to SNAP25 (Figure in Introduction). In solution, syntaxin alternates between such a closed conformation and an extended 'open conformation'. Hence, the rate of formation of the binary complex can give useful insights into the availability of the SNARE domain of syntaxin for SNARE-complex formation and thus, the extent of auto-inhibition of a certain syntaxin.

Syntaxin homologs differ in the rate of binary complex formation

To determine the on-rate for the binary complex between SNAP25 and each of the secretory syntaxins, I followed the change in fluorescence anisotropy of labeled SNAP25 as seen earlier (Section 4.3). The second-order reaction for the binary complex can be treated as pseudo-first order, if one of the components is kept constant and the other is used in excess. In this experiment, a fixed concentration of labeled SNAP25 (50nM) was mixed with Syx at different concentrations in the micromolar range. Each reaction was fit to a single exponential to obtain the pseudo-first order rate constant, which was then plotted as a function of the Syx concentration. The slopes of the linear fits gave the second order rates of the reaction.

The binary on rates were calculated for all the secretory syntaxins. For each Syx, the H3 (SNARE) domain construct was used as a control for kinetic studies to determine the rate without auto-inhibition by the Habc domain.

The rate constants for the H3 domains of Syx1a, 2, 3 and 4 are in the same range in the order of 10^3 $M^{-1}s^{-1}$ (Figure 4.14a). However, the rates differ for the cytoplasmic domains of the syntaxin homologs. The rate of binary complex formation for Syx4 and Syx2 was slower than for Syx1a, suggesting that the closed conformation for these syntaxins is tighter. The rate of Syx3-SNAP25 binary complex formation was even slower and the rate couldn't be computed with this approach, suggesting that Syx3 resides in an even tighter closed conformation. Thus, the stability of the closed conformation and the extent of auto-inhibition by Habc domain varies for the different syntaxin homologs.

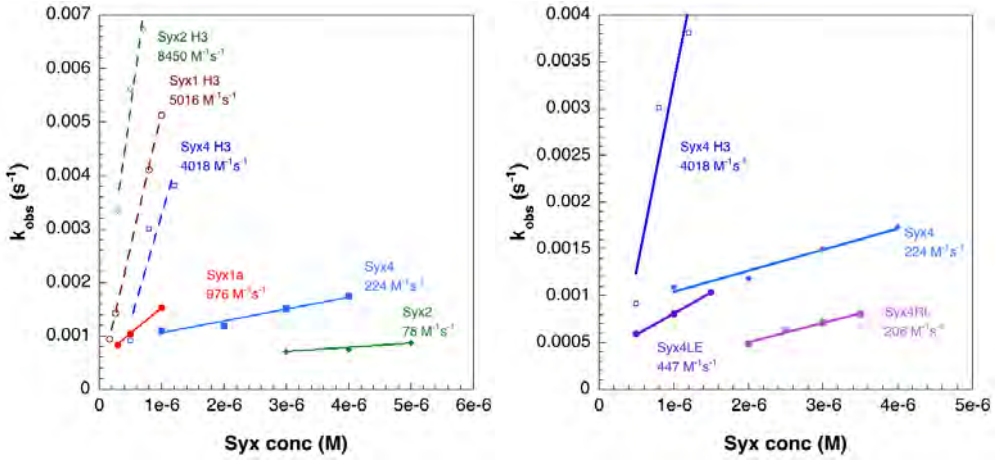

(a) (b)

Figure 4.14 – **The rate of binary complex formation depends on the stability of the Syx closed conformation.**
The reactions for the interaction of 50nM SNAP25^{130OG} with different concentrations of Syx variants were fit to a single exponential to obtain the pseudo-first order rate constant, which was then plotted as a function of the syntaxin variant concentration. The slope of the linear fits gave the second order rate constant. (a) The Syx homologs had similar rates for binding of their SNARE domain to SNAP25, but for the entire cytoplasmic domain the rates differed. Thus, the interaction of the Habc domain with the SNARE domain differs in different syntaxins. (b) The Syx4LE mutant was two times faster than the Syx4 cytoplasmic domain, but it was still slower than the Syx4H3 domain. The RL mutation did not cause any change in the rate of interaction with SNAP25 compared to Syx4 wt.

The rate of binary complex kinetics for Syx4LE is faster than for Syx4

In solution, the equilibrium for the 'LE' mutant of Syx1a is shifted towards an open conformation rather than a closed conformation. Consequently, it assembles into a binary complex with SNAP25 faster than Syx1a wt (Syx1aLE binary rate $\approx$ 3320 $M^{-1}s^{-1}$, Syx1a binary rate $\approx$ 700 $M^{-1}s^{-1}$). The binary complex formation rate for Syx1LE is still slower than that for the Syx1a H3 domain ($\approx$ 6000 $M^{-1}s^{-1}$), indicating that Syx1LE is not in a fully open conformation (Burkhardt et al., 2008).

When I tested the Syx4LE mutant, I found that its rate of binary complex formation was only double than that for the Syx4 wt and much lesser than that for the Syx4 H3 domain (Figure 4.14b). Hence, the shift in equilibrium towards the open conformation is less pronounced for Syx4LE than for Syx1aLE.

Syx1a mutants with a mutation in the N-peptide domain have similar binary kinetics as Syx1a wt. The Syx4RL mutant, where the N-peptide cannot interact with Munc18c, also shows similar binary kinetics as Syx4 wt. Hence, the N-terminal peptide does not affect the rate of binary complex formation.

4.6.2 The off-rates of binary complex formation differ for the syntaxin homologs

In the last section, I described the on-rate at which the binary SNARE complex assembles. Next, I determined the rate at which the binary complex falls apart for the syntaxin homologs and mutants. For this, SNAP25^{130OG} was incubated overnight with different syntaxin variants to pre-form the binary complex.

In order to measure the off-rate, I added excess of unlabeled SNAP25 to the pre-formed binary complex. With this procedure, Syx4 leaving the pre-formed SNAP25^{130OG}-Syx4 complex will be bound by unlabeled SNAP25. The decrease in fluorescence anisotropy of SNAP25^{130OG} denotes the falling apart of the binary complex. The anisotropy data was fitted to an exponential decay to calculate the off-rate of the binary SNARE complex.

The off rates were determined for the binary complexes of syntaxin homologs Syx1, Syx2 and Syx4 with SNAP25. The off-rates for the binary complexes of Syx2 and Syx4 with SNAP25 were found to be in the range of $10^{-5}s^{-1}$, while the off-rate for Syx1a was 10 times higher (Figure 4.15a). Hence, the binary complex of Syx4 and Syx2 homologs falls apart slower than that of Syx1a.

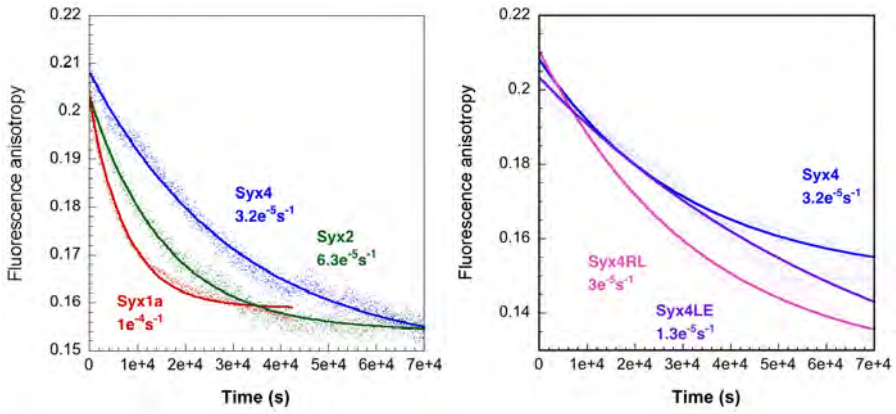

(a) Syx4 LE (b) Syx4 RL

Figure 4.15 – **Off rates for the binary complex of SNAP25 with different Syx constructs.** 100nM SNAP25^{130OG} was incubated with 200nM Syx4. To measure the off rate, excess (5μM) unlabeled SNAP25 was added to the premix and the decrease in fluorescence anisotropy was measured as the complex falls apart. (a) Off rates for the binary complexes of Syx2 and Syx4 were slower than that for Syx1a. (b) Off rates for the binary complexes of Syx4 variants were similar.

The off-rates were also determined for the binary complexes of aforementioned Syx4 mutants with SNAP25. The off-rates for binary complexes of Syx4 1-270, Syx4RL mutant and the Syx4LE mutant were found to be in the same range of $10^{-5}s^{-1}$. The off rates for binary complexes of Syx1a variants are also similar (Table 4.2).

Table 4.2 – **Kinetic rate constants for binary complex formation with SNAP25.**

Equation	k_{on} ($M^{-1}s^{-1}$)	k_{off} ($M^{-1}s^{-1}$)	K_d (nM)
Syx4+SNAP25	230	3.2e−5	140
Syx4LE+SNAP25	450	1.4e−5	31
Syx4RL+SNAP25	206	3.0e−5	145
Syx1a+SNAP25*	730	1e−4	137
Syx1aLE+SNAP25*	3320	1e−4	30
Syx1a(25-262)+SNAP25*	760	1e−4	131
Syx2+SNAP25	78	6.3e−5	800

k_{on} and k_{off} are determined experimentally, and K_d is calculated as k_{off}/k_{on}
*The values for binary complexes of Syx1a variants are from
Burkhardt et al. (2008), some of which were also confirmed in this study.

4.6.3 The Munc18c-Syx4 complex falls apart faster than the Munc18a-Syx1a complex

In order to monitor the binding of Munc18c with Syx4 by fluorescence anisotropy, I labeled Syx4 (1-270) at Cys1 with Oregon Green dye (Syx4 1-270^{1OG}), in close proximity to the N-terminal binding site. When Munc18c was added to labeled Syx4, an increase in anisotropy was observed, which indicates formation of the complex. This change can be attributed to the interaction of Munc18c with Syx4 N-peptide region. Addition of Munc18a to labeled Syx4 did not show any change in the fluorescence anisotropy, in accordance with earlier results where no interaction was observed between Munc18a and Syx4 (Section 4.4). Syx1a (1-262) labeled similarly at Cys1 (Syx1 1-262^{1OG}) was also used to study the binding of Munc18a and of Munc18c. In this case too, an increase in anisotropy was observed on addition of either Munc18a or Munc18c indicating complex formation. The high on-rates for all the Munc18-Syx complexes indicate that they interact instantaneously (Table 4.3). The on-rates are too fast to be measured by a hand-mixing approach, and were thus calculated indirectly.

The off-rate for the Syx4 1-270^{1OG}-Munc18c complex was determined by competitive dissociation as mentioned in the previous section for SNAP25^{130OG}-Syx complexes. In this case, Syx4 1-270^{1OG} was pre-incubated with Munc18c to form a complex. The falling apart of the complex on addition of excess unlabeled Syx4 was followed as a decrease in the fluorescence anisotropy. The data was fitted to an exponential decay to calculate the off-rate. Similar off-rate assays were performed for Syx1 1-262^{1OG} complexes with Munc18a and Munc18c.

The off-rate was calculated for the Munc18c-Syx4 complex, and compared with the off rates of Munc18a-Syx1a and Munc18c-Syx1a complexes. The off-rates for the Munc18c-Syx4 complex and the Munc18c-Syx1a complex were 10x faster than that for the Syx1a-Munc18a complex (Figure 4.16 and Table 4.3). I tried to fit the data to an exponential decay, but the dissociation was too fast for the Munc18c-Syx4 complex and for the Munc18c-Syx1 complex to get a good fit. Nonetheless, we can conclude that the complexes of Munc18c with Syx1 and Syx4 fall apart

faster than the Munc18a-Syx1 complex. Hence, in the presence of Munc18c, compared to Munc18a, it is easier for SNAP25 to bind to Syx and form the binary SNARE complex.

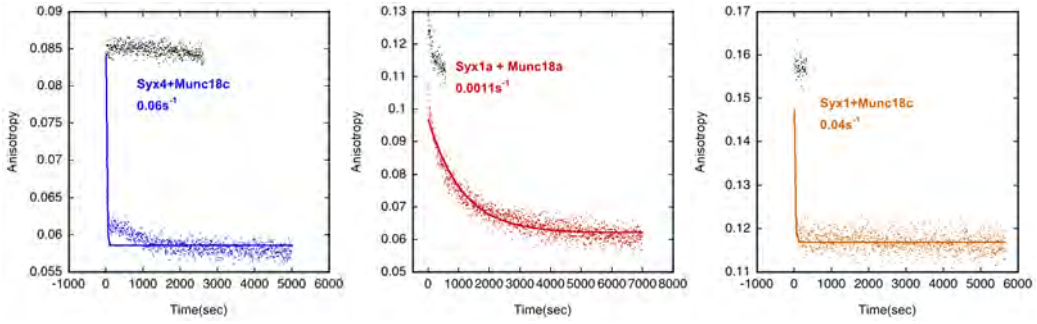

(a) Munc18c-Syx4 complex (b) Munc18a-Syx1a complex (c) Munc18c-Syx1a complex

Figure 4.16 – **The Munc18c-Syx4 complex falls apart faster than the Munc18a-Syx1a complex.** (a) The fluorescence anisotropy of 100nM Syx4 1-270^{1OG} increased rapidly when incubated with 200nM Munc18c, indicating complex formation. On addition of excess (5μM) of unlabeled Syx4 to the reaction mixture, there was a decrease in the anisotropy. (b) The fluorescence anisotropy of 100nM Syx1 1-262^{1OG} increased rapidly when incubated with 200nM Munc18a. On addition of excess (5μM) of unlabeled Syx1 to the reaction mixture, there was a decrease in the anisotropy. (c) The fluorescence anisotropy of 100nM Syx1 1-262^{1OG} increased rapidly when incubated with 200nM Munc18c, indicating complex formation. On addition of excess (5μM) of unlabeled Syx1 to the reaction mixture, there was a decrease in the anisotropy. The decay for complexes (a) and (c) was too fast to obtain a good fit. The off-rate was calculated as the rate of decrease in fluorescence anisotropy.

Table 4.3 – **Kinetic rate constants for Munc18-Syx complex formation.**

Equation	k_{on} ($M^{-1}s^{-1}$)	k_{off} ($M^{-1}s^{-1}$)	k_d (nM)
Syx4+Munc18c	6e+6	0.06	10
Syx1a+Munc18c	2e+6	0.04	20
Syx1a+Munc18a*	5e+6	0.0011	1.4

K_d and k_{off} are determined experimentally, and k_{on} is calculated as k_{off}/K_d.
*The values for binary complexes of Syx1a variants are from
Burkhardt et al. (2008), some of which were also confirmed in this study.

4.7 Interaction of Munc18c with the SNARE complex

In the previous sections, I reported that Syx4 binds tightly to Munc18c through both its N-peptide and the closed conformation. When bound, Syx4 is inhibited from participating in SNARE complex formation. However, it has been suggested that Munc18 proteins have another role in SNARE-mediated fusion besides binding to syntaxin. It is purported that Munc18 binds to the SNARE complex after it is formed, and mediates fusion. According to this hypothesis, Munc18 could bind to either the N-peptide of syntaxin or directly to the ternary

complex bundle, after or during SNARE complex formation. I explored the interaction of Munc18 with the Syx N-peptide and the SNARE core complex using fluorescence anisotropy assays.

4.7.1 Munc18 dissociates from the Syx N-peptide on SNARE complex formation

Munc18 dissociates from Syx N-peptide on binary SNARE complex formation

As seen earlier, the fluorescence anisotropy of Syx4 1-270^{1OG} changes upon binding of Munc18c. This rapid change is likely due to the interaction of Munc18c with the N-peptide of Syx4. In order to find out if Munc18c remains bound to the N-terminus of Syx4 or dissociates from it when the Syx4/SNAP25 complex forms, I added excess SNAP25 to the reaction.

On addition of excess SNAP25 to the Syx4 1-270^{1OG}-Munc18c complex, I observed a decrease in fluorescence anisotropy (Figure 4.17a). This indicates that Munc18c dissociates from Syx4 while the binary Syx4/SNAP25 complex forms. The decrease in anisotropy was gradual and reduced almost to the anisotropy of uncomplexed Syx4 only after overnight incubation. Note that, little or no change in the anisotropy was observed on interaction of Syx4 1-270^{1OG} with SNAP25. When the SNAP25 concentration was increased, the anisotropy dropped faster, but only to a certain extent. This suggests that, SNAP25 probably does not actively pull out Syx4 from the complex with Munc18, but rather binds to the free Syx4 available from the dissociation of the Munc18c/Syx4 complex. Although the Munc18c/Syx4 complex falls apart relatively quickly as shown earlier (Figure 4.16), the binding of SNAP25 to Syx4 is relatively slow. Both reactions seem to sufficiently describe the observed change on addition of SNAP25 to the Syx4/Munc18c complex. Similar results were obtained for the Syx1 1-262^{1OG}-Munc18a complex on addition of excess SNAP25, but the reduction in anisotropy is more gradual compared to that for the Munc18c-Syx4 complex (Figure 4.17b). It cannot be excluded, however, that SNAP25 binds to Syx4 while Syx4 is still in complex with Munc18c, and that Munc18c then gradually dissociates from the Munc18c/Syx4/SNAP25 complex.

Munc18 does not bind to the Syx N-peptide after ternary SNARE complex formation

The ternary SNARE complex was pre-formed by overnight incubation of Syx4 1-270^{1OG} with excess SNAP25 and Syb. The fluorescence anisotropy of Syx4 1-270^{1OG} was observed to change only slightly on formation of the SNARE complex. The interaction of Munc18c with the Syx4 N-peptide was studied after ternary SNARE complex formation was complete. When Syx4 1-270^{1OG} is in the free state, addition of Munc18c causes a jump in the fluorescence anisotropy, as seen earlier. However, when Munc18c was added to the SNARE complex containing Syx4 1-270^{1OG}, there was very little increase in the fluorescence anisotropy that soon changed back to the baseline value (Figure 4.18a). Hence, there is little or no interaction of Syx4 N-peptide with Munc18c, when it is a part of the SNARE complex.

Similar results were obtained when Munc18a was added to the SNARE complex containing

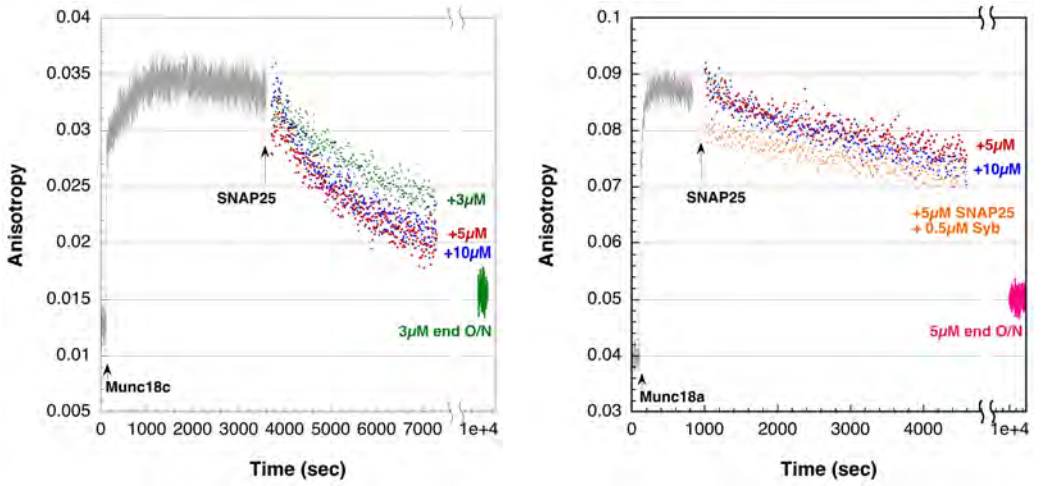

(a) Syx4 1-270^{1OG}/ Munc18c complex + excess SNAP25

(b) Syx1 1-262^{1OG}/ Munc18a complex + excess SNAP25

Figure 4.17 – **Addition of excess SNAP25 to Syx-Munc18 complex can overcome the inhibition by Munc18.**
(a) The anisotropy of 50nM Syx4 1-270^{1OG} rapidly increased on addition of 100nM Munc18c. There is a second phase of slower increase in anisotropy after the fast jump. Some of the Syx4 might be oligomerized, and this second phase probably reflects binding to this pool of oligomerized Syx4. When an excess of SNAP25 (3–10μM) was added to the Munc18c-Syx4 complex, the florescence anisotropy decreased, eventually reducing almost to the starting value. (b) The anisotropy of 50nM Syx1 1-262^{1OG} increased rapidly on addition of 100nM Munc18a. The increase in anisotropy was not biphasic as seen for Syx4 in (a). When an excess of SNAP25 (5–10μM) was added to this Munc18a-Syx1 complex, the florescence anisotropy reduced gradually and after overnight incubation reached almost the starting value. Inclusion of 500nM synaptobrevin in addition to SNAP25 did not cause further reduction in anisotropy.

Syx1 1-262^{1OG}. The rapid jump in the fluorescence anisotropy observed on the addition of Munc18a to free Syx1 1-262^{1OG} was highly reduced when Munc18a was added to SNARE complex containing Syx1 1-262^{1OG} (Figure 4.18b). Hence, it seems that there is very little interaction of Syx1 with Munc18a after ternary SNARE complex formation.

4.7.2 Munc18c might interact with the SNARE core complex

The SNARE core complex assembly was followed as an increase in fluorescence anisotropy on incubating Syx4H3 domain, SNAP25 and Syb 1-96^{61OG} as described in Section 4.3. When Munc18c was included in the reaction mixture, I saw an additional increase in the anisotropy, beyond that observed for the core complex formation. Note that the N-peptide and Habc domain of Syx4 were absent, and hence Munc18c could not have interacted with these sites. This observation was interesting and indicated something new. I probed this further by adding Munc18c after the SNARE core complex formation was almost complete (anisotropy reached

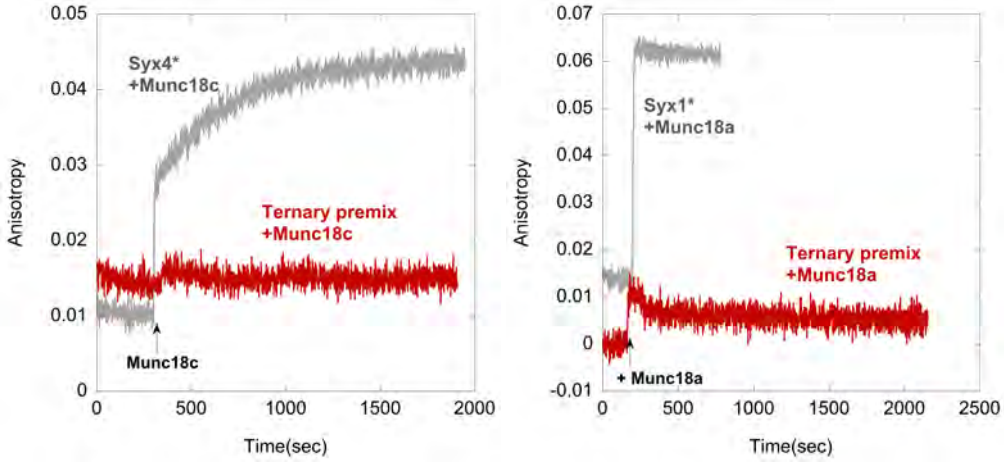

(a) (b)

Figure 4.18 – **Munc18 does not bind to Syx N-peptide region after SNARE complex formation.**
(a) A ternary SNARE complex (red trace) was formed by premixing 50nM Syx4 1-270^{1OG}, 500nM SNAP25 and 750nM Syb. The anisotropy of the SNARE complex was similar to free Syx4 1-270^{1OG}. Munc18c was added as shown by the arrow resulting in little change in the fluorescence anisotropy. When Munc18c was added to free Syx4 1-270^{1OG}, a rapid increase in anisotropy was observed (gray trace). (b) A ternary SNARE complex (red trace) was formed by premixing 50nM Syx1 1-262^{1OG}, 500nM SNAP25 and 750nM Syb. The anisotropy of the SNARE complex was similar to free Syx1 1-262^{1OG}. Munc18a was added as shown by the arrow resulting in little change in the fluorescence anisotropy. When Munc18c was added to free Syx1 1-262^{1OG}, a rapid increase in anisotropy was observed (gray trace).

a plateau). On addition of Munc18c, an immediate jump in the fluorescence anisotropy was observed (Figure 4.19a). This suggested that Munc18c might affect the mobility of the fluorescent dye attached at Cys61, possibly by binding to the surface of the SNARE core complex.

The assay was also carried out by using the entire cytoplasmic domain of Syx4. Due to the auto-inhibition by Syx4 Habc domain, the SNARE complex assembly was slower in this case, and was allowed to incubate for an hour prior to addition of Munc18c. A similar jump in the fluorescence anisotropy was also observed when Munc18c was added to the SNARE complex with Syx4wt (Figure 4.19b). Hence, despite the presence of the N-peptide and Habc domain of Syx4, Munc18c appears to interact with the SNARE core complex. In this case, it is possible that Munc18c interacts with both the N-terminal peptide and the core complex. No change in anisotropy was seen when Munc18c was added to free Syb 1-96^{61OG}, indicating that Munc18c interacts only with the assembled SNARE complex.

The Cys61 position is present in the central region of Syb. Other single cysteine variants of Syb were also used to follow the binding of Munc18c to the SNARE core complex – Syb labeled

at Cys28 with Oregon Green (Syb 1-96^{28OG}) and Syb labeled at Cys79 with Alexa488 (Syb 1-96^{79Ax}). However, the change in anisotropy was not observed when the dye was attached at N-terminal or C-terminal positions on the core complex (Figures 4.19c and 4.19d). Thus, Munc18c affected the mobility of the fluorescent dye when the ternary complex contained a label at position 61 on Syb, but not at positions Cys28 or Cys79.

The interaction of Munc18a with the SNARE core complex containing either Syb 1-96^{61OG} or Syb 1-96^{79Ax} was also analysed. Addition of Munc18a resulted in an increase in anisotropy for the SNARE core complex containing Syb 1-96^{61OG} but not Syb 1-96^{79Ax} (Figure 4.20). Note that a higher concentration of Munc18a was required to see this effect, compared to Munc18c. Additional experiments need to be carried out to further investigate and confirm the interaction of Munc18 with the SNARE core complex.

4.8 Similarities and differences in Munc18 homologs

The structures available for most of the secretory Munc18 proteins (Burkhardt et al., 2011; Hackmann et al., 2013; Hu et al., 2007; Misura et al., 2001) show high structural conservation. Like other SM proteins, they adopt an arch-shaped structure formed by three distinct domains. In the Munc18a/Syx1a structure, the cavity enclosed by the arch forms the binding site for the closed conformation of syntaxin. In this structure, the N-peptide of Syx1a extends outside this cavity and binds at another site on the surface of Munc18a. The structure of Munc18c is resolved in complex with only the N-peptide of Syx4, while Munc18b was cystallized without any partner. The vertebrate Munc18 homologs show high sequence conservation. Munc18b has ≈64% sequence identity with Munc18a, while Munc18c has ≈51% sequence identity with Munc18a (≈49% sequence identity between Munc18b and Munc18c).

Along with Dr. Nickias Kienle, I collected and annotated ≈250 sequences for Munc18 from several metazoan species. A phylogenetic tree (Appendix A.2) was calculated from the multiple sequence alignment of these sequences. The phylogenetic tree showed that most non-vertebrates have a single Munc18, while most vertebrates have three variants - Munc18a, Munc18b and Munc18c. This suggests that the repertoire of secretory Munc18s expanded during the evolution of vertebrates. Although the three Munc18 homologs are closely related, they form distinct clusters that are distinguished by their sequence patterns. The vertebrate sequences from each Munc18 cluster (≈ 60 sequences each) were used to create sequence weblogos (Appendix A.3) to reveal the similarities and differences between the subgroups. Overall, the Munc18 sequences are highly conserved and show many similarities. However, some differences between the sequences were observed between the sub-groups.

To identify residues that differ between the subtypes, but are conserved within individual subtypes, the 'Hannenhalli' method was used (Hannenhalli and Russell, 2000). This method uses the multiple sequence alignments and the phylogenetic tree as inputs. This analysis was carried out by Nicee Srivastava in my laboratory. The highest scoring sites are shown in Table A.2. Some of the sites identified in the Hannenhalli analysis are found on the outer

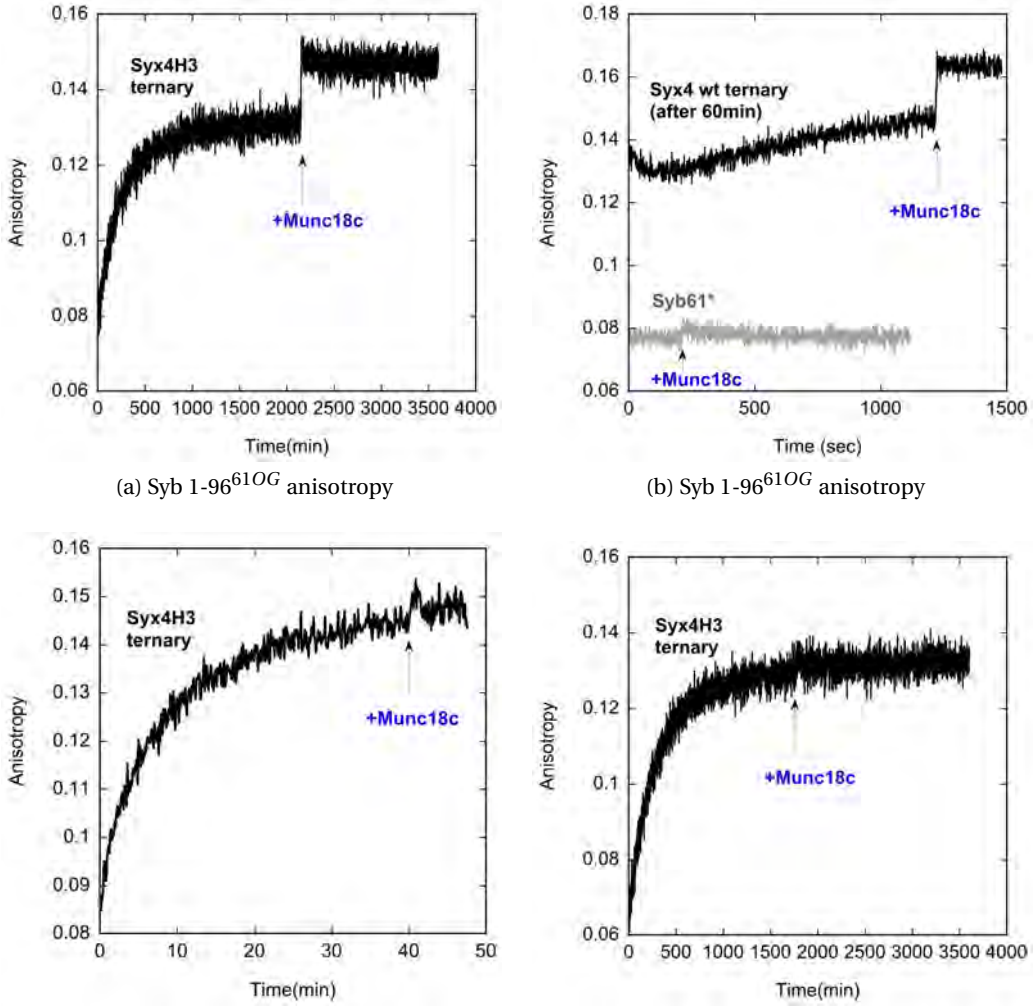

(a) Syb 1-96^{61OG} anisotropy

(b) Syb 1-96^{61OG} anisotropy

(c) Syb 1-96^{28OG} anisotropy

(d) Syb 1-96^{79Ax} anisotropy

Figure 4.19 – **Munc18c could interact with the SNARE core complex.**
(a) The SNARE core complex consisting of only the SNARE domains was pre-formed from 500nM Syx4H3, 1μM SNAP25 and 40nM Syb 1-96^{61OG}. After SNARE complex formation was complete, addition of 750nM Munc18c caused a jump in the fluorescence anisotropy. (b) 40nM Syb 1-96^{61OG}, 1μM SNAP25, 500nM Syx4 (1-270) was incubated for an hour before starting the assay to allow SNARE complex formation. Addition of 700nM Munc18c resulted in a jump in the anisotropy. (c & d) The SNARE core complex assembly similar to (a) was also carried out using (c) Syb 1-96^{28OG} or (d) Syb 1-96^{79Ax}. After SNARE complex formation was complete, addition of 750nM Munc18c did not cause a change in anisotropy.

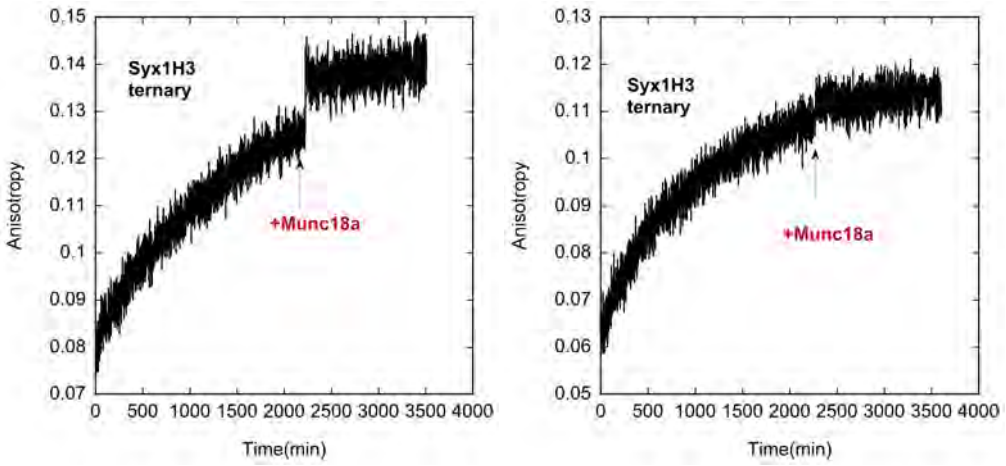

(a) Syb 1-96^{61OG} anisotropy

(b) Syb 1-96^{79Ax} anisotropy

Figure 4.20 – **Munc18a could interact with the SNARE core complex.**
(a) The SNARE core complex consisting of only the SNARE domains was pre-formed from 500nM Syx1H3, 750nM SNAP25 and 40nM Syb 1-96^{61OG}. After SNARE complex formation was complete, addition of 1.2μM Munc18a caused a jump in the fluorescence anisotropy. (b) The SNARE core complex consisting of only the SNARE domains was pre-formed from 500nM Syx1H3, 750nM SNAP25 and 40nM Syb 1-96^{79Ax}. After SNARE complex formation was complete, addition of 1.2μM Munc18a did not cause a change in anisotropy.

surface of Munc18. They might have significance in binding to other proteins such as Rab proteins.

The residues differences observed between the Munc18 homologs were mapped onto the available structures of mammalian Munc18a, Munc18b and Munc18c. The following sections describe the differences observed in the Munc18 structures, specifically at the syntaxin binding sites. These differences might explain their specificities for certain syntaxins. Standard one-letter and three-letter codes are used for the amino acids, and the chemical property of their side chains is color-coded in some cases (See Appendix A.1 for amino acid codes and types). The structures and domain architectures of Munc18a and Syx1a are illustrated in Figure 1.3 and are representative of the Munc18 and Syx homologs.

4.8.1 N-peptide binding site

The Syx N-peptide and the corresponding binding site in Munc18 proteins are highly conserved across species and subtypes (Figure 4.21). The central residues Asp3, Arg4, and Leu8 are highly conserved in almost all syntaxin N-peptides. The N-peptide binding site in Munc18 has an acidic groove, a basic region and a hydrophobic pocket that are generally highly conserved. However, there are some distinct differences between the syntaxin and Munc18 subgroups. Syx4, for example, has high conservation of N-peptide residues which might indicate that

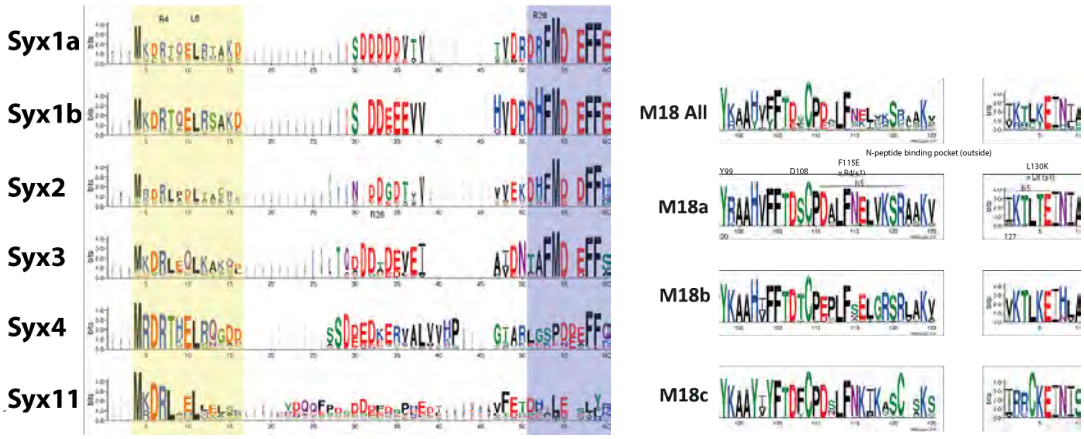

(a) (b)

Figure 4.21 – **The Syntaxin N-peptide and corresponding N-peptide binding site on Munc18.**
(a) The weblogos for the N-peptide of Syx 1a, 1b, 2, 3 and 4 from different vertebrate species are shown. The residues shaded in yellow form the N-peptide, while the residues shaded in blue are part of the Ha domain. Important residues are annotated in Syx1a with the sequence position. (b) The weblogos for domain 1 and domain 2 show the N-peptide binding site for, from top to bottom, all Munc18 sequences, Munc18a, Munc18b and Munc18c, from various vertebrate species. The important residues in Munc18a that interact with Syx1 are annotated. For the complete weblogos see Appendix A.3

it has evolved for specific binding. Indeed, Syx4 was found to bind only Munc18c, but not Munc18a and Munc18b (Tellam et al., 1997, Section 4.4). The Syx2 N-peptide, on the other hand, has weak conservation of the N-peptide in different species, which might be a possible explanation for why it can interact with all the Munc18 homologs. However, the N-peptide is not the only binding site, and the rest of the protein could also contribute to the specificity. Generally, the N-peptide affinities of vertebrate syntaxins are not as strong as the binding of Sed5p, Tlg2p or Syx16 to their respective SMs (Burkhardt et al., 2008; Demircioglu et al., 2014; Furgason et al., 2009; Hu et al., 2011)

The Syx N-peptide binding site on Munc18 is mainly present on the surface of domain 1. Interestingly, a coil in domain 2 of Munc18c that joins helix α8 and strand β9, just before the domain 3 insertion (Figure 1.3) is in close proximity to the N-peptide binding site. The Munc18c residue Glu223 on this coil forms a hydrogen bond with the main chain N of Asp3 in Syx4 N-peptide (Figure 4.22). The corresponding residues in Munc18a (Asp216) and Munc18b (Thr216) are further away from the N-peptide as they are located on a shorter coil. The neighbouring residue Lys224 in Munc18c forms a salt bridge with Glu189. This residue is a proline in Munc18a and Munc18b and hence the interaction is absent.

In Munc18c, Tyr218 (located on domain 1) is also present close to the N-peptide binding site. It forms a hydrogen bond with Asn137 that in turn, forms a hydrogen bond with residue Arg2 of the Syx4 N-peptide. Tyr218 is conserved in Munc18c for most species (His in others). However,

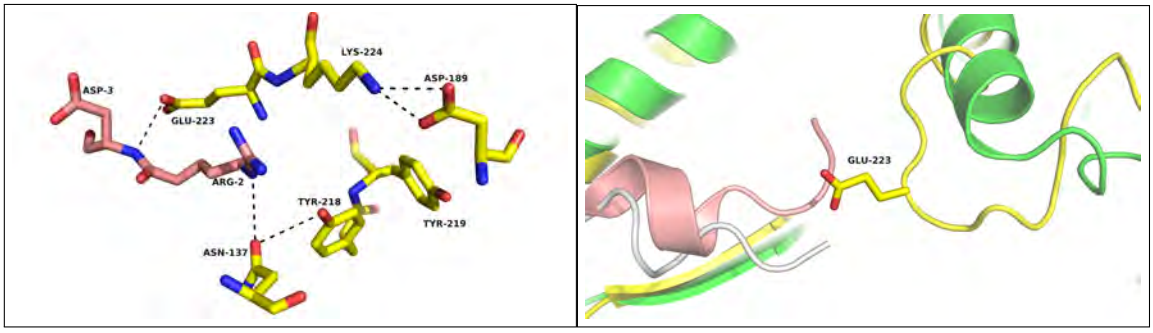

(a) (b)

Figure 4.22 – **Glu223 and Tyr218 in Munc18c interact with the N-peptide of Syx4.** (a) In Munc18c (yellow), Glu223 is present on a longer loop and forms a salt bridge with the main chain N of Asp3 in Syx4 (beige). (b) This loop is much shorter in Munc18a (green) and Munc18b (not shown). The Tyr218 of Mun18c is also close to the N-peptide binding site, and along with Asn137 interacts with Arg2 of Syx4 N-peptide. Lys224 forms a salt bridge with Asp189. These interactions are absent in Munc18a and Munc18b.

Munc18a and Munc18b have a conserved Ala211 corresponding to this position. Tyr218 is followed by another conserved Tyr at position 219 in Munc18c. This position corresponds to Tyr212 in Munc18a, that was suggested to be a part of the electrostatic network connecting the N-peptide binding site to the closed conformation. The phosphorylation of Tyr219 in Munc18c is thought to affect the Munc18c/Syx4 interaction (Jewell et al., 2008; Oh and Thurmond, 2006; Ramalingam et al., 2014). In Munc18b, a conserved Phe residue (Phe212) is present at this site.

Subtle differences are seen in the hydrophobic binding pocket of Leu8 of the Syx N-peptide, between the Munc18 homologs (Table 4.4). For example, the corresponding residues for Val119 in Munc18a are the charged Gly119 in Mucn18b and positively charged Lys123 in Munc18c. In Munc18c, the hydrophobic binding pocket also has a few other positively charged residues on the periphery. The helix containing Ala124 is a random coil in Munc18c and is not close to the hydrophobic pocket. These subtle differences could account for some of the observed binding preferences between Munc18/Syx pairs.

Table 4.4 – **Amino acid differences in the hydrophobic binding region for the syntaxin N-peptide in vertebrate Munc18s.** (See Appendix A.3).

M18a	V119	L118	F115	A124	L130	I127	V104
M18b	G119	L118	F115	A124	L130	V127	I104
M18c	K123	I122	F119		C133	I130	I108

4.8.2 Munc18a Gly26 hydrogen bond with Arg28 in Syx1a is not conserved

The N-peptide of Syx1a is connected to the Ha helix of the Habc domain by a loop that goes around Munc18a domain 1. This loop is not resolved in the Munc18a/Syx1a structure, and is

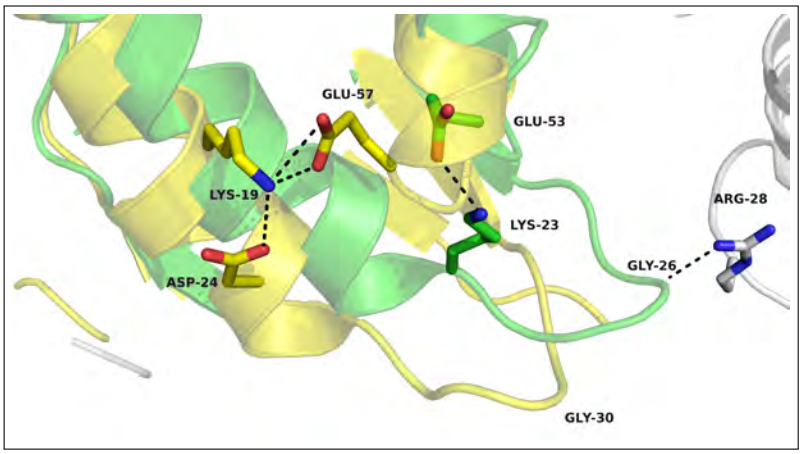

Figure 4.23 – **A hydrogen bond between Gly26 from Munc18a and Arg28 from Syx1a is not conserved in other Munc18/Syx pairs.**
(a) In Munc18c (yellow), Glu57 forms salt bridges with Lys19 and Asp24. This appears to pull the helix containing Glu57 more towards the helix containing Asp24. The corresponding residue in Munc18a (green), Glu53, forms a salt bridge with Lys23 at a lower position in the helix. (b) The displacement of the helix in Munc18c results in a difference in the position of the loop containing Gly30. The corresponding residue in Munc18a (green), Gly26 interacts with Arg28 from Syx1a Ha domain (white). This interaction is probably absent in Munc18c (yellow).

probably flexible. In Munc18a, Gly26 present on a loop between α1-β1 in domain 1, forms a hydrogen bond with Arg28 from Syx1a located at the beginning of the Ha domain. However, the corresponding position in Munc18b and Munc18c (Gly30) is shifted, because of a change in the loop positioning. This shift might abrogate interaction with their partner syntaxins at this position. The crystal structures of Munc18b and Munc18c are not resolved bound to the closed conformation of their cognate syntaxins, although the residues forming the closed conformation binding site are highly conserved in the Munc18 homologs. Thus, it is likely that Munc18b and Munc18c bind to their cognate syntaxins in a closed conformation. The biochemical data presented in the previous sections strongly support this idea. However, the lack of high resolution structures makes it difficult to determine the precise location of the residues involved in binding to Syx.

The shift in the Gly26 loop is probably due to structural differences in Munc18c and Munc18b compared to Munc18a in the helices flanking this loop (Figure 4.23). In Munc18c, the helix containing Glu57 is pulled away through salt bridges to Asp24 and Lys19 in the adjacent helix. Asp24 is conserved only in Munc18c (Arg in Munc18b and Lys in Munc18a). However, the site for Glu57 is conserved in the Munc18 homologs. In Munc18a, the loop containing the corresponding conserved Glu53 is not pulled away because it forms a salt bridge with Lys23 that is present at a lower position in the helix. These structural differences result in the different positioning of the loop containing Gly26(Munc18a)/Gly30(Munc18c). Hence this loop might not be involved in syntaxin binding in Munc18c. Interestingly, the residue Arg28 in Syx1a that

interacts with Munc18a Gly26, is not conserved in any other Syx subgroup, including Syx1b (Figure 4.21). This residue is also not conserved in the choanoflagellate Munc18.

4.8.3 β10 - β11 beta hairpin is shorter in Munc18c

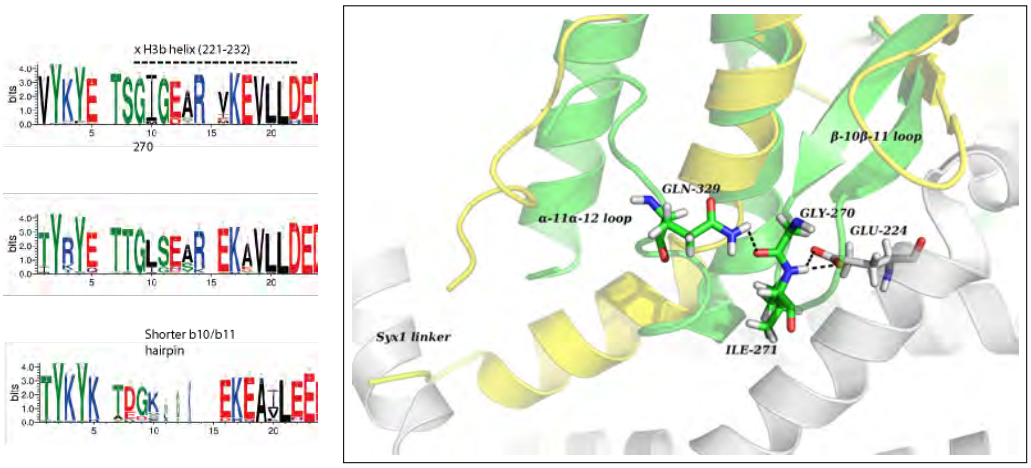

(a) (b)

Figure 4.24 – **The β10 - β11 hairpin loop is shorter in Munc18c.**
(a) Weblogo representation of Munc18a/b/c show that the β10 - β11 loop is conserved in Munc18a and Munc18b, but has a deletion in Munc18c. (b) The shorter Munc18c β10 - β11 loop is also seen in a superimposition of Munc18a (green) and Munc18c (yellow) structures. In Munc18a, Gln329 in the folded α11-α12 loop and Glu224 from Syx1a (white) interact with residues in the β10 - β11 loop. The α11-α12 loop needs to fold in all Munc18 homologs to accommodate the Syx linker. The absence of the β10 - β11 loop in Munc18c might indicate a lack of the interactions linking Syx binding to the folding of the α11-α12 loop, and hence slower binding.

The Munc18a-Syx1a crystal structure shows that Munc18a binds to the closed conformation of Syx1 consisting of the Habc and H3 domains. The linker helix connecting the Habc and H3 domains is suggested to be important because a conformation change in the linker results in opening of the Habc-H3 domain. The linker region lies outside the arch-shaped cavity, but causes a steric hindrance for the α11-α12 helix loop in Munc18a domain 3a. This loop is observed to bend at a conserved proline. The corresponding loops in Munc18b and Munc18c structures are extended, probably because these structures were resolved in the absence of the closed conformation of their cognate syntaxins. However, the conservation of the proline residue in the loop suggests that Munc18b and Munc18c must also bend similarly on Syx binding to avoid steric hindrance with the Syx linker region.

In the Munc18a-Syx1a structure, sandwiched between the Munc18a α11-α12 folded loop and the Syx1a H3c domain, is the β10 - β11 hairpin loop (Figure 4.24). There is a hydrogen bond connection linking Gln329 from the α11-α12 folded loop, Ile271 and Gly270 from the β10 -

β11 loop and Glu224 from Syx1a. This hydrogen bonding network might be responsible for the folding of the α11-α12 loop on binding of Syx1a.

The β10 - β11 hairpin loop is conserved in Munc18b, but in Munc18c there is a deletion resulting in a shorter loop (Figure 4.24). This might result in differences in the folding of Munc18c α11-α12 on binding of its partner Syx4. Notably, the structure of choanoflagellate Munc18 has a loop similar to that seen in Munc18a and Munc18b, indicating that the loop deletion could be a special characteristic of Munc18c.

4.8.4 The electrostatic network reported in Munc18a is not conserved

In the last couple of years, it has become evident that SM proteins can interact with their cognate syntaxins via two spatially separated binding sites – the first one on the surface that binds to the Syx N-peptide and the second one in the arch-shaped cavity interacting with rest of the syntaxin. Biochemical experiments suggest that binding at both sites occurs simultaneously. It is unclear, however, how the two sites communicate within the SM protein. A possible electrostatic connection between the two binding sites has been described for Munc18a by Colbert et al. (2013) (Figure 4.25).

Table 4.5 – **Amino acid differences in the electrostatic network connecting N-peptide binding site and SNARE binding site in Munc18b and Munc18c with respect to Munc18a.** The first and last residue in *italics* is from the partner syntaxin (Syx4 for Munc18c, Syx3 for Munc18b). The residue differences where amino acid type is changed are shown in gray. The differences shown are conserved for each homolog in different species (See Munc18a/b/c weblogos in Appendix A.3).

M18a	*K2*	E132	S109	D108	Y212	R171	S149	D148	R39	N261	*E234*
M18b	*K2*	E132	T109	D108	F212	V/A171	A149	D148	R39	Q261	*E234*
M18c	*R2*	E135	F113	D112	Y219	V/A176	V152	D/N151	K43	N266	*E242*

The residues that form this electrostatic network in Munc18a are highly conserved (Section A.3). However, I found that many of these residues were not conserved in Munc18b and Munc18c (Table 4.5). This could imply that this connection is either a special feature of Munc18a, or the network is somewhat different in the other Munc18 homologs. Thus, in Munc18b and Munc18c there might be other residues contributing to the putative electrostatic link. For example, in Munc18b, the electrostatic network might proceed through Gln174 that is conserved in most Munc18b species (Glu in Munc18a,c). As seen in Figure 4.26, Asp108 near the N-peptide binding site forms a hydrogen bond with Gln174. The electrostatic network can continue through Gln175, Leu147, Asp148 and eventually ending at Arg39. When Syx1a structure in complex with Munc18a is overlapped with the Munc18b structure, the Munc18b Arg39 lies close to the Syx1a Glu234, similar to the corresponding position in Munc18a.

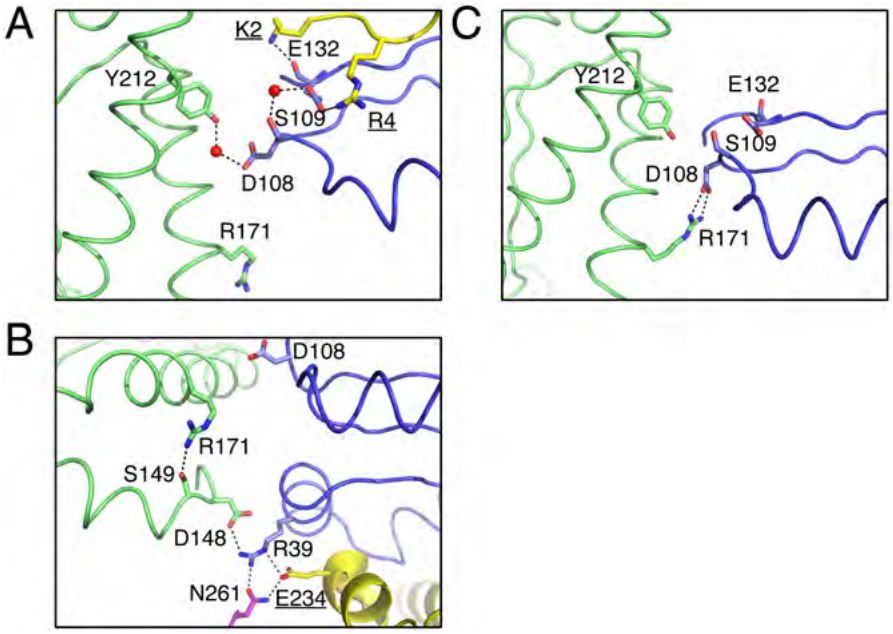

Figure 4.25 – **Possible electrostatic network connecting the Syx1a N-peptide and SNARE-binding regions of Munc18a.**
The structural details for different regions of the electrostatic network are shown. (A) Syx1a N-peptide (yellow), Munc18a domain 1 (blue) and domain 2 (green) residues, and water molecules (red spheres) are linked through several hydrogen bonds (dashed lines). Syx1a residues are underlined. Starting from the N-peptide site, there are hydrogen bonds between K2 and/or R4 in the Syx1a N-peptide and E132 in Munc18a. Two ordered water molecules coordinate E132, S109, and D108 in Munc18a domain 1. (B) The pathway continues through the interface of Munc18a domains 1 and 2, from D108 to N261 (purple) of the SNARE-binding region of Munc18a domain 3a, forming hydrogen bonds with E234 in the Syx1a SNARE domain (yellow). In the Munc18a–Syx1a wt structure, the electron density is weak for R171, possibly indicating that it interacts dynamically with other polar residues when the N-peptide is present. Finally, Munc18a residues R39 and N261 form hydrogen bonds with E234 of the Syx1a SNARE domain. (C) Munc18a residues D108 in domain 1 and R171 in domain 2 form a salt bridge in the absence of Syx1a N-peptide. These observations suggest that disruption of the Munc18a–Syx1a N-peptide interaction may lead to a rearrangement of the electrostatic network, with the D108–R171 salt bridge breaking a connection with the Syx1a SNARE domain. This was suggested to enable SNARE complex formation. Adapted from Colbert et al. (2013).

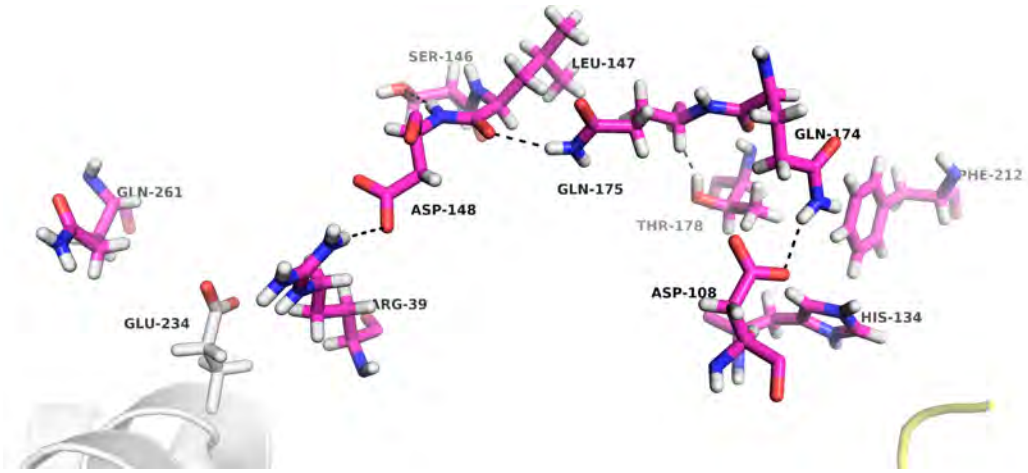

Figure 4.26 – **Suggested alternative electrostatic network in Munc18b connecting N-peptide binding site with the SNARE domain binding site.**
In Munc18b (pink), Asp108 forms a hydrogen bond with Gln174. These residues, along with F212 and H134, are close to the N-peptide of Syx4 (yellow). Gln175 forms a hydrogen bond with main chain of Leu147. Asp148 forms a salt bridge with Arg39, both of which are also a part of the Munc18a electrostatic network. Arg39 as well as Gln261 are close to the Glu234 from Syx1aH3 domain (white, overlayed from Munc18a/Syx1a structure), suggesting that they could form hydrogen bonds.

5 Discussion

Vesicle fusion is a vital process involved in transport and signaling in eukaryotic cells and is facilitated by a repertoire of proteins. The SNARE and Sec1/ Munc18 (SM) proteins are thought to be the central players of vesicle fusion (See reviews Jahn and Fasshauer (2012); Jahn and Scheller (2006); Rizo and Xu (2015); Südhof and Rothman (2009) and '2013 Nobel prize in Physiology or Medicine' lectures by Rothman et al. (2013)). The SNARE proteins located on vesicles and target membrane "zip up" to form a tight helical bundle that snaps the two membranes together, overcoming the energetic barrier to membrane fusion. SM proteins are thought to regulate vesicle fusion by binding to the Qa-SNARE, syntaxin (Syx).

The SM and SNARE families are highly conserved and consist of several members that function at different vesicle trafficking steps. The SM and Syx family members are thought to have evolved along with the repertoire of protein machinery functioning at various trafficking steps through duplication and diversification events from a primordial set of proteins. Also, the SM proteins functioning in different steps show high sequence and structural conservation. The SM proteins whose structures have been resolved show a similar arch-shaped structure and domain architecture (Baker et al., 2013; Bracher and Weissenhorn, 2002; Burkhardt et al., 2008, 2011; Hackmann et al., 2013; Hu et al., 2007; Misura et al., 2000). Hence, they probably have a common mechanism of action. Most SM proteins interact with their partner Syx at two binding sites. The closed conformation comprising of the Habc and SNARE (H3) domains of Syx binds inside the SM arch-shaped cavity and the N-terminal peptide of Syx binds at a site on the outer surface.

The SM protein family is sub-divided into four subgroups according to the trafficking steps at which they function – Sly1 (ER-Golgi), Vps45 (Golgi-endosome), Vps33 (Golgi-vacuole) and Munc18 (exocytosis). Most organisms have a single homolog of the Munc18 protein involved in secretion. However, vertebrates express three paralogs, Munc18a, Munc18b and Munc18c. The Qa-SNARE syntaxin involved in secretion has also undergone duplication in vertebrates and has six paralogs – syntaxins 1 (1a, 1b), 2, 3, 4, 11, 19, 21. The studies on Munc18 proteins in invertebrates (*C.elegans*, *D.melanogaster*) show that they are essential for neuro-transmission in these organisms (Brenner, 1974; Gengyo-Ando et al., 1993; Harrison et al., 1994). The

vertebrate homologs are also found to be essential for vesicle fusion in various tissues, and lead to a lethal phenotype (Kanda et al., 2005; Kim et al., 2012; Verhage et al., 2000). In this study, I focused on the SNARE and SM protein machinery involved in exocytosis, where fusion between vesicles and the plasma membrane leads to secretion or surface presentation of vesicle contents.

The structural information has been resolved for all the three Munc18 homologs in vertebrates. Munc18a, that participates in synaptic exocytosis, is the most well studied of these. Munc18a binds to its partner Syx1a at both the binding sites simultaneously as seen through the X-ray crystal structure and biochemical studies (Burkhardt et al., 2008; Misura et al., 2001). Munc18a is also known to inhibit SNARE complex formation *in vitro* by a mechanism that requires binding at both the Syx1a N-peptide and closed conformation. Such a binding mode and function was also found to be conserved in the secretory Munc18/Syx from choanoflagellate, a group of single-celled eukaryotes that are the closest living relatives of animals (Burkhardt, 2015; Burkhardt et al., 2011). The homolog of Munc18 in Drosphila, ROP, has reduced interaction with its Syx in the presence of a SNARE domain mutation, indicating that binding to the Syx SNARE domain contributes to the affinity (Wu et al., 1999, 2001). The structures for Munc18b and Munc18c are highly similar to the Munc18a structure. This suggests that the secretory SM proteins are likely to have a similar binding mode and function. However, several reports have been published that suggest that Munc18a, "which must be at the pinnacle of the evolutionary path, is something special" and its binding mode and function, that evolved specifically for neuronal exocytosis, does not exist for other SM proteins including Munc18c (Christie et al., 2012; Shin, 2013; Yu et al., 2013).

The primary aim of this study was to examine the binding mode and function of Munc18c, a vertebrate homolog of Munc18a, that is probably involved in exocytosis in almost all tissues. It is mainly studied in pancreatic insulin secretion and GLUT4 vesicle exocytosis in insulin-responsive cells. Munc18c is known to interact with its cognate partner Syx4, but the exact mode of binding and mechanism of action are not clear. Recent publications have concluded that Munc18c interacts with only the N-peptide of Syx4 and not the closed conformation (Christie et al., 2012; Hu et al., 2007; Yu et al., 2013). It was also reported that Munc18c accelerates the rate of liposome fusion. The findings published for the binding mode of Munc18c thus contradict the high sequence and structural similarity between the exocytotic Munc18 proteins in vertebrates. Moreover, the action of Munc18c on SNARE complex assembly has not been well characterized. The question thus was if Munc18c binding and function are indeed different from Munc18a, and what sequence and structural differences cause this divergence. Moreover, are these differences suitable for the tissue specific roles of Munc18a and Munc18c in synaptic exocytosis and glucose uptake respectively. Since Munc18c is a close homolog of Munc18a in vertebrates, it could also be used as another system to study the function of SM proteins in general and Munc18a in particular.

5.1 Munc18c is similar to Munc18a in its binding mode and function

5.1.1 Syx4 binds tightly to Munc18c through both its N-peptide and closed conformation

The interaction of Munc18c with Syx4 has been studied earlier by other groups, and the two proteins were found to interact at a relatively high affinity (Christie et al., 2012; Jewell et al., 2008). However, most studies on Munc18c were performed by expressing Munc18c using recombinant baculovirus infected insect cells. The expression of Munc18c in *E.coli* was reported but probably yielded low quantities of pure protein since only qualitative studies were published with this expression system. In order to study the Munc18c/Syx4 interaction using sensitive biophysical methods I required pure protein in micromolar quantities. I overcame this hurdle by optimizing the expression and purification protocol for Munc18c using the *E.coli* expression system. I was able to obtain pure Munc18c at 10-12μM concentration through my protocol. After I had established this protocol, J. Martin's group published a similar protocol for Munc18c expression in *E.coli* cultures (Rehman et al., 2013). However, they stored Munc18c at −80°C after purification. I used freshly purified Munc18c for experiments, since I observed reduced activity on freezing and thawing. I also tried to express and purify Munc18b, but was not able to obtain enough quantities for sensitive experiments, and hence this protein was not studied.

The first step in elucidating the binding mode of Munc18c was to determine the binding affinity between Munc18c and Syx4. I tested binding of the purified proteins through qualitative binding assays such as GST-pulldown and analytical gel filtration as well as the quantitative and sensitive method of ITC. I found that Munc18c and the cytoplasmic domain of Syx4, Syx4(1-270), bind to each other in a 1:1 stoichiometry and with a high affinity similar to Munc18a-Syx1a interaction (Figure 4.3). Note that I obtained better thermodynamic parameters for the Munc18c-Syx4 interaction ($K_d \approx$ 10nM and $\Delta H \approx -14.3$ kcal/mol) than published by Christie et al. (2012) ($K_d \approx$ 95nM and $\Delta H \approx -6$ kcal/mol). This could be because Christie et al. used a mutant, Syx4 C141S, while I used Syx4 wt. Binding kinetics carried out by surface plasmon resonance studies (Jewell et al., 2008) gave a dissociation constant of 32nM, which is similar to that observed by me.

Next, I determined which domains of Syx4 contribute to the binding affinity. The Munc18c structure has been solved in complex with the N-terminal 19 residues of Syx4 (N-peptide). Hence, it is evident that the N-peptide binds to Munc18c, but the binding of the rest of the Syx4 protein to Munc18c is not clear. It is possible that the equilibrium for Syx4 is shifted towards an open conformation, making it difficult for Munc18c to bind to the transient closed conformation. However, I found that Syx4 does exist in a closed conformation in solution, that is in fact tighter than the closed conformation of Syx1a (Figure 4.14a). Since Syx4 is able to form a closed conformation in solution, I tried to determine if Munc18c binds to this closed conformation.

Several lines of evidence from my results suggest that Munc18c indeed binds to the closed conformation of Syx4 (Figures 4.2b and 4.4). Using analytical gel filtration and ITC, I found that a deletion mutant of Syx4 lacking the N-peptide, Syx4 (25-270) binds to Munc18c, although with reduced affinity than Syx4 (1-270). Thus, Syx4 can bind to Munc18c even in the absence of its N-peptide, suggesting that the rest of the protein also contributes to the binding affinity. Moreover, a deletion mutant of Syx4, Syx4 (1-191), containing the N-peptide but lacking the SNARE domain had reduced affinity to Munc18c. This suggests that the SNARE domain contributes to the interaction between Syx4/Munc18c. Further I found that a combination of two fragments of Syx4, the SNARE domain (Syx4H3) and the rest of the protein (Syx4 1-191), bind to Munc18c with a higher affinity than as individual fragments. This strongly suggests that the two fragments interact to form a closed conformation that is then bound by Munc18c.

Christie et al. (2012) had reported through ITC experiments and GST-pulldown assays that Syx4 lacking the N-peptide does not bind to Munc18c. Their findings seem to be in contrast to my results. How can this be explained? Christie et al. obtained a binding affinity of 95nM for the interaction of Munc18c with Syx4 cytoplasmic domain, whereas I observed an affinity of ≈10nM. This suggests that the proteins used for my experiments were of better quality. Furthermore, I observed an affinity of ≈700nM for the interaction of Munc18c/Syx4 in absence of the N-peptide interaction. This affinity range is close to the detection limit of ITC. Considering that Christie et al. observed a 10x lower affinity for the Munc18c/Syx4 interaction, probably due to proteins of lower quality, they would not have been able to detect binding for Syx4 lacking the N-peptide. They also suggested from low-resolution solution structure models that Munc18c and Munc18a bind to the syntaxin in an extended (open) conformation, through only its N-peptide. However, the results for Munc18a/Syx1a interaction could not be confirmed by Colbert et al. (2013) using similar methods. Moreover, note that J. Martin's group reported a binding affinity of ≈1.5μM for Munc18c interaction with Syx4 N-peptide (Hu et al., 2011), which is ≈15x lower than the affinity of Munc18c/Syx4 reported by them. Therefore, binding of only the Syx4 N-peptide to Munc18c seems to be inadequate to explain the Munc18c/Syx4 interaction.

It should be noted that my results are consistent with qualitative pulldown assays that proposed binding of Munc18c to Syx4 with or without the N-peptide (Aran et al., 2009; Beest et al., 2005). D'Andrea-Merrins et al. (2007) also found that I241A mutation in the Syx4 H3 domain reduces binding of Munc18c to Syx4. In conclusion, it is highly probable that Munc18c interacts with both the N-peptide and closed conformation of Syx4 simultaneously.

5.1.2 Munc18c has an inhibitory effect on SNARE complex assembly

My findings suggest that Munc18c binds to Syx4 not only through its N-peptide, but also the closed conformation, similar to the binding mode of Munc18a. Hence, the next step was to determine if it had an effect on the speed of SNARE complex formation. An increase in the fluorescence anisotropy of labeled Synaptobrevin 2 (Syb) on addition of Syx4 and

SNAP25 indicated SNARE complex formation. SNAP23 is known to be the physiological SNARE partner of Syx4 in GLUT4 vesicle fusion, along with Syb. However, SNARE complex formation with SNAP23 was much slower and I used SNAP25 instead of SNAP23 for practical reasons (Appendix A.2). When Munc18c was included in the reaction mixture, there was a decrease in the rate at which SNARE complex formation took place (Figure 4.5). Hence, Munc18c seems to inhibit SNARE complex formation of Syx4 similar to Munc18a/Syx1.

The Munc18 homologs are able to interact with different syntaxin homologs, although they have certain preferences as well. Munc18a can interact with Syx 1, 2 and 3 but not Syx4, while Munc18c interacts with Syx 1, 2 and 4 but not Syx3. A detailed discussion of the interaction specificities of Munc18/Syx interaction can be found in Section 5.5. I checked the effect of Munc18c on the SNARE complex assembly of Syx1a and Syx2 in addition to Syx4, and the effect of Munc18a on Syx1 and Syx2. This also allowed a direct comparison of the inhibitory effects of Munc18a and Munc18c. Both Munc18a and Munc18c had an inhibitory effect on SNARE complex formation with Syx1a and Syx2 (Figure 4.10). However, the inhibitory effect of Munc18a was stronger than that of Munc18c for both the syntaxins.

The role of Munc18c in SNARE complex formation has been explored till now only through structural studies and *in vivo* experiments. The structural studies on binding to Syx4 focused on the interaction with the N-peptide but neglected the effect of Munc18c in the ability of Syx4 to engage in SNARE complex formation. The *in vivo* studies on Munc18c function carried out in cell lines show contradictory results (Jain et al., 2012; Khan et al., 2000; Macaulay et al., 2002; Oh et al., 2005; Tamori et al., 1998; Thurmond et al., 1998). The Munc18c knockout mice die in the uterus or soon after birth, and show a slightly stronger phenotype than the Munc18a knockouts. Hence, the effect of deleting Munc18c cannot be directly studied as done for Munc18a.

As mentioned above, the direct effect of Munc18c on the kinetics of SNARE complex assembly has not been studied rigorously. I have established an assay for the first time that can directly measure this effect. Earlier studies have used a liposome fusion assay to study the effect of Munc18c on vesicle fusion with contradictory findings. A recent study by Yu et al. (2013) showed that Munc18c accelerates fusion, but an earlier study by Brandie et al. (2008) had shown that Munc18c plays an inhibitory role. Note that liposome fusion assays can measure SNARE complex formation only indirectly by monitoring lipid mixing. Although this assay can measure the SNARE enzymatic activity, it can suffer from artifacts. For example, Munc18 alone can cause membrane bridging and hemi-fusion in the absence of SNAREs (Xu et al., 2011). Munc18a has been shown to accelerate liposome fusion (Shen et al., 2007), although this effect requires a longer preincubation period at 4°C. However, Schollmeier et al. (2011) later reported that Munc18a inhibited fusion when the Syx-liposomes were pre-incubated with Munc18a and SNAP25, but stimulated fusion when Syb-liposomes were also added before incubation.

5.1.3 Do the two binding sites on Munc18c work together for regulating SNARE assembly?

Earlier studies from my laboratory found that the SNARE complex assembly consisting of Syx1a, SNAP25 and synaptobrevin2 (Syb) is inhibited by Munc18a (Burkhardt et al., 2008). The interaction between Munc18a/Syx1a at both the binding sites is required for this inhibitory effect. In the absence of the Syx1a N-peptide, Munc18a could no longer block SNARE assembly. A similar effect was observed for Syx1LE mutant that has a double mutation (L165A/L166A) in the Syx1a linker region, destabilizing its closed conformation. Syx1LE has a high affinity for Munc18a, however, the SNARE complex assembly with the Syx1LE mutant had no effect (or only slightly affected) in the presence of Munc18a. Thus, the two binding sites in Munc18a collaborate to exert the block on the SNARE complex assembly, although it is not clear how the two sites communicate in the complex. Colbert et al. (2013) proposed a putative electrostatic network connecting the two binding sites in Munc18a, that is severed in the absence of N-peptide binding.

If the mechanism of Munc18c inhibition is similar to that of Munc18a, then lack of binding at one of two sites would alter Munc18c inhibition of SNARE assembly. First, I tested the action of Munc18c on SNARE complex assembly in the absence of the N-peptide interaction. A double mutant, Syx4 R4A L8A (Syx4RL) with mutations at two highly conserved residues of the N-peptide was used for this purpose. The enthalpy and binding affinity of Syx4RL to Munc18c is similar to that of Syx4 (25-270), which lacks the N-peptide region altogether. I used the Syx4RL mutant instead of the truncated variant for these experiments to avoid effects of oligomerization observed for the truncated variant. The SNARE complex assay with Syx4RL did not show any inhibition by Munc18c for formation of both binary and ternary SNARE complexes (Figure 4.6). Hence, these results are similar to those obtained for Syx1a/Munc18a in the absence of N-peptide interaction, indicating that the N-peptide of Syx4, similar to that of Syx1, is important for the inhibitory effect exerted by Munc18c.

Along with the Syx4 N-peptide, Munc18c was also found to interact with the rest of Syx4 probably through a closed conformation. I wanted to study the inhibitory effect of Munc18c on SNARE complex assembly in absence of binding at the closed conformation. It is not possible to study this effect directly, because the SNARE domain cannot be deleted or mutated without affecting the rate of SNARE complex formation. Hence, I used a Syx4LE mutant (L173A/E174A in the linker region between the Habc and H3 domain) analogous to Syx1LE mutant for this purpose. The LE mutation is thought to shift the equilibrium between the open and closed conformations of syntaxin towards a more open state.

The affinity of Syx4LE for Munc18c (≈160nM) was lower than that for Syx4 wt (10nM). The Syx4LE mutant was able to form a SNARE complex with SNAP25 and Syx4, and the kinetics was faster than observed for Syx4wt. The on-rates for binary SNARE complex determined for different Syx variants showed that Syx4LE binds to SNAP25 only two times faster than Syx4 wt, while this difference is ≈10 times faster between Syx1LE and Syx1a wt (Figure 4.14a). Thus, for

Syx4LE mutant the equilibrium is shifted towards a more closed conformation compared to the Syx1LE mutant. In the presence of Munc18c, there was a decrease in the rate of SNARE complex assembly of Syx4LE (Figure 4.7). The inhibition by Munc18c could result from a tighter closed conformation of Syx4LE. Thus, Munc18c can bind to this closed conformation resulting in inhibition of the SNARE complex. Since, Munc18c is able to interact with Syx1 and probably Syx1LE, I tested the effect of Munc18c on the SNARE complex assembly of Syx1LE. Munc18c was observed to slow down the rate of SNARE complex formation with Syx1a LE mutant as well (Figure 4.11). Munc18a used as a control did not result in any inhibition as expected. It is difficult to explain this effect, but it is probably due to minor differences in binding between Munc18a and Munc18c.

Overall, the results obtained in this study suggest that Munc18c has a similar binding mode and effect on SNARE complex assembly, as that observed for Munc18a. The exocytotic protein of choanoflagelate *M.brevicollis* was also seen to have a similar mode of binding and mechanism of action (Burkhardt, 2015; Burkhardt et al., 2011). Hence, binding at both the N-peptide as well as the closed conformation seems to be a conserved feature of secretory SM proteins in animals. Also, binding at both the sites is required for the high affinity interaction of Munc18/Syx and regulation of SNARE assembly.

5.2 The reaction rates for SNARE complex formation depend on the equilibria of individual reactions

5.2.1 Binary SNARE complex kinetics

The process of SNARE assembly is thought to start with the formation of a binary Syx-SNAP25 complex. In the closed conformation of Syx, the Habc domain binds to the H3 domain and presents a hurdle to SNARE complex formation. Deletion of the Habc domain can remove the 'auto-inhibition' by Syx and should result in faster complex formation. I studied the rate of binary complex formation for the entire cytoplasmic domain as well as the SNARE domain for the different Syx homologs, to observe if there are any differences in auto-inhibition.

The rates measured for binary complex formation for H3 domains of the different Syx were found to be in the same range ($\approx 5 \times 10^3$ $M^{-1}s^{-1}$). Therefore, the SNARE domains themselves have similar on-rates for SNAP25 binding in the absence of the Habc domain. Further, when the entire cytoplasmic domains were used, the rates were lower for all syntaxins in general. However, the rate for binding of Syx1 to SNAP25 (≈ 900 $M^{-1}s^{-1}$) was found to be higher than the rates for Syx4 ($\approx$220 $M^{-1}s^{-1}$) and Syx2 ($\approx$78 $M^{-1}s^{-1}$). The rate for Syx3-SNAP25 complex formation was too slow to be measured with this approach. Thus, Syx1 seems to have a more open conformation, while Syx3 seems to have a tight closed conformation. The more open conformation of Syx1 compared to the other vertebrate syntaxins involved in secretion could be an adaptation for (fast) neuronal secretion, although this is speculative. A very tight closed conformation has been observed for the secretory Syx, Sso1p and the Syx involved in ER-Golgi

transport, Sed5p, both from yeast (Demircioglu et al., 2014; Nicholson et al., 1998). The rate of binary complex formation for Sso1p is very slow (≈3 $M^{-1}s^{-1}$) indicating that it has a very tight closed conformation, comapared to the secretory syntaxins.

The rate at which the Syx-SNAP25 complex falls apart was also measured for the different Syx homologs. The off-rate was measured as the decrease in fluorescence anisotropy when excess unlabeled SNAP25 is added to a pre-formed complex of labeled SNAP25-Syx. The off-rate for Syx1a-SNAP25 complex (≈10^{-4} $M^{-1}s^{-1}$) was an order higher than those for the binary complexes with Syx4 and Syx2 (≈10^{-5} $M^{-1}s^{-1}$). The value for the dissociation constant calculated as k_{off}/k_{on} was found to be similar for Syx1a and Syx4 binary SNARE complexes (K_d ≈ 140nM). The Syx1a binary complex with SNAP25 is thought to form a 1:1 as well as a 2:1 complex. Wiederhold and Fasshauer (2009) had measured the binding of Syx1a H3 domain with SNAP25, and found that binding of the first Syx1aH3 molecule occurs with high affinity (K_d ≈ 5nM) whereas the second binds with moderate affinity (K_d ≈ 234nM) to form the 2:1 complex. It is possible that other vertebrate syntaxins might also form a 2:1 complex in addition to the 1:1 complex with SNAP25.

5.2.2 Kinetics of Munc18/Syx complexes

Munc18a and Munc18c seem to stabilize the closed conformation of Syx, since they prevent the bound syntaxin from forming SNARE complexes. Hence, the off-rate of the Munc18-Syx complex can give an idea about the availability of free Syx for SNARE complex formation. The dissociation of the Munc18-Syx complexes was studied by following the fluorescence anisotropy of Syx4 and Syx1 labeled near the N-peptide. The off-rates for the complex of Munc18c with Syx1a and Syx4 were found to be higher (≈ 10^{-2} s^{-1}) than that for Munc18a-Syx1a (≈ 10^{-3} s^{-1}). Thus, the complexes with Munc18c fall apart faster than those with Munc18a. The on-rate was calculated indirectly from the off rate and the K_d measured by ITC. The on-rate for all the Munc18-Syx complexes studied here was calculated to be in the order of 10^{+6} $M^{-1}s^{-1}$, indicating that the Munc18-Syx interaction is almost instantaneous. The on-rate and off-rate for the Munc18a-Syx1a complex were in the same range as determined by Burkhardt et al. (2008). The kinetics for Munc18c/Syx4 complex studied by surface plasmon resonance (Jewell et al., 2008) gave similar values for association rate (9.2 ×10^{+5} $M^{-1}s^{-1}$) and dissociation rate (2.9 ×10^{-2} s^{-1}).

5.2.3 The direction of reaction depends on individual equilibria

As seen in the previous sections, Syx can form complexes with both Munc18 and SNAP25. Thus, when all three proteins are present in solution, Munc18 and SNAP25 will compete for binding to Syx (Figure 5.1). The association and dissociation rates of Munc18/Syx and Syx/SNAP25 complexes slightly differ between the homologs. However, in general the association and dissociation rates for the Munc18/Syx complex (k_{on} ≈10^{+6} $M^{-1}s^{-1}$,k_{off} ≈10^{-3}–10^{-2} s^{-1}) are faster than those for the Syx/SNAP25 complex (k_{on} ≈10^{+2} $M^{-1}s^{-1}$,k_{off} ≈10^{-5}–10^{-4} s^{-1}).

In other words, the Munc18/Syx complex forms instantly but also falls apart faster compared to the slowly assembling SNAP25/Syx complex. Therefore, the Munc18/Syx complex predominates over a shorter time period, but eventually Syx pairs with SNAP25 on a longer time frame. Moreover, in the presence of Syb, the binary SNARE complex will form an almost irreversible ternary SNARE complex. The direction of the reaction is thus dictated by the equilibria of the individual reactions and the concentrations of the proteins.

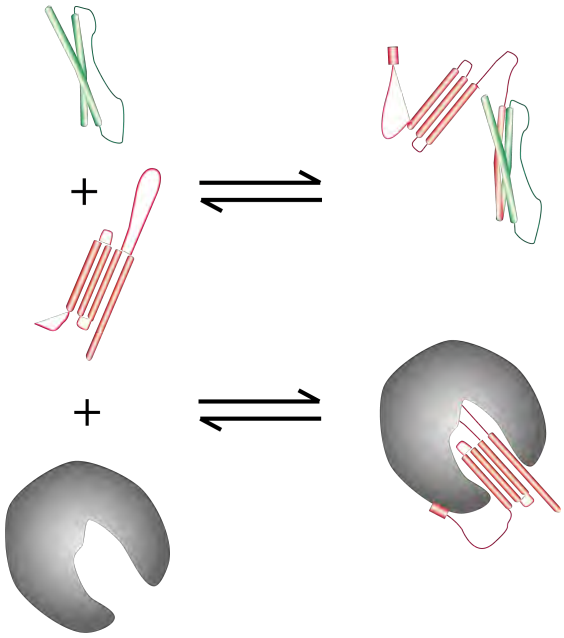

Figure 5.1 – **Reactions involved in binary SNARE complex formation.**
Syntaxin (red) binds to Munc18 (gray) in a closed conformation, and the SNARE domain of Syntaxin interacts with SNAP25 (green) in an open conformation. In solution, Syx can bind to either SNAP25 or Munc18 through reversible reactions. The direction of the reaction would depend on the kinetic rate constants of the individual reactions and the concentrations of the proteins.

In order to see how the reaction rates affect the progress of the reaction, I simulated the binary SNARE complex assembly with Syx4 and Syx1a by feeding the constants obtained by individual association and dissociation experiments into the Matlab Simbiology package. This also gives a way to compare the SNARE complex assembly involved in synaptic exocytosis and GLUT4 vesicle fusion. The binary assembly of Syx1a proceeds at a faster rate than the Syx4 binary assembly when identical concentrations of the components are used (Figure 5.2). This is consistent with the results of the fluorescence anisotropy experiments where I observed faster binary SNARE complex assembly with Syx1 compared to Syx4. Moreover, the binary assembly is inhibited to a higher extent by Munc18a than by Munc18c. The primary reason for this observation is the lower off-rate of the Munc18a/Syx1 complex compared to the Munc18c/Syx1 complex. I also observed a higher inhibitory effect of Munc18a compared to Munc18c on the SNARE complex formation rate with Syx1 and Syx2 through fluorescence anisotropy experiments.

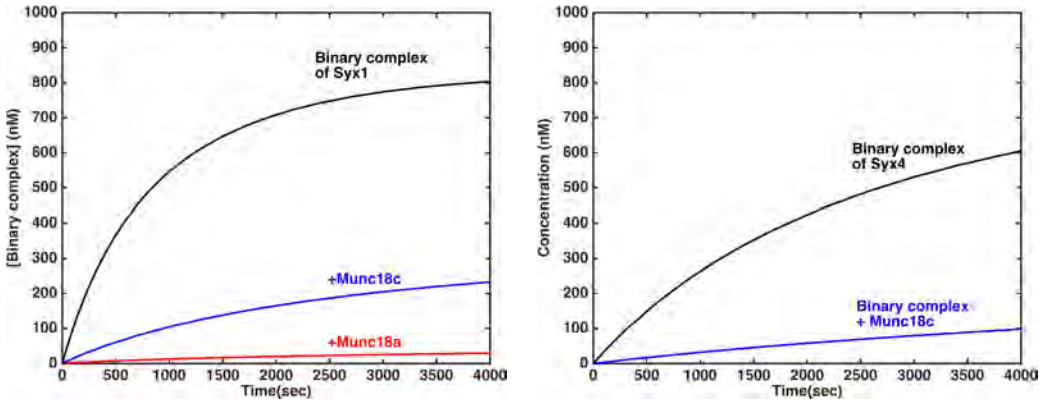

(a) (b)

Figure 5.2 – **Simulation of binary complex assembly of Syx1 and Syx4 and the effect of Munc18a and Munc18c.**
The x axis shows the time after start of reaction and the y axis shows the concentration of the binary complex in nM. The concentrations of the free proteins and Syx/Munc18 complex are not shown for ease of viewing. The simulations were performed using the Matlab Simbiology package. (a) The binary complex of 1μM Syx1a (black line) with 1.5μM SNAP25 was simulated by using the rate constants obtained through experiments. When 1μM Munc18a or Munc18c was included in the reaction mixture, an inhibition of the binary complex was observed. (b) The binary complex of 1μM Syx4 (black line) with 1.5μM SNAP25 was simulated by using the rate constants obtained through experiments. When 1μM Munc18c was included in the reaction mixture, an inhibition of the binary complex was observed.

As seen earlier, Munc18 binds to Syx instantaneously but also dissociates quickly. Addition of excess SNAP25 to a Munc18c-Syx4 complex would thus favor formation of the binary complex. I observed that the complexes of Munc18a and Munc18c with their respective Syxs fall apart in the presence of excess SNAP25 (Section 4.7.1). A simulation of the reaction shows the formation of the binary complex even in the presence of Munc18c (Figure 5.3). However, this observation does not support the idea that SNAP25 actively pulls out Syx from the M18/Syx complex. But how would an "increase in SNAP25 concentration" help to overcome Munc18 inhibition? Increasing the SNAP25 levels is an experimental trick. In the cell, the binding of Munc18 to Syx would need to be weakened by other mechanisms such as phosphorylation of Munc18. However, this process is not very fast and requires the presence of a kinase enzyme. Other factors such as Munc13 might be able to facilitate the binding of SNAP25 and exit of Munc18 from Syx (Ma et al., 2011; Rizo and Xu, 2015).

5.3 Interaction of Munc18 with the SNARE complex

The mechanism of action of Munc18 proteins is baffling because on one hand, they are essential for SNARE-mediated vesicle fusion, and on the other hand, the molecular level studies suggest that Munc18 prevents Syx from forming a SNARE complex. To reconcile the

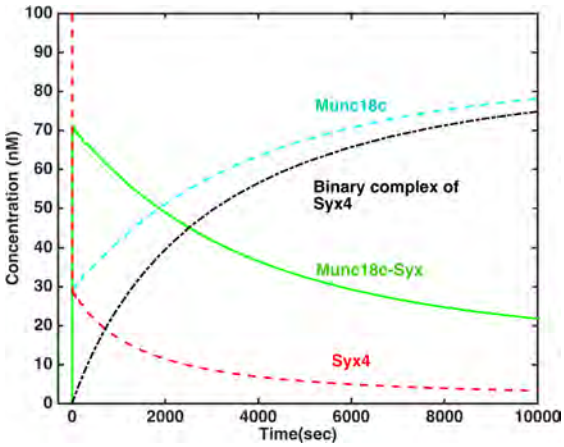

Figure 5.3 – **Excess SNAP25 shifts the equilibrium of the reaction (simulation).**
The simulation shows the change in concentrations of different species when excess (5μM) SNAP25 is added to 100nM Syx4 and 100nM Munc18c. The Munc18c/Syx4 complex (green) forms instantaneously, but dissociates with time. The binary complex of Syx4/SNAP25 (black) increases slowly with time. The concentrations of Munc18c (blue) and Syx4 (red) drop quickly due to Munc18/Syx complex formation. Munc18c concentration then rises with the dissociation of the Munc18c/Syx4 complex while Syx4 concentration (red) decreases gradually as it forms the SNARE complex.

essential role of Munc18 proteins, it has been suggested that Munc18 binds to the ternary SNARE complex during or before membrane fusion occurs (Toonen and Verhage, 2007). Whether Munc18 contributes to the assembly of the ternary complex, or directly to membrane fusion is left open. Under this hypothesis, Munc18 might remain bound to the N-peptide of Syx or to the SNARE helical bundle (core complex) or both. I investigated these putative interactions for Munc18a and Munc18c (referred to here as Munc18) with Syx1a and Syx4 (referred to here as Syx) respectively using fluorescence anisotropy.

5.3.1 Munc18 does not interact with Syx N-peptide after SNARE complex formation

As mentioned earlier, the binding affinity of Munc18c to Syx4 is reduced drastically in the absence of the SNARE domain (Figure 4.4a). A similar experiment also showed that the SNARE domain is needed for a tight interaction between Munc18a and Syx1a (Burkhardt et al., 2008). In the absence of the SNARE domain, the affinity of the rest of the Syx (N-peptide and Habc domain) for Munc18 is very low. Thus, I wanted to determine if this low affinity is adequate to keep Munc18 bound to the N-peptide of Syx as the SNARE complex formation takes place.

I observed through separate assays that Munc18a and Munc18c dissociate from the Syx N-peptide during or after SNARE complex formation. The fluorescence anisotropy change of Syx labeled near the N-peptide (Syx4 1-270^{1OG}) was used to follow the binding and dissociation of Munc18 with the Syx N-peptide. Excess SNAP25 was then added to study what happens when

Syx enters the binary SNARE complex in the presence of Munc18. The fluorescence anisotropy of Munc18/Syx complex decreased on adding excess SNAP25, indicating that Munc18 dissociates from the Syx N-peptide. In another assay, I observed no change in fluorescence anisotropy on addition of Munc18 to a pre-mixed ternary SNARE complex containing Syx4 1-270^{1OG}. Therefore, in the concentration range used for the experiments, Munc18 cannot bind to the N-peptide region of Syx. This does not rule out that Munc18 is able to bind to the N-peptide in the cellular environment, as it is possible that Munc18 is kept at the site of the assembling snare complex through other interactions, such as with the membrane. However, an interaction of Munc18 with the core complex cannot be ruled out.

5.3.2 Munc18 might bind to the SNARE core complex

I monitored the SNARE core complex formation as an increase in fluorescence anisotropy of Syb labeled at Cys61 on addition of SNAP25 and Syx H3 domain. After SNARE complex formation was complete, addition of Munc18 resulted in a sudden jump in the anisotropy. No change in anisotropy was observed when Munc18 was added to free Syb. Hence, the anisotropy change is possibly due to binding of Munc18 on the surface of the SNARE core complex. The position Cys61 is in the center of the SNARE complex (Figure 5.4). When Syb labeled at N- or C-terminal parts was used to form the core complex, the binding of Munc18 was not observed, possibly because the other labelled positions used are not influenced by binding of Munc18. Hence, Munc18 might bind to the core complex at the central position. When the core complex was formed using Syx4 cytoplasmic domain instead of only the SNARE domain, the binding of Munc18c to the core complex was still visible. In conclusion, Munc18 might interact on the surface of the SNARE core complex, although additional experiments are required to confirm that this is true. To have concrete evidence of Munc18 binding, other positions on the surface of the SNARE core complex need to be tested. As the fluorescence change was observed using labeled Syb, it is not clear whether Munc18 can bind to the surface of the Syx/SNAP25 binary complex as well.

Earlier studies have reported low affinity interactions of Munc18a or Munc18c with the SNARE complex using NMR, ITC and FRET assays (Brünger et al., 2015; Dulubova et al., 2007; Xu et al., 2010; Yu et al., 2013). However, these studies use full length Syx making it difficult to understand if binding takes place at the N-peptide or the SNARE core complex or both. One study reported binding of Munc18 to the C-terminal end of free Syb (residues 75-96) using NMR and ITC (Xu et al., 2010). When only the SNARE core complex is used, very weak or no interaction was observed with Munc18a (Burkhardt et al., 2008; Xu et al., 2010). The interaction of Munc18 with the SNARE complex is possibly a low affinity interaction that could not be identified by ITC. Binding to the SNARE core complex was also observed for the yeast secretory ortholog, Sec1p (Carr et al., 1999; Togneri et al., 2006). However, these studies are based on qualitative pulldown assays and no concrete evidence is available to support this binding mode.

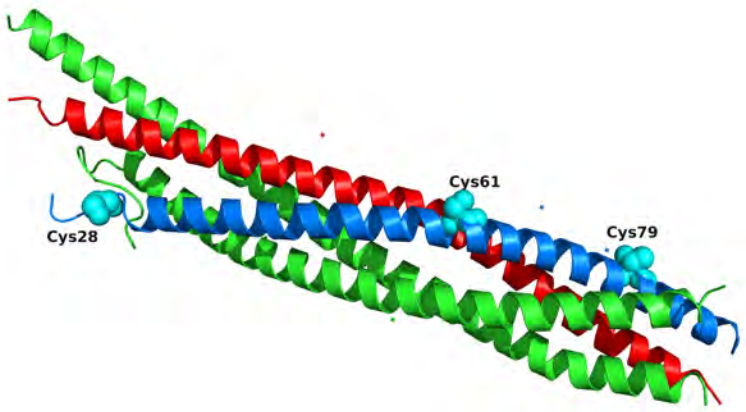

Figure 5.4 – **Labeled positions of Syb in the SNARE core complex.**
When the SNARE core complex is labeled at Cys61 of Syb, binding of Munc18 is observed as an increase in anisotropy of the dye. However, when the Cys79 or Cys28 position of Syb are labeled, Munc18 interaction with the core complex is not observed.

But what is the significance of Munc18 binding to assembled SNARE complexes that have completed fusion? It is possible that Munc18 might aid the formation of the SNARE complex. Any evidence of Munc18 binding to partially assembled SNAREs would thus be interesting. A recent study published the crystal structures of Vps33 with the SNARE domains of Qa (Vam3) and R-SNAREs (Nyv1) seperately. The Vam3 SNARE domain binds inside the arch-shaped cavity while Nyv1 interacts at a nearby position with its '0'-layer close to that of Vam3. Hence, Vps33 might serve as a template to aid the zipping up of the SNARE complex by interacting with SNAREs on opposing membranes. However, it remains to be seen if this mechanism is true for all SM proteins. Vps33 is different from the other SM sub-groups since it functions as a part of a HOPS tethering complex, that binds to trans-SNARE complexes (Collins and Wickner, 2007). Note also that Vam3 is different from other syntaxins as it has no canonical N-peptide that can bind to Vps33, and it has been reported to reside in an open conformation (Dulubova et al., 2001). It is therefore possible that the interaction of the SM protein Vps33 is somewhat different compared to other SM proteins, since it does not have to open its cognate syntaxin first. It is possible that the Vps33 structure with Vam3 and Nyv1 represents a later stage in the SNARE assembly process, that has not yet been identified for Munc18s.

5.4 Implications of Munc18c function in insulin response

Munc18c has been studied in insulin mediated exocytosis of GLUT4 storage vesicles (GSVs) in skeletal muscles and fat cells. Munc18c and Syx4 are implicated to be responsible for development of insulin resistance and diabetes. Despite several *in vivo* studies on Munc18c/Syx4 interaction and its role in vesicle fusion, the mechanism of action of Munc18c remains elusive. Munc18c knockout mice do not survive, and hence it is difficult to study the role of Munc18c as that elucidated for Munc18a. Munc18a is the single most well-studied SM protein in exo-

cytosis because the synaptic exocytosis system is amenable to sensitive measurements with electrophysiology and other methods. To study the exocytosis of GSVs in adipocytes, on the other hand, is difficult because exocytosis is not localized to a particular site on the plasma membrane. *In vitro* experiments can thus provide another means to study the function of Munc18c in SNARE complex assembly.

I found that Munc18c binds to Syx4 with a high affinity at two binding sites and inhibits SNARE complex formation *in vitro*. However, it is not clear how SNARE complex formation can take place in the presence of Munc18c. Increasing the levels of SNAP25 might be one mechanism to achieve this. Another mechanism that has been explored is the phosphorylation of Munc18c. The insulin signaling cascade proceeds through a number of phosphorylation and de-phosphorylation cycles of individual components. However it is not clear how these signaling pathways transmit the signal for SNARE-mediated GSV fusion. A plausible mechanism is the phosphorylation of Munc18c that has been observed under basal conditions, and to higher levels under stimulus, in MIN6β cells and in 3T3L1 adipocytes (Oh and Thurmond, 2006; Schmelzle, 2006; Umahara et al., 2007). Phosphorylation is studied *in vitro* and in cell lines by using a kinase to phosphorylate the protein, or using mutations that mimic phosphorylation, 'phosphomimetic mutants' (Y→E). Several publications cite that phosphorylation of Munc18c at Tyr521 or at Tyr219 (or use of phospho-mimetic mutants) can reduce Munc18 binding to Syx and increase surface GLUT4 levels and glucose uptake (Aran et al., 2011; Bakke et al., 2013; Jewell et al., 2011; Umahara et al., 2007). The Tyr219 residue is present within 8Å of the Syx4 N-peptide binding site while Tyr521 is present in close proximity of Tyr219 but in a disordered region in the Munc18c structure (Jewell et al., 2011). Disordered regions are thought to be critical sites for important post-translational modifications and conformational changes. The Insulin receptor (IR) kinase is thought to be directly responsible for phosphorylating Munc18c (Aran et al., 2011; Jewell et al., 2011), thus placing Munc18c phosphorylation as one of the earliest events in insulin signaling.

I used a Munc18c phospho-mimetic mutant Y521E that mimicks phosphorylation at this site. The interaction of Munc18c Y521E with Syx4 and Syx2 was measured by ITC. A reduction in enthalpy and binding affinity was observed for both Syx4 and Syx2 compared to Munc18c wt, although binding was still observed. It is possible that actual phosphorylation causes a further reduction in affinity that is not captured through this mutation. Moreover, another phosphorylation site Y219 has also been reported to cause reduction in Syx4 binding. Phosphorylation at both these sites might lead to further decrease in enthalpy and binding affinity. These sites were not found to be conserved in Munc18a and Munc18b (Jewell et al., 2011), suggesting that the mechanism might be Munc18c-specific.

I also observed that Munc18c might bind to the SNARE complex. Hence, Munc18c might be responsible for an inhibitory function earlier in SNARE complex formation, and an essential function during vesicle fusion. *In vivo* functional studies show contrary observations for the role of Munc18c. Overexpression of Munc18c *in vivo* was shown to reduce GLUT4 externalization in most studies indicating an inhibitory effect (Khan et al., 2000; Macaulay

et al., 2002; Tamori et al., 1998; Thurmond et al., 1998). However, recent studies with RNAi and heterozygous mice indicate that Munc18c is essential for glucose uptake (Jain et al., 2012; Jewell et al., 2011; Oh et al., 2005). A recent review proposes that it is the balance between Munc18c and Syx4 that is critical for SNARE mediated exocytosis, since high or low levels of Munc18c than optimum result in insulin resistance (Ramalingam et al., 2014).

5.5 Munc18 and Syntaxin subgroups - interactions and specificities

5.5.1 Munc18/Syx specificities

Most organisms possess a single copy of syntaxin and Munc18 that function in exocytosis, but duplication events in vertebrates has lead to several homologs. There are three Munc18 homologs in vertebrates - Munc18 a, b and c, while six isoforms of Syx are found - Syx 1, 2, 3, 4, 11, 19 and 21. The most studied syntaxins are Syx 1, 2, 3, 4 and 11. Syx11 is somewhat different as it has a post-translational modification for membrane attachment instead of a trans-membrane domain. Whether it is able to function as a fusogenic SNARE protein had not been firmly established at the outset of my work. Therefore, I have only used the canonical Syx 1, 2, 3 and 4 for my biochemical investigations.

Previous studies had already observed through qualitative pull-down assays that different Munc18 homologs are specific for certain syntaxin homologs (Hackmann et al., 2013; Hata and Südhof, 1995; Tamori et al., 1998; Tellam et al., 1997). I tested the interaction specificities between Munc18a and Munc18c and syntaxins 1, 2, 3 and 4 through quantitative assays. I found that Munc18a binds to Syx1, Syx2 and to a lesser extent to Syx3 but not to Syx4. Munc18c was found to interact with Syx2, 4 and 1 but not with Syx3. The Munc18c-Syx1 interaction had not been documented previously. As mentioned before, I was not able to purify Munc18b and hence it was not included. Munc18b has been shown to have a similar interaction pattern as Munc18a, binding to Syx1, 2, 3 and 11.

The different Munc18 and Syx homologs differ in their tissue localization (Table 1.2), but certain homologs are known to function together. Munc18a/Syx1 regulate synaptic exocytosis in neurons and first phase of insulin release in pancreas (Hata et al., 1993; Jewell et al., 2010; Tomas et al., 2008), Munc18b is found to associate with Syx3 and Syx11 in secretory tissues and immune cells (Al Hawas et al., 2012; Côte et al., 2009; Kim et al., 2012; Riento, 2000), while Munc18c/Syx4 is thought to be involved in insulin-stimulated GLUT4 exocytosis and insulin secretion (Jewell et al., 2010; Oh and Thurmond, 2009; Thurmond and Pessin, 2000). However, some tissues have two or more homologs of Munc18 and syntaxin that are able to interact with each other. How is the cell able to determine which Munc18/Syx pair is supposed to function for a particular exocytosis event?

The cross-reactivity between syntaxin and Munc18 proteins can be explained to some extent by the localized expression of these proteins. Munc18c is a ubiquitous protein found in many cell types, but Munc18a and Munc18b are expressed only in certain cell types. For

example, Munc18b and Munc18c are co-localized in epithelial cells, but function at different locations. Munc18b is involved in apical membrane secretion, while Munc18c functions at the basolateral membrane (Rodriguez-Boulan et al., 2005). Since Munc18b has not been found to interact with Syx4 and Munc18c does not interact with Syx3, their specific functions in these cells can probably be segregated. Another possibility is that the Syx/Munc18 pairs could be targeted specifically to their respective membranes in the polar epithelial cells. Such polarity could explain why Syx1 functions along with Munc18a at the synaptic bouton, while Syx3 is found to be active in long-term potentiation at the post-synaptic membrane (Jurado et al., 2013).

The most complex scenario seems to be in the case of pancreatic β-cells, which express all three homologs of Munc18, and many of the Syx homologs. In this case, Syx1 deficient cells show a marked reduction in first phase of insulin release that occurs from pre-docked granules, but not the second phase where granules need to be translocated from intracellular pools (Ohara-Imaizumi et al., 2007). Syx4 heterozygous mice have defects in both the first and second phase (Jewell et al., 2010), but Munc18c depletion affects only the second sustained phase of insulin release (Oh and Thurmond, 2009). Note that I observed an interaction between Munc18c and Syx1, which might be functional in β-cells. However, it is also possible that the Munc18/Syx pairs function at different steps of insulin release within the islet cells.

5.5.2 Munc18 specificities could be explained by minor differences between the homologs

The sequences for secretory Munc18 and syntaxin homologs for various species of vertebrates are highly conserved. However, the different homologs are divided into various subgroups in a phylogenetic analysis by subtle differences that are conserved with each sub-group (Appendix A.2). A study of the sequence divergence revealed some interesting differences between the subtypes which might shed more light on the Munc18/Syx specificities. However, due to the lack of structural data for all Syx homologs, especially in complex with their partner Munc18s, it is difficult to identify if these differences indeed lead to steric clashes or structural aberrations that do not allow binding of certain Munc18/Syx pairs. Thus, the following findings should be considered with discretion.

The Syx N-terminal peptide is highly conserved, but the weblogo representation shows differences between the Syx paralogs. For example, the Syx4 N-peptide has high conservation, while that of Syx2 is more variable. This could correlate with the high specificity of Syx4 that interacts with only Munc18c, and the low specificity of Syx2 that seems to interacts with all the Munc18 homologs. Hence, it is possible that the N-terminal peptide might contribute to specificity. Beest et al. (2005) constructed chimeras of Syx3 and Syx4 with their N-peptides exchanged, and tested interaction with Munc18b and Munc18c through qualitative pulldowns. They found that a chimera with Syx4 N-peptide grafted on Syx3 could bind to both Munc18b and Munc18c. However, the chimera with Syx3 N-peptide attached to the rest of Syx4, could bind to Munc18c

but not Munc18b. These findings need to be confirmed through quantitative experiments, but they suggest that both the binding sites probably contribute to the interaction specificity. Also, they show that the Syx sequence, especially at the N-terminal end might be important for targeting with Munc18 or other factors in kidney cells. Hu et al. (2011) tested the binding of the N-peptides of Syx1 and Syx4 with Munc18a and Munc18c using ITC. They found that Syx4 N-peptide interacts with non-cognate Munc18a but with 20x lower affinity than with its partner Munc18c. The Syx1 N-peptide bound weakly with both Munc18a and Munc18c, although affinity to Munc18c was slightly higher. Thus, it is possible that the Syx4 N-peptide has evolved for (or maintained) high affinity binding with Munc18c.

The Syx N-peptide binding site on the surface of domain 1 of Munc18 also has some differences between the homologs. The hydrophobic patch within the N-peptide binding site is smaller for Munc18c, compared to Munc18a and Munc18b (Table 4.4, Hackmann et al. (2013)). Interestingly, a coil in domain 2 of Munc18c that joins α8-helix and β9-sheet, comes close to the N-peptide binding site. In Munc18a and Munc18b, this coil is much shorter, and hence is not close to the N-peptide binding site. The Munc18c residue Glu223 on this coil forms a hydrogen bond with the main chain N-H of Asp3 of Syx4 N-peptide (Figure 4.22). Could this interaction be responsible for the specificity of Munc18c for the Syx4 N-peptide?

The N-peptide of Syx1a is followed by a loop that goes around Munc18a domain 1 and connects with the Ha helix of the Habc domain that binds inside the Munc18a arch. In Munc18a, Gly26 present on a loop between α1-β1 in domain 1, forms a hydrogen bond with Arg28 from Syx1a located at the beginning of the Ha domain. However, the corresponding position in Munc18b and Munc18c (Gly30) is shifted because of a change in the loop positioning which might abrogate interaction with their partner syntaxins. The Syx1a residue Arg28 is not conserved in any other Syx homologs, but the Gly26 residue is conserved in other Munc18s. This interaction is also not conserved in Munc18/Syx from Monosiga. However, note that Munc18a structure is in complex with the closed conformation, while the Munc18c structure is in association with only the N-peptide and Munc18b structure is monomeric. Is it possible that binding at the N-peptide causes a change in conformation in this part of the structure? Accordingly, the conformational change between the homologs might indicate a change that occurs on Syx binding. This might be important for our understanding of the 'opening' of the bound Syx. Moreover, binding of Munc18b and Munc18c to the closed conformation of Syx might be weaker than in Munc18a due to absence of this interaction.

The linker helix in Syx connecting the Habc and H3 domains is suggested to be important because a conformational change in the linker results in opening up of the Syx closed conformation. The Syx1 linker region lies outside the Munc18a arch-shaped cavity, but causes a steric hindrance for the α11-α12 helix loop in Munc18a domain 3a. Hence, the α11-α12 helix loop is 'closed' in the structure of Munc18a-Syx1 complex. Interestingly, Colbert et al. (2013) showed that this hairpin loop is unstructured in the complex of Munc18a with Syx1 lacking the N-peptide. Hence, removal of the N-peptide interaction could lead to opening up of the α11-α12 loop and dissociation of Syx. This hairpin loop is extended in Munc18b and Munc18c struc-

tures, but would probably need to fold when binding to the Syx closed conformation. In the Munc18a-Syx1a structure, a hydrogen bond network connects the Munc18a α11-α12 folded loop with the Munc18a β10 - β11 hairpin loop and the Syx1a H3 domain (Figure 4.24). The β10 - β11 hairpin loop has a deletion in Munc18c, that is not present in Munc18a, Munc18b or even the Munc18 from Monosiga. The absence of this loop in Munc18c might disrupt the hydrogen bonding network connecting the folded α11-α12 loop with binding of Syx H3 domain.

5.6 Bringing it all together

The primary aim of my study was to investigate if Munc18c differs from most other studied Munc18 proteins in its binding mode to Syx and action on SNARE complex assembly. I found that Munc18c indeed binds to both the N-terminal peptide and the closed conformation of Syx and inhibits SNARE complex formation. Hence, my results along with the studies on vertebrate Munc18a (Burkhardt et al., 2008) and Munc18b (Hackmann et al., 2013) as well as Munc18 homologs from other metazoans (Johnson et al., 2009; Wu et al., 1999, 2001) and choanoflagellates (Burkhardt et al., 2011), suggest that all animal Munc18 proteins bind to Syx with a high-affinity interaction at two sites.

An important question in the field is how can Syx escape the tight grip of Munc18 to participate in the SNARE complex assembly? The biochemical studies I presented here provide some mechanisms through which Munc18/Syx complex could dissociate (Figure 5.5, Scheme 1). My studies suggest that phosphorylation of Munc18c at Tyr521 (and possibly also Tyr 219) could reduce its interaction with Syx. Similarly, it has been shown that the phosphorylation of Munc18a at Ser 306 and Ser 313 by protein kinase C (PKC) prevents its interaction with Syx (Fujita et al., 1996; Genç et al., 2014). I also found that the presence of excess SNAP25 can alter the reaction equilibria favoring formation of the SNARE complex, thus overcoming the inhibition by Munc18. Similar effects *in vivo* or additional factors such as Munc13 (Ma et al., 2011) could help to open up Syx to allow SNARE complex formation. My results suggest that during SNARE complex formation, Munc18 does not remain attached to the N-peptide of Syx. However, it is possible that Munc18 might associate with the SNARE core complex.

But how could the high-affinity binding of Munc18 to Syx and its inhibitory role *in vitro* correlate with its essential function in exocytosis? One possibility is that Munc18 locks Syx away from the formation of off-pathway SNARE complexes such as the 2:1 Syx/SNAP25 complex, thus providing a regulatory mechanism for correct SNARE complex formation (Rizo and Xu, 2015). Another possibility is that Munc18 could somehow aid in the formation of the SNARE complex, besides its inhibitory role. A recent paper by Baker et al. (2015) shows that the SM protein Vps33 binds to the SNARE domains of its partner Qa- (Vam3) and R- (Nyv1) SNAREs. Since the binding sites are close to each other, Vps33 is thought to provide a framework for the assembly of the SNARE complex. However, note that Vam3 is different from other syntaxins, because it lacks a canonical N-peptide and is known to reside in an open conformation (Dulubova et al., 2001).

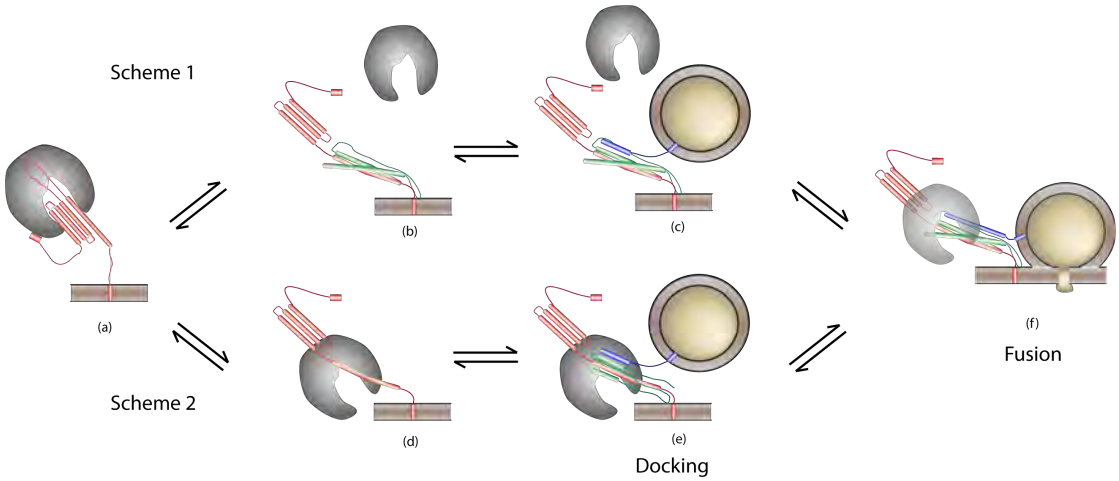

Figure 5.5 – **Model for the role of Munc18 in vesicle fusion.**
(a) Munc18c was found to interact with both the N-peptide and closed conformation of Syx4, similar to the binding mode of its vertebrate homolog, Munc18a as well as the Munc18 from choanoflagellates. Thus, all Munc18 proteins (gray) have a high-affinity to their partner syntaxins (red) and interact with both the N-peptide and closed conformation. (b & c) 'Scheme 1' suggests that Munc18 needs to dissociate from Syx for SNARE complex formation to proceed. The dissociation of the Munc18-Syx complex could occur by decrease in the binding affinity through phosphorylation, changes in local concentrations (of SNAP25, etc.) or by changes in reaction equilibria caused by factors such as Munc13. SNAP25 (green) and Syb (blue) from the vesicles can then interact with syntaxin to form the SNARE complex. (d & e) An alternative 'Scheme 2' is possible where Munc18 plays a direct role in vesicle fusion, similar to the scheme suggested for the role of Vps33 by Baker et al. (2015). Syx could open up while still bound to Munc18 through its SNARE domain. The opening of syntaxin could occur through the dissociation of its N-peptide and/or perturbations in its linker region caused by factors similar to those mentioned in (b & c). Munc18 could then bind the other SNARE proteins, Syb and SNAP25, and act as a framework for the nucleation and formation of the SNARE complex. (f) After formation of the SNARE complex and in the presence of required signals, vesicle fusion can take place. Munc18 could stay attached to the SNARE complex during this step or dissociate.

A function similar to Vps33 could be possible for Munc18, but only after the Munc18 inhibition is relieved and Syx opens up (Figure 5.5, Scheme 2). The SM proteins Sly1 (and possibly Vps45) are known to function directly in the opening up of their partner Syx (Demircioglu et al., 2014). In Munc18, such a function could be provided by external factors such as Munc13, Rabs or modifications such as phosphorylation. The energy barrier for the opening up of the syntaxin could be overcome in two ways. Removal of the N-peptide interaction is sufficient to eliminate the inhibition exerted by both Munc18a and Munc18c as shown by my results and Burkhardt et al. (2008). This could be a plausible mechanism to open up Syx while it is still bound to Munc18 through its SNARE domain. In the Vps33 structure with Vam3, the domain 3 hairpin loop ($\alpha 11 - \alpha 12$) is in an 'open' configuration (Baker et al., 2013). Such an open configuration is observed in Munc18b and Munc18c structures that are not in complex with the entire Syx,

while Munc18a bound to the full-length Syx shows a 'closed' hairpin loop (See Section 4.8.3). An open hairpin loop causes a steric hindrance for binding of the Syx linker region (that connects Habc and SNARE domains). Hence, opening up of the Munc18 domain 3a hairpin loop could also help to free up Syx SNARE motif from the Habc domain. The removal of Syx N-peptide and linker region interactions could also contribute simultaneously to the opening of Syx. Colbert et al. (2013) observed that in the complex of Munc18 with Syx lacking the N-peptide, the domain 3a hairpin loop is unstructured, suggesting an allosteric link between the two sites.

Through my studies, I found some evidence to indicate that Munc18 interacts with Syb as part of the SNARE core complex. Interestingly, the interaction is observed around the '0-layer' of Syb, which is similar to the binding site proposed for Vps33 binding to R-SNARE (Baker et al., 2013). However, this binding needs to be investigated further. If Munc18 indeed functions as a framework for SNARE assembly, in its absence SNARE complex assembly could be slow or erroneous, thus providing evidence for its essential role in exocytosis.

In the SM protein, Sly1, an extra loop blocks the putative R-SNARE binding site. Interestingly, a mutation in this loop of Sly1 overcomes the effects of deleting a Rab protein, Ypt1 (Dascher et al., 1991; Ossig et al., 1991). Hence, Ypt1 might help to release the block by the Sly1 loop for formation of the SNARE complex. This indicates that, Rab proteins known to be involved in vesicle trafficking, might also function by associating with SM proteins. Rab proteins are also known to interact with other proteins involved in docking, such as tethering complexes. Munc13, a type of tethering protein, is also thought to be involved in releasing Syx from binding to Munc18. Consequently, the SM proteins and SNAREs form the central actors in vesicle fusion that is orchestrated by a repertoire of other interacting proteins.

6 Summary and Future directions

The Soluble N-ethylmaleimide-sensitive factor Attachment protein Receptors (SNAREs) and Sec1/Munc18 (SM) proteins are found to be essential players involved in vesicle fusion events. The SNARE proteins drive vesicle fusion by zipping up to form a SNARE complex, while SM proteins are thought to regulate fusion by binding to the Qa SNARE (syntaxin) through two spatially separated binding sites. The syntaxin helices form a closed conformation that binds in the arch-shaped cavity of the SM proteins, while the N-terminal peptide binds at another site on the surface of the SM protein. The SNARE and SM protein family members have highly conserved sequences and similar domain architecture. The most well-studied SM protein, Munc18a, belongs to the SM sub-family involved in secretion and functions in neurotrasmitter release at synapses. Munc18a binds to its partner Syx1a through both the closed conformation as well as the N-peptide binding site and is known to inhibit SNARE complex formation *in vitro*. A Munc18 from choanoflagellates, the closest living relatives of animals, was found to have a similar mode of binding as Munc18 and also inhibited SNARE complex assembly. Thus, it was expected that exocytotic Munc18 proteins in metazoans would have a similar mode of binding and effect on SNARE assembly. Surprisingly, a close vertebrate homolog of Munc18a, called Munc18c, was found in earlier studies to interact with only the N-peptide of its cognate Syx4. It was therefore suggested that Munc18a, "which must be at the pinnacle of the evolutionary path, is something special" and its binding mode and function, that evolved specifically for neuronal exocytosis, does not exist for other SM proteins including Munc18c (Christie et al., 2012; Shin, 2013; Yu et al., 2013). The major question I tried to address was if Munc18c is indeed different from Munc18a in its mode of binding and mechanism of action.

I found through sensitive biochemical and biophysical experiments that Munc18c does have a similar binding mode as Munc18a, and interacts with its cognate partner Syx4 through both the N-peptide and the closed conformation. Moreover, Munc18c had an inhibitory effect on SNARE assembly with both binding sites contributing to inhibition, similar to the effect of Munc18a. However, the inhibition by Munc18a was found to be stronger than Munc18c. The lower inhibitory activity of Munc18c could be a result of the higher off-rate of the Munc18c/Syx4 complex compared to Munc18a/Syx1a complex.

Munc18 inhibits the first step in SNARE complex formation, that is the formation of the binary complex between SNAP25 and Syx. Thus, Munc18 and SNAP25 compete for binding to Syx. The rates for association and dissociation of Munc18/Syx and SNAP25/Syx complexes are slightly different between Syx and Munc18 homologs. However, I found that the kinetics for the Munc18/Syx complex occurs on a faster time scale compared to the SNAP25/Syx complex. Thus, the block of SNARE complex assembly by Munc18 was effective on a shorter time scale, but SNAP25 could eventually bind to syntaxin resulting in SNARE complex formation. Extending this observation, I also found that addition of excess SNAP25 shifts the equilibrium in favor of formation of the SNAP25/Syx complex instead of the Munc18/Syx complex.

I further observed that Munc18 could have a putative binding site on the surface of the SNARE core complex. The mobility of a dye bound at Cys61 at the center of Syb was affected on addition of Munc18, but not when the dye was present at the N-terminal or C-terminal region. However, this preliminary finding needs to be confirmed by rigorous testing using different methods to measure the affinity of binding and location of the binding site(s). Although, the structure and function of SM proteins from various organisms has been extensively studied, the exact mechanism of action of SM proteins remains to be uncovered. A recent paper by Baker et al. (2015) proposes that the SM protein Vps33 acts as a template for assembly of SNARE complex by binding to partially assembled Qa and R-SNAREs near the '0'-layer. Thus, it needs to be tested if Munc18 could also act as a template in SNARE assembly similar to Vps33. This could solve one of the long-standing questions in the field regarding the controversial functions of Munc18 *in vivo* (essential for fusion) and *in vitro* (inhibition of SNARE assembly by tight binding to syntaxin).

Vertebrates express three Munc18 homologs and six Syx homologs. Although, only certain Munc18/Syx pairs have been studied, earlier publications show that there are some overlaps (Hata and Südhof, 1995; Tamori et al., 1998; Tellam et al., 1995). Qualitative pulldown assays showed that Munc18a and Munc18b can bind to Syx1, 2, 3 while Munc18c can interact with Syx2 and Syx4. I confirmed these interaction specificities for Munc18a and Munc18c through quantitative studies, and found a new interaction between Munc18c/Syx1a, that was not reported earlier. However, the specific structural differences that result in the Munc18/Syx interaction specificities remains to be elucidated. When I compared the sequences and structures of the different vertebrate Munc18 homologs, I found some subtle differences at binding sites especially between Munc18a and Munc18c. However, it is difficult to arrive at conclusive evidence unless the structures of the syntaxin homologs in complex with different Munc18 homologs are available.

The function of Munc18c and Syx4 is mostly studied in the exocytosis of GLUT4 containing vesicles (GSVs) and are implicated in the development of insulin resistance and diabetes. The insulin-mediated signaling cascade eventually results in GLUT4 externalization and glucose uptake, but the molecular entities connecting the two events are not resolved. It is proposed that the insulin signaling cascade might result in phosphorylation of Munc18c, thus changing its activity and resulting in fusion of GSVs. I found that a phospho-mimetic mutant of Munc18c

had a lower affinity for Syx4 compared to Munc18c wt. Thus, Munc18c phosphorylation could be one of the mechanisms by which SNARE-mediated GSV fusion is regulated.

The results obtained by me suggest that secretory Munc18 proteins have a conserved two-site mode of binding to Syx. Through this mode, Munc18 binds to Syx and keeps it from participating in the SNARE assembly. Syx1 and SNAP25 have been shown to form an off-pathway 2:1 complex in addition to the 1:1 complex that is supposed to lead to a functional SNARE complex. The binding of Munc18 to Syx could also be an important mechanism to keep Syx from entering 2:1 dead-end complexes with SNAP25, thus making sure that SNARE complex formation can proceed smoothly. However, it is still not clear how Syx could be released from Munc18 to achieve fast exocytosis as seen in neurons. I found that increasing the concentration of SNAP25 can allow binary SNARE complex formation in the presence of Munc18. However, the cell might be employing other mechanisms to facilitate this change. Modifications such as phosphorylation of Munc18 could be one mechanism for releasing Munc18. Other factors such as Munc13 and Rabs could also be involved. Munc13 is supposed to play a role in releasing syntaxin from the tight grip of Munc18a in synaptic exocytosis (Ma et al., 2011). In insulin-mediated GSV fusion, a regulatory protein called Synip binds to Syx4. Interestingly, Synip binds to Syx4, but not Syx 1, 2 or 3, and hence it will be interesting to study its effect on Syx4 SNARE complex assembly (Min et al., 1999). Doc2β is another protein found to be a key positive regulator of GSV fusion. Interestingly, it is known to bind to phosphorylated Munc18c in a manner that precludes its binding to Syx4 (Jewell et al., 2008). Thus, the next step for further understanding the vesicle fusion process would be to study the effect of other interacting partners on SNARE complex assembly.

The role of Syx and Munc18 proteins *in vivo* can be tested on cell lines. I have provided Syx4 and Munc18 proteins to Iaroslav Savtchouk from Andrea Volterra's group in my department to study the function of Syx4 in astrocytes. In order to study if Syx4 is involved in exocytosis, he injected the cytoplasmic domain of Syx4 to observe if it reduces exocytosis by an indirect measurement. He used Syx4 protein lacking the SNARE domain as a control. In this preliminary analysis he observed a difference between test and control cases, indicating that Syx4 might be participating in exocytosis. He is further investigating glutamate release by astrocytes using fluorescently labeled Syx4. Moreover, micro-injection of Munc18c could also be carried out to measure its effect on exocytosis. Similar studies can be done on adipocyte cell lines by measuring glucose uptake and GLUT4 presentation on the cell surface.

A Appendix

A.1 Classification of the Amino Acids

Each of the 20 different amino acids has distinctive physical and chemical properties, primarily based on their side chain (or "R group"). They can be classified into four categories based upon the major chemical properties of the R group. Below are the names of the amino acids, their 3 letter abbreviations, and their standard one letter symbols.

1. Positively charged (and therefore basic) amino acids.

Arginine	Arg	R
Histidine	His	H
Lysine	Lys	K

2. Negatively charged (and therefore acidic) amino acids.

Aspartic acid	Asp	D
Glutamic acid	Glu	E

3. Polar amino acids . Though uncharged overall, these amino acids have an uneven charge distribution. Because of this uneven charge distribution, these amino acids can form hydrogen bonds with water. As a consequence, polar amino acids are called *hydrophilic*, and are often found on the outer surface of folded proteins, in contact with the watery environment of the cell.

Asparagine	Asn	N
Cysteine	Cys	C
Glutamine	Gln	Q
Glycine	Gly	G
Serine	Ser	S
Threonine	Thr	T
Tyrosine	Tyr	Y

4. Nonpolar amino acids. These amino acids are uncharged and have a uniform charge distribution. Because of this, they do not form hydrogen bonds with water, are called *hydrophobic*, and tend to be found on the inside surface of folded proteins.

Alanine	Ala	A
Isoleucine	Ile	I
Leucine	Leu	L
Methionine	Met	M
Phenylalanine	Phe	F
Proline	Pro	P
Tryptophan	Trp	W
Valine	Val	V

A.2 Use of SNAP25 instead of SNAP23 for kinetic studies

SNAP23 is known to be the physiological SNARE partner of Syx4 in GLUT4 vesicle fusion, along with Synaptobrevin 2 (Syb). SNAP23 is a homolog of the synaptic protein SNAP25, and is enriched in adipocyte cell lines and to a lesser extent in skeletal muscle cells (Wong et al., 1997).

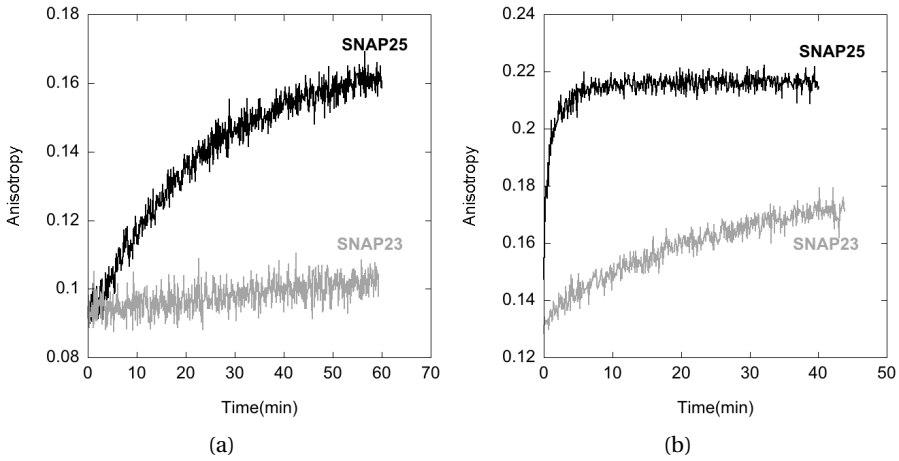

Figure A.1 – **The assay with SNAP25 is faster than with SNAP23.**
Comparison of ternary SNARE complex formation rates for SNAP23 or SNAP25 (700nM) with 350nM Syx4 and labeled Syb (40nM) (a) without pre-incubation (b) with pre-incubation of Syx4 and SNAP23/SNAP25.

The kinetics of SNARE complex formation with SNAP23 was compared with SNAP25, using Syx4 and Syb2 partner SNAREs. The rate of SNARE complex formation with SNAP23 was found to be much slower than SNAP25, even on pre-incubation with Syx4 (Figure. A.1). The SNARE complex formation using only Syx4H3 domain instead of the complete cytoplasmic domain also gave similar results. Thus, I used SNAP25 for all the kinetic experiments, in order

to visualize changes on a shorter time scale.

SNAP25, that has two homologs 'a' and 'b', is found to be expressed only in the nervous system and neuroendocrine cells such as pancreatic islets of Langerhans (Jacobsson et al., 1994; Sadoul et al., 1995), adrenal chromaffin cells (Roth and Burgoyne, 1994) and anterior pituitary cells but not in adipocytes (Volchuk et al., 1996). However, one study by Jagadish et al. (1996) detected SNAP25 mRNA and protein in adipocytes and skeletal muscles using sensitive methods such as reverse-transcription PCR combined with southern hybridization and immunoblot analysis of plasma membranes from subcellular fractionation. They found that the SNAP25a homolog was the major species in adipose tissue, while the SNAP25b homolog, involved in fast synaptic responses, is present in skeletal muscles. Moreover, they also found that a pre-formed complex of SNAP25 and Syx4 binds to GLUT4 vesicles. Hence, it is possible that SNAP25 might be involved in forming a SNARE complex with Syx4 in adipocytes and skeletal muscles.

A.3 Sequence analysis of vertebrate SM and Syx proteins

The sequences for Munc18 and Syx homologs were collected from NCBI non-redundant database and RefSeq. Along with Dr. Nickias Kienle, I annotated and curated these sequences in our database (Table A.1). These sequences were then used to obtain multiple sequence alignments for each sub-group. The weblogo and phylogenetic trees were then constructed from the multiple sequence alignments.

Table A.1 – **Number of sequences used for multiple sequence alignment of Munc18 and Syx homologs.** The number of sequences for each homolog of Munc18 and syntaxin that were collected and annotated are mentioned here. These sequences were then used for multiple sequence alignment of Munc18 and Syx homologs. The phylogenetic trees and weblogos were created from the multiple sequence alignments.

Protein homolog	Number of sequences
Syx vertebrate all	615 sequences
Syx1a	74 sequences
Syx1b	72 sequences
Syx2	83 sequences
Syx3	90 sequences
Syx4	76 sequences
Syx11	124 sequences
Syx19	81 sequences
Syx21	15 sequences
Munc18 all	249 sequences
Munc18a	67 sequences
Munc18b	52 sequences
Munc18c	63 sequences

The phylogenetic tree for the SM protein family shows the four sub-groups of SM proteins that are involved in trafficking at various steps in the secretory pathway (Figure A.2). This tree was constructed by Dr. Tobias Kloepper in my laboratory. The proteins that belong to the Munc18 sub-group involved in secretion, form three lineage-specific clusters of fungi, plants and animals. The metazoan Munc18 proteins cluster along with the Munc18 proteins from chanoflagellates, single-celled eukaryotes that are the closest living relatives of animals. Most organisms have a single Munc18, but the vertebrates have three paralogs evolved through duplication – Munc18a, Munc18b and Munc18c. Although the three Munc18 homologs are closely related, they form distinct clusters that are distinguished by their sequence patterns. The vertebrate sequences from each Munc18 cluster were used to create sequence weblogos to reveal the similarities and differences between the subgroups (Figure A.3).

The Syx sequences are highly conserved, but they form distinct clusters that are distinguished by their sequence patterns. The syntaxin family of proteins has six isoforms in vertebrates, that probably arose through duplication. The vertebrate sequences from each Syx cluster were used to create sequence weblogos to reveal the similarities and differences between the subgroups (Figure A.3). The phylogenetic trees were calculated from the multiple sequence alignment for the Syx homologs in vertebrates (Figure A.3).

The 'Hannenhalli' method identifies residues that differ between the subtypes, but are conserved within each individual subtype (Hannenhalli and Russell, 2000). This method uses the multiple sequence alignments and the phylogenetic tree as inputs. Several sites were identified to have a conserved residue within each sub-type, but which varies between the different sub-types (Table A.2). The sites that are identified to be differing between the sub-types are numbered according to the position in the multiple sequence alignment. These positions can be checked in the weblogos that are also constructed from the multiple sequence alignments. This analysis was carried out by Nicee Srivastava in my laboratory.

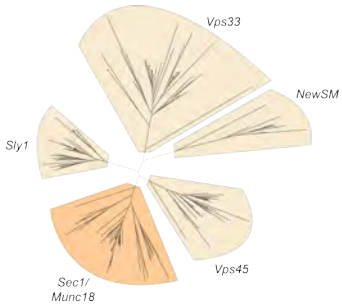

(a) SM family

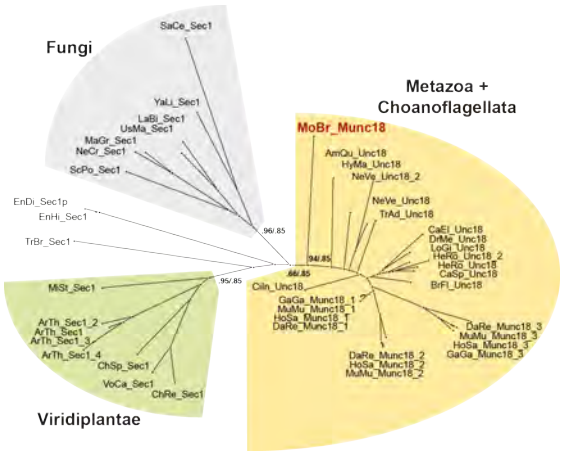

(b) Munc18 subgroups

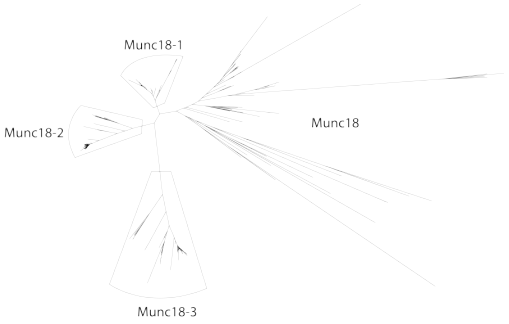

(c) Animal Munc18 classification

Figure A.2 – **Phylogenetic analysis of SM protein family with focus on the SM proteins in secretion.**
(a) A phylogenetic analysis of the SM protein family shows five sub-groups – Munc18, Sly1, Vps33, Vps45 and a newly identified subgroup termed 'new-SM'. (b) A phylogenetic analysis of the Munc18 proteins involved in secretion shows clustering into species-specific sub-groups – fungi, plants and metazoa. The Munc18 proteins from metazoans cluster together with the Munc18s from choanoflagellates (*Monosiga brevicollis* Munc18 shown in red), single-celled eukaryotes that are the closest living relatives of animals. (c) The metazoan phylogenetic tree for Munc18 shows that most in-vertebrates have a single Munc18, but duplication in vertebrates results in three Munc18 homologs - Munc18a, b and c.

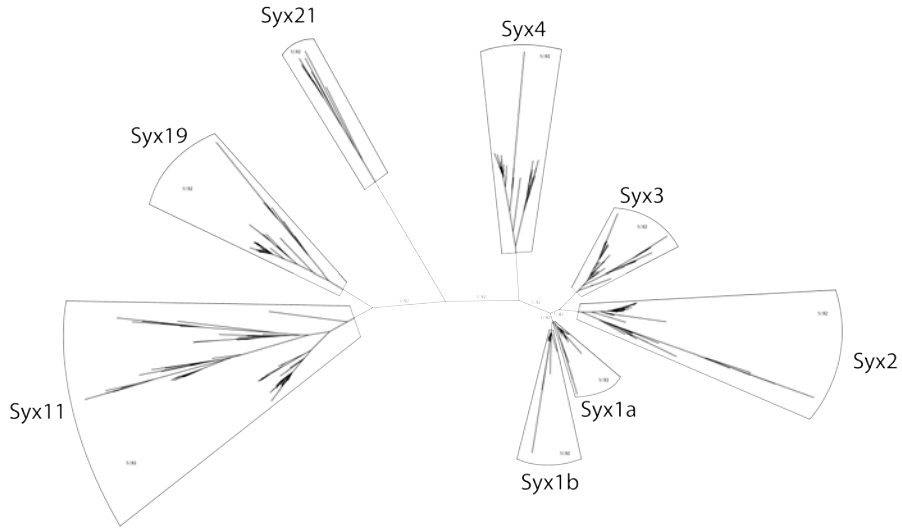

Figure A.3 – **Phylogenetic analysis of Qa.IV family of syntaxin proteins in vertebrates.** The Qa.IV family of secretory syntaxin proteins has six homologs in vertebrates.

Table A.2 – **The highest scoring Hannenhalli predicted sites.** The sites that had the highest score from the Hannenhalli analysis are conserved in each of the subtypes. The position indicates the corresponding site in the multiple sequence alignment of all Munc18 homologs, and can be checked in the weblogo. The residues are color coded according to their chemistry as polar, acidic, basic, neutral and hydrophobic.

Position in weblogo	Munc18a residue	Munc18b residue	Munc18c residue
94	M	L	K
100	K	S	D
118	L	P	F
176	P	T	K
201	V	G	K
332	K	E	L
342	Q	L	E
526	S	T	D
559	Q	K	E
563	R	E	K
630	R	S	K
696	P	Q	E
706	M	L	W
787	I	R	S
790	Q	P	E
817	H	L	E
824	R	P	C
829	F	S	N
917	E/D	L	K

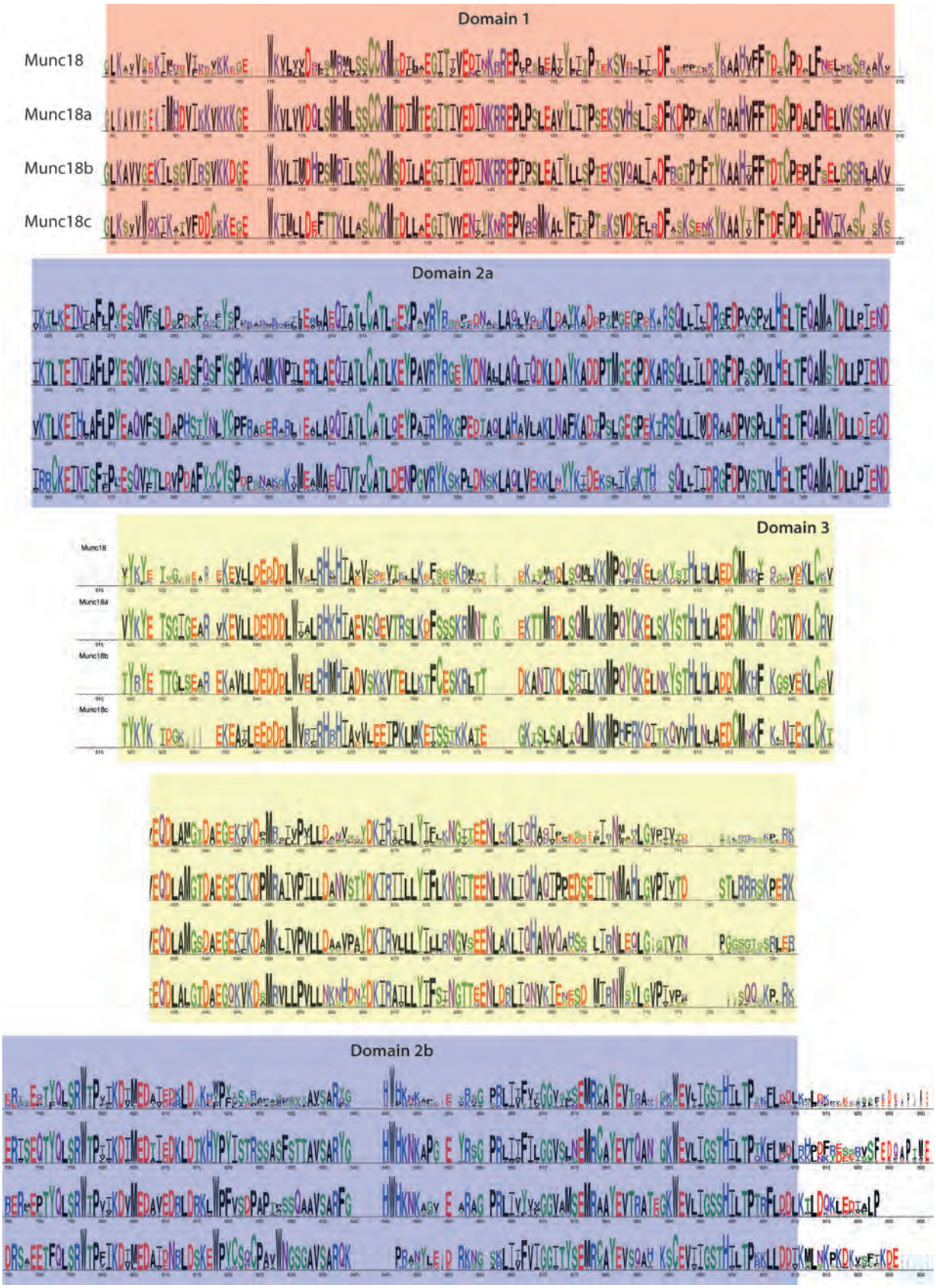
Domain 1
Munc18
Munc18a
Munc18b
Munc18c
Domain 2a
Domain 3
Domain 2b

Figure A.4

Figure A.3 *(previous page)* – **Weblogo representations for Munc18 homologs in animals.** The weblogos were constructed from the multiple sequence alignments of ≈250 Munc18 sequences from animals and vertebrate Munc18 homologs. The weblogos for the Munc18 domains are shown here for, from top to bottom, Munc18 from animals, Munc18a, Munc18b, Munc18c. The different domains are colored to distinguish them. The domain 3 weblogo (yellow) is split to accommodate the sequence. See the attached file sent through email for the complete weblogo.

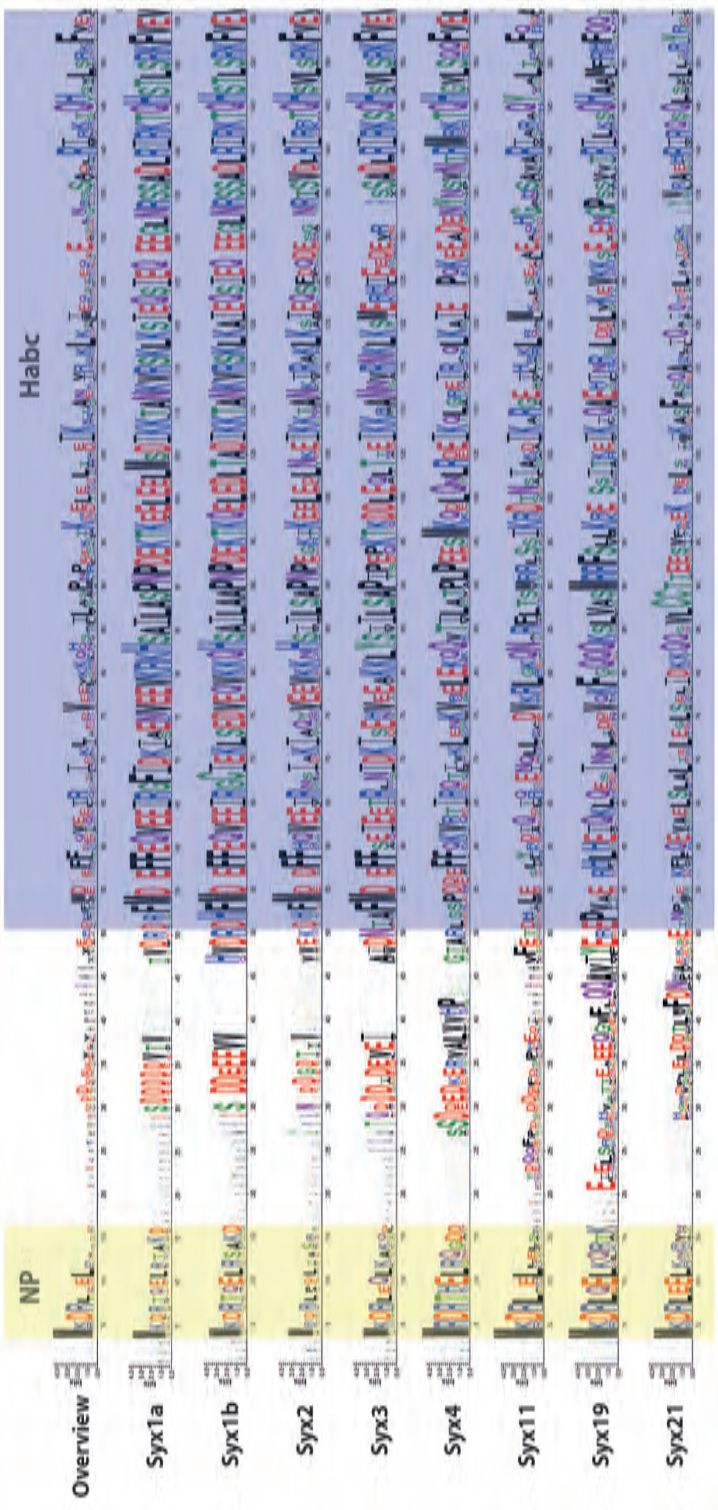
Habc
NP
Overview
Syx1a
Syx1b
Syx2
Syx3
Syx4
Syx11
Syx19
Syx21

Figure A.4

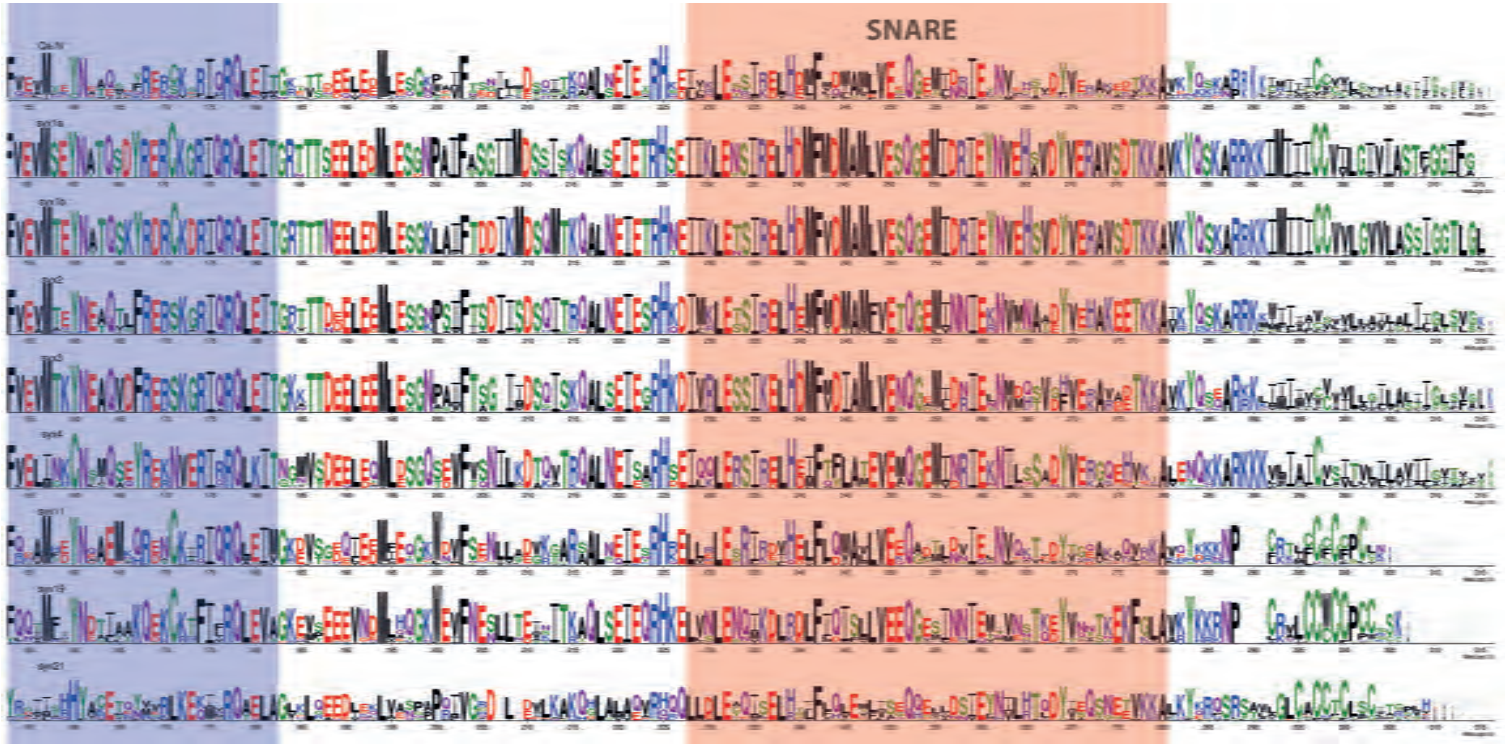

Figure A.3 – **Weblogo representations for Syx homologs in vertebrates.**
The weblogos were constructed from the multiple sequence alignments of ≈600 Syx sequences from vertebrates. The weblogo for the Syx homologs are annotated with the domains - N-peptide, Habc and SNARE domains. The weblogo is split on two pages to accommodate the entire sequence. The split occurs in the Habc domain, and a part of the sequence is repeated for sake of continuity.

Bibliography

Al Hawas, R., Q. Ren, S. Ye, Z. A. Karim, A. H. Filipovich, and S. W. Whiteheart (2012). Munc18b/STXBP2 is required for platelet secretion. *Blood*, 120(12):2493–2500.

Araki, S., Y. Tamori, M. Kawanishi, H. Shinoda, J. Masugi, H. Mori, T. Niki, H. Okazawa, T. Kubota, and M. Kasuga (1997). Inhibition of the Binding of SNAP-23 to Syntaxin 4 by Munc18c. *Biochemical and Biophysical Research Communications*, 234:257–262.

Aran, V., F. M. Brandie, A. R. Boyd, T. Kantidakis, E. J. Rideout, S. M. Kelly, G. W. Gould, and N. J. Bryant (2009). Characterization of two distinct binding modes between syntaxin 4 and Munc18c. *Biochemical Journal*, 419(3):655.

Aran, V., N. J. Bryant, and G. W. Gould (2011). Tyrosine phosphorylation of Munc18c on residue 521 abrogates binding to Syntaxin 4. *BMC Biochemistry*, 12(1):19.

Baker, R. W., P. D. Jeffrey, and F. M. Hughson (2013). Crystal Structures of the Sec1/Munc18 (SM) Protein Vps33, Alone and Bound to the Homotypic Fusion and Vacuolar Protein Sorting (HOPS) Subunit Vps16*. *PLoS ONE*, 8(6):e67409.

Baker, R. W., P. D. Jeffrey, M. Zick, B. P. Phillips, W. T. Wickner, and F. M. Hughson (2015). A direct role for the Sec1/Munc18-family protein Vps33 as a template for SNARE assembly. *Science*, 349(6252):1111–1114.

Bakke, J., A. Bettaieb, N. Nagata, K. Matsuo, and F. G. Haj (2013). Regulation of the SNARE-interacting protein Munc18c tyrosine phosphorylation in adipocytes by protein-tyrosine phosphatase 1B. *Cell Communication and Signaling*, 11(1):57.

Beest, M. B. A. t., S. J. Chapin, D. Avrahami, and K. E. Mostov (2005). The Role of Syntaxins in the Specificity of Vesicle Targeting in Polarized Epithelial Cells. *Molecular Biology of the Cell*, 16:5784–5792.

Bennett, M. K., J. Garcia-Arrarás, L. A. Elferink, K. Peterson, A. M. Fleming, C. D. Hazuka, and R. H. Scheller (1993). The syntaxin family of vesicular transport receptors. *Cell*, 74(5):863–873.

Bergman, B. C., M.-A. Cornier, T. J. Horton, D. H. Bessesen, and R. H. Eckel (2008). Skeletal muscle munc18c and syntaxin 4 in human obesity. *Nutrition & Metabolism*, 5:21.

Bracher, A. and W. Weissenhorn (2002). Structural basis for the Golgi membrane recruitment of Sly1p by Sed5p. *The EMBO Journal*, 21(22):6114–6124.

Bradford, M. M. (1976). A Rapid and Sensitive Method for the Quantitation of Microgram Quantities of Protein Utilizing the Principle of Protein-Dye Binding. *Analytical Biochemistry*, 72:248–254.

Brandie, F. M., V. Aran, A. Verma, J. A. McNew, N. J. Bryant, and G. W. Gould (2008). Negative Regulation of Syntaxin4/SNAP-23/VAMP2-Mediated Membrane Fusion by Munc18c In Vitro. *PLoS ONE*, 3(12):e4074.

Brenner, S. (1974). The genetics of Caenorhabditis elegans. *Genetics*, 77(1):71–94.

Brünger, A. T., D. J. Cipriano, and J. Diao (2015). Towards reconstitution of membrane fusion mediated by SNAREs and other synaptic proteins. *Critical Reviews in Biochemistry and Molecular Biology*, 00(00):1–11.

Burkhardt, P. (2015). The origin and evolution of synaptic proteins - choanoflagellates lead the way. *Journal of Experimental Biology*, 218(4):506–514.

Burkhardt, P., D. A. Hattendorf, W. I. Weis, and D. Fasshauer (2008). Munc18a controls SNARE assembly through its interaction with the syntaxin N-peptide. *The EMBO Journal*, 27(7):923–933.

Burkhardt, P., C. M. Stegmann, B. Cooper, T. H. Kloepper, C. Imig, F. Varoqueaux, M. C. Wahl, and D. Fasshauer (2011). Primordial neurosecretory apparatus identified in the choanoflagellate Monosiga brevicollis. *Proceedings of the National Academy of Sciences, USA*, 108(37):15264–15269.

Carpp, L. N., L. F. Ciufo, S. G. Shanks, A. Boyd, and N. J. Bryant (2006). The Sec1p/Munc18 protein Vps45p binds its cognate SNARE proteins via two distinct modes. *The Journal of Cell Biology*, 173(6):927–936.

Carr, C. M., E. Grote, M. Munson, F. M. Hughson, and P. J. Novick (1999). Sec1p Binds to SNARE Complexes and Concentrates at Sites of Secretion. *The Journal of Cell Biology*, 146(2):333–344.

Christie, M. P., A. E. Whitten, G. J. King, S.-H. Hu, R. J. Jarrott, K.-E. Chen, A. P. Duff, P. Callow, B. M. Collins, D. E. James, and J. L. Martin (2012). Low-resolution solution structures of Munc18:Syntaxin protein complexes indicate an open binding mode driven by the Syntaxin N-peptide. *Proceedings of the National Academy of Sciences, USA*, 109(25):9816–9821.

Colbert, K. N., D. A. Hattendorf, T. M. Weiss, P. Burkhardt, D. Fasshauer, and W. I. Weis (2013). Syntaxin1a variants lacking an N-peptide or bearing the LE mutation bind to Munc18a in a closed conformation. *Proceedings of the National Academy of Sciences, USA*, Pp. 1–6.

Collins, K. M. and W. T. Wickner (2007). trans-SNARE complex assembly and yeast vacuole membrane fusion. *Proceedings of the National Academy of Sciences, USA*, 104(21):8755–8760.

Côte, M., M. M. Ménager, A. Burgess, N. Mahlaoui, C. Picard, C. Schaffner, F. Al-Manjomi, M. Al-Harbi, A. Alangari, F. Le Deist, A. R. Gennery, N. Prince, A. Cariou, P. Nitschke, U. Blank, G. El-Ghazali, G. Ménasché, S. Latour, A. Fischer, and G. de Saint Basile (2009). Munc18-2 deficiency causes familial hemophagocytic lymphohistiocytosis type 5 and impairs cytotoxic granule exocytosis in patient NK cells. *Journal of Clinical Investigation*, 119(12):3765–3773.

Dacks, J. B. and M. C. Field (2007). Evolution of the eukaryotic membrane-trafficking system: origin, tempo and mode. *Journal of Cell Science*, 120(17):2977–2985.

D'Andrea-Merrins, M., L. Chang, A. D. Lam, S. A. Ernst, and E. L. Stuenkel (2007). Munc18c Interaction with Syntaxin 4 Monomers and SNARE Complex Intermediates in GLUT4 Vesicle Trafficking. *Journal of Biological Chemistry*, 282(22):16553–16566.

Dascher, C., R. Ossig, D. Gallwitz, and H. D. Schmitt (1991). Identification and structure of four yeast genes (SLY) that are able to suppress the functional loss of YPT1, a member of the RAS superfamily. *Molecular and Cellular Biology*, 11(2):872–885.

Deàk, F., Y. Xu, W.-P. Chang, I. Dulubova, M. Khvotchev, X. Liu, T. Sudhof, and J. Rizo (2009). Munc18-1 binding to the neuronal SNARE complex controls synaptic vesicle priming. *The Journal of Cell Biology*, 184(5):751–764.

Demircioglu, F. E., P. Burkhardt, and D. Fasshauer (2014). The SM protein Sly1 accelerates assembly of the ER-Golgi SNARE complex. *Proceedings of the National Academy of Sciences, USA*, 111(38):13828–13833.

Dulubova, I., M. Khvotchev, S. Liu, I. Huryeva, T. C. Südhof, and J. Rizo (2007). Munc18-1 binds directly to the neuronal SNARE complex. *Proceedings of the National Academy of Sciences, USA*, 104(8):2697–2702.

Dulubova, I., S. Sugita, S. Hill, M. Hosaka, I. Fernandez, T. C. Südhof, and J. Rizo (1999). A conformational switch in syntaxin during exocytosis: role of munc18. *The EMBO Journal*, 18:4372–4382.

Dulubova, I., T. Yamaguchi, Y. Gao, S.-W. Min, I. Huryeva, T. C. Südhof, and J. Rizo (2002). How Tlg2p/syntaxin 16 'snares' Vps45. *The EMBO Journal*, 21(14):3620–3631.

Dulubova, I., T. Yamaguchi, Y. Wang, T. C. Südhof, and J. Rizo (2001). Vam3p structure reveals conserved and divergent properties of syntaxins. *Nature Structural Biology*, 8(3):258–264.

Fasshauer, D., W. Antonin, V. Subramaniam, and R. Jahn (2002). SNARE assembly and disassembly exhibit a pronounced hysteresis. *Nature Structural Biology*, 9(2):144–151.

Fasshauer, D., W. K. Eliason, A. T. Brünger, and R. Jahn (1998a). Identification of a Minimal Core of the Synaptic SNARE Complex Sufficient for Reversible Assembly and Disassembly. *Biochemistry*, 37(29):10354–10362.

Fasshauer, D. and M. Margittai (2004). A Transient N-terminal Interaction of SNAP-25 and Syntaxin Nucleates SNARE Assembly. *Journal of Biological Chemistry*, 279(9):7613–7621.

Fasshauer, D., R. B. Sutton, A. T. Brünger, and R. Jahn (1998b). Conserved structural features of the synaptic fusion complex: SNARE proteins reclassified as Q- and R-SNAREs. *Proceedings of the National Academy of Sciences, USA*, 95:15781–15786.

Ferro-Novick, S. and R. Jahn (1994). Vesicle fusion from yeast to man. *Nature*, 370(6486):191–193.

Fujita, Y., T. Sasaki, K. Fukui, H. Kotani, T. Kimura, Y. Hata, T. C. Südhof, R. H. Scheller, and Y. Takai (1996). Phosphorylation of Munc-18/n-Sec1/rbSec1 by protein kinase C: its implication in regulating the interaction of Munc-18/n-Sec1/rbSec1 with syntaxin. *The Journal of Biological Chemistry*, 271(13):7265–7268.

Furgason, M. L. M., C. MacDonald, S. G. Shanks, S. P. Ryder, N. J. Bryant, and M. Munson (2009). The N-terminal peptide of the syntaxin Tlg2p modulates binding of its closed conformation to Vps45p. *Proceedings of the National Academy of Sciences, USA*, 106(34):14303–14308.

Garcia, E. P., E. Gatti, M. Butler, J. Burton, and P. De Camilli (1994). A rat brain Sec1 homologue related to Rop and UNC18 interacts with syntaxin. *Proceedings of the National Academy of Sciences, USA*, 91(6):2003–2007.

Garrido-Sanchez, L., X. Escote, L. Coin-Aragüez, J. C. Fernandez-Garcia, R. El Bekay, J. Vendrell, E. Garcia-Fuentes, and F. J. Tinahones (2013). Munc18c in Adipose Tissue Is Downregulated in Obesity and Is Associated with Insulin. *PLoS ONE*, 8(5):e63937.

Genç, Ö., O. Kochubey, R. F. Toonen, M. Verhage, and R. Schneggenburger (2014). Munc18-1 is a dynamically regulated PKC target during short-term enhancement of transmitter release. *eLife*, 3:e01715.

Gengyo-Ando, K., Y. Kamiya, A. Yamakawa, K. Kodaira, K. Nishiwaki, J. Miwa, I. Hori, and R. Hosono (1993). The C. elegans unc-18 gene encodes a protein expressed in motor neurons. *Neuron*, 11(4):703–711.

Grimsley, G. R. and C. N. Pace (2003). Spectrophotometric Determination of Protein Concentration. *Current Protocols in Protein Science*, Pp. 3.1.1–3.1.9.

Grote, E., C. M. Carr, and P. J. Novick (2000). Ordering the final events in yeast exocytosis. *The Journal of Cell Biology*, 151(2):439–452.

Gurkan, C., A. V. Koulov, and W. E. Balch (2000). *An Evolutionary Perspective on Eukaryotic Membrane Trafficking*. Madame Curie Bioscience Database [Internet]. Austin (TX): Landes Bioscience.

Hackmann, Y., S. C. Graham, S. Ehl, S. Honing, K. Lehmberg, M. Arico, D. J. Owen, and G. M. Griffiths (2013). Syntaxin binding mechanism and disease-causing mutations in Munc18-2. *Proceedings of the National Academy of Sciences, USA*, Pp. 1–10.

Hannenhalli, S. S. and R. B. Russell (2000). Analysis and prediction of functional sub-types from protein sequence alignments. *Journal of Molecular Biology*, 303(1):61–76.

Harrison, S. D., K. Broadie, J. v. d. Goor, and G. M. Rubin (1994). Mutations in the drosophila Rop gene suggest a function in general secretion and synaptic transmission. *Neuron*, 13(3):555–566.

Hata, Y., C. A. Slaughter, and T. C. Südhof (1993). Synaptic vesicle fusion complex contains unc-18 homologue bound to syntaxin. *Nature*, 366(6453):347–351.

Hata, Y. and T. C. Südhof (1995). A novel ubiquitous form of Munc-18 interacts with multiple syntaxins. Use of the yeast two-hybrid system to study interactions between proteins involved in membrane traffic. *The Journal of Biological Chemistry*, 270(22):13022–13028.

Houng, A., J. Polgar, and G. L. Reed (2003). Munc18-Syntaxin Complexes and Exocytosis in Human Platelets. *Journal of Biological Chemistry*, 278(22):19627–19633.

Hu, S.-H., M. P. Christie, N. J. Saez, C. F. Latham, R. Jarrott, L. H. L. Lua, B. M. Collins, and J. L. Martin (2011). Possible roles for Munc18-1 domain 3a and Syntaxin1 N-peptide and C-terminal anchor in SNARE complex formation. *Proceedings of the National Academy of Sciences, USA*, 108(3):1040–1045.

Hu, S.-H., C. L. Gee, C. F. Latham, S. W. Rowlinson, U. Rova, A. Jones, J. A. Halliday, N. J. Bryant, D. E. James, and J. L. Martin (2003). Recombinant expression of Munc18c in a baculovirus system and interaction with syntaxin4. *Protein Expression and Purification*, 31(2):305–310.

Hu, S.-H., C. F. Latham, C. L. Gee, D. E. James, and J. L. Martin (2007). Structure of the Munc18c/Syntaxin4 N-peptide complex defines universal features of the N-peptide binding mode of Sec1/Munc18 proteins. *Proceedings of the National Academy of Sciences, USA*, 104(21):8773–8778.

Jacobsson, G., A. J. Bean, R. H. Scheller, L. Juntti-Berggren, J. Deeney, P.-O. Berggren, and B. Meister (1994). Identification of synaptic proteins and their isoform mRNAs in compartments of pancreatic endocrine cells. *Cell*, 91:12487–12491.

Jagadish, M. N., C. S. Fernandez, D. R. Hewish, S. L. Macaulay, K. H. Gough, J. Grusovin, A. Verkuylen, L. Cosgrove, A. Alafaci, M. J. Frenkel, and C. W. Ward (1996). Insulin-responsive tissues contain the core complex protein SNAP-25 (synaptosomal-associated protein 25) A and B isoforms in addition to syntaxin 4 and synaptobrevins 1 and 2. *Biochemical Journal*, 317:945–954.

Jahn, R. and D. Fasshauer (2012). Molecular machines governing exocytosis of synaptic vesicles. *Nature*, 490(7419):201–207.

Jahn, R. and R. H. Scheller (2006). SNAREs — engines for membrane fusion. *Nature Reviews Molecular Cell Biology*, 7(9):631–643.

Jain, S. S., L. A. Snook, J. F. C. Glatz, J. J. F. P. Luiken, G. P. Holloway, D. C. Thurmond, and A. Bonen (2012). Munc18c provides stimulus-selective regulation of GLUT4 but not fatty acid transporter trafficking in skeletal muscle. *FEBS Letters*, 586(16):2428–2435.

James, D. E. (2005). MUNC-ing around with insulin action. *Journal of Clinical Investigation*, 115(2):219–221.

Jewell, J., E. Oh, S. Bennett, S. Meroueh, and D. C. Thurmond (2008). The Tyrosine Phosphorylation of Munc18c Induces a Switch in Binding Specificity from Syntaxin 4 to Doc2ß. *Journal of Biological Chemistry*, 283(31):21734–21746.

Jewell, J. L., E. Oh, L. Ramalingam, M. A. Kalwat, V. S. Tagliabracci, L. Tackett, J. S. Elmendorf, and D. C. Thurmond (2011). Munc18c phosphorylation by the insulin receptor links cell signaling directly to SNARE exocytosis. *The Journal of Cell Biology*, 193(1):185–199.

Jewell, J. L., E. Oh, and D. C. Thurmond (2010). Exocytosis mechanisms underlying insulin release and glucose uptake: conserved roles for Munc18c and syntaxin 4. *AJP: Regulatory, Integrative and Comparative Physiology*, 298(3):R517–R531.

Johnson, J. R., P. Ferdek, L.-Y. Lian, J. W. Barclay, R. D. Burgoyne, and A. Morgan (2009). Binding of UNC-18 to the N-terminus of syntaxin is essential for neurotransmission in Caenorhabditis elegans. *Biochemical Journal*, 418(1):73–80.

Jurado, S., D. Goswami, Y. Zhang, A. J. M. Molina, T. C. Südhof, and R. C. Malenka (2013). LTP Requires a Unique Postsynaptic SNARE Fusion Machinery. *Neuron*, 77(3):542–558.

Kanda, H., Y. Tamori, H. Shinoda, M. Yoshikawa, M. Sakaue, J. Udagawa, H. Otani, F. Tashiro, J.-i. Miyazaki, and M. Kasuga (2005). Adipocytes from Munc18c-null mice show increased sensitivity to insulin-stimulated GLUT4 externalization. *Journal of Clinical Investigation*, 115(2):291–301.

Khan, A. H., D. C. Thurmond, C. Yang, B. P. Ceresa, C. D. Sigmund, and J. E. Pessin (2000). Munc18c Regulates Insulin-stimulated GLUT4 Translocation to the Transverse Tubules in Skeletal Muscle. *Journal of Biological Chemistry*, 276(6):4063–4069.

Kim, K., Y. M. Petrova, B. L. Scott, R. Nigam, A. Agrawal, C. M. Evans, Z. Azzegagh, A. Gomez, E. M. Rodarte, V. M. Olkkonen, R. Bagirzadeh, L. Piccotti, B. Ren, J. H. Yoon, J. A. McNew, R. Adachi, M. J. Tuvim, and B. F. Dickey (2012). Munc18b is an essential gene in mice whose expression is limiting for secretion by airway epithelial and mast cells. *Biochemical Journal*, 446(3):383–394.

Kloepper, T. H., C. N. Kienle, and D. Fasshauer (2007). An Elaborate Classification of SNARE Proteins Sheds Light on the Conservation of the Eukaryotic Endomembrane System. *Molecular Biology of the Cell*, 18:3463–3471.

Klöpper, T. H., N. Kienle, D. Fasshauer, and S. Munro (2012). Untangling the evolution of Rab G proteins: implications of a comprehensive genomic analysis. *BMC Biology*, 10(1):71.

Koumandou, V. L., J. B. Dacks, R. M. Coulson, and M. C. Field (2007). Control systems for membrane fusion in the ancestral eukaryote; evolution of tethering complexes and SM proteins. *BMC Evolutionary Biology*, 7:29–29.

Laemmli, U. K. (1970). Cleavage of Structural Proteins during the Assembly of the Head of Bacteriophage T4. *Nature*, 227(5259):680–685.

Lam, P. P. L., M. Ohno, S. Dolai, Y. He, T. Qin, T. Liang, D. Zhu, Y. Kang, Y. Liu, M. Kauppi, L. Xie, W. C. Y. Wan, N.-R. Bin, S. Sugita, V. M. Olkkonen, N. Takahashi, H. Kasai, and H. Y. Gaisano (2013). Munc18b is a major mediator of insulin exocytosis in rat pancreatic β-cells. *Diabetes*, 62:2416–2428.

Latham, C. F., J. A. Lopez, S.-H. Hu, C. L. Gee, E. Westbury, D. H. Blair, C. J. Armishaw, P. F. Alewood, N. J. Bryant, D. E. James, and J. L. Martin (2006). Molecular Dissection of the Munc18c/Syntaxin4 Interaction: Implications for Regulation of Membrane Trafficking. *Traffic*, 7(10):1408–1419.

Leto, D. and A. R. Saltiel (2012). Regulation of glucose transport by insulin: traffic control of GLUT4. *Nature Reviews Molecular Cell Biology*, 13(6):383–396.

Ma, C., W. Li, Y. Xu, and J. Rizo (2011). Munc13 mediates the transition from the closed syntaxin–Munc18 complex to the SNARE complex. *Nature Publishing Group*, 18(5):542–549.

Ma, C., L. Su, A. B. Seven, Y. Xu, and J. Rizo (2013). Reconstitution of the Vital Functions of Munc18 and Munc13 in Neurotransmitter Release. *Science*, 339(6118):421–425.

Macaulay, S. L., J. Grusovin, V. Stoichevska, J. M. Ryan, L. A. Castelli, and C. W. Ward (2002). Cellular munc18c levels can modulate glucose transport rate and GLUT4 translocation in 3T3L1 cells. *FEBS Letters*, 528:154–160.

Margittai, M. (2001). Homo- and Heterooligomeric SNARE Complexes Studied by Site-directed Spin Labeling. *Journal of Biological Chemistry*, 276(16):13169–13177.

Meijer, M., P. Burkhardt, H. de Wit, R. F. Toonen, D. Fasshauer, and M. Verhage (2012). Munc18-1 mutations that strongly impair SNARE-complex binding support normal synaptic transmission. *The EMBO Journal*, 31(9):2156–2168.

Meijer, M., T. Cijsouw, R. F. Toonen, and M. Verhage (2015). Synaptic Effects of Munc18-1 Alternative Splicing in Excitatory Hippocampal Neurons. *PLoS ONE*, 10(9):e0138950.

Min, J., S. Okada, M. Kanzaki, J. S. Elmendorf, K. J. Coker, B. P. Ceresa, L.-J. Syu, Y. Noda, A. R. Saltiel, and J. E. Pessin (1999). Synip: A Novel Insulin-Regulated Syntaxin 4–Binding Protein Mediating GLUT4 Translocation in Adipocytes. *Nature Reviews Molecular Cell Biology*, 3:751–760.

Misura, K. M. S., L. C. Gonzalez, A. P. May, R. H. Scheller, and W. I. Weis (2001). Crystal Structure and Biophysical Properties of a Complex between the N-terminal SNARE Region of SNAP25 and Syntaxin 1a. *Journal of Biological Chemistry*, 276(44):41301–41309.

Misura, K. M. S., R. H. Scheller, and W. I. Weiss (2000). Three-dimensional structure of the neuronal-Sec1-syntaxin 1a complex. *Nature*, 404:355–362.

Munson, M., X. Chen, A. E. Cocina, S. M. Schultz, and F. M. Hughson (2000). Interactions within the yeast t-SNARE Sso1p that control SNARE complex assembly. *Nature Structural & Molecular Biology*, 7(10):894–902.

Nicholson, K. L., M. Munson, R. B. Miller, T. J. Filip, R. Fairman, and F. M. Hughson (1998). Regulation of SNARE complex assembly by an N-terminal domain of the t-SNARE Sso1p. *Nature Structural Biology*, 5(9):793–802.

Novick, P. and R. Schekman (1979). Secretion and cell-surface growth are blocked in a temperature-sensitive mutant of Saccharomyces cerevisiae. *Proceedings of the National Academy of Sciences, USA*, 76(4):1858–1862.

Oh, E., B. A. Spurlin, J. E. Pessin, and D. C. Thurmond (2005). Munc18c Heterozygous Knockout Mice Display Increased Susceptibility for Severe Glucose Intolerance. *Diabetes*.

Oh, E. and D. C. Thurmond (2006). The Stimulus-induced Tyrosine Phosphorylation of Munc18c Facilitates Vesicle Exocytosis. *Journal of Biological Chemistry*, 281(26):17624–17634.

Oh, E. and D. C. Thurmond (2009). Munc18c Depletion Selectively Impairs the Sustained Phase of Insulin Release. *Diabetes*, 58(5):1165–1174.

Ohara-Imaizumi, M., T. Fujiwara, Y. Nakamichi, T. Okamura, Y. Akimoto, J. Kawai, S. Matsushima, H. Kawakami, T. Watanabe, K. Akagawa, and S. Nagamatsu (2007). Imaging analysis reveals mechanistic differences between first- and second-phase insulin exocytosis. *The Journal of Cell Biology*, 177(4):695–705.

Ossig, R., C. Dascher, H. H. Trepte, H. D. Schmitt, and D. Gallwitz (1991). The yeast SLY gene products, suppressors of defects in the essential GTP-binding Ypt1 protein, may act in endoplasmic reticulum-to-Golgi transport. *Molecular and Cellular Biology*, 11(6):2980–2993.

Otsuka, M., H. Oguni, J.-S. Liang, H. Ikeda, K. Imai, K. Hirasawa, K. Imai, E. Tachikawa, K. Shimojima, M. Osawa, and T. Yamamoto (2010). STXBP1 mutations cause not only Ohtahara syndrome but also West syndrome–result of Japanese cohort study. *Epilepsia*, 51(12):2449–2452.

Peng, R. (2002). Sly1 protein bound to Golgi syntaxin Sed5p allows assembly and contributes to specificity of SNARE fusion complexes. *The Journal of Cell Biology*, 157(4):645–655.

Peng, R.-W. (2005). Decoding the Interactions of SM Proteins with SNAREs. *TheScientificWorldJOURNAL*, 5:471–477.

Peng, R.-W., C. Guetg, E. Abellan, and M. Fussenegger (2010). Munc18b regulates core SNARE complex assembly and constitutive exocytosis by interacting with the N-peptide and the closed-conformation C-terminus of syntaxin 3. *Biochemical Journal*, 431:353–361.

Pevsner, J., S.-C. Hsu, J. E. A. Braun, N. Calakos, A. E. Ting, M. K. Bennett, and R. H. Scheller (1994a). Specificity and Regulation of a Synaptic Vesicle Docking Complex. *Neuron*, 13:353–361.

Pevsner, J., S. C. Hsu, and R. H. Scheller (1994b). n-Sec1: a neural-specific syntaxin-binding protein. *Proceedings of the National Academy of Sciences, USA*, 91(4):1445–1449.

Pobbati, A. V., A. Stein, and D. Fasshauer (2006). N- to C-terminal SNARE complex assembly promotes rapid membrane fusion. *Science*, 313(5787):673–676.

Prekeris, R., J. Klumperman, and R. H. Scheller (2000). Syntaxin 11 is an atypical SNARE abundant in the immune system. *European Journal of Cell Biology*, 79(11):771–780.

Price, A., W. Wickner, and C. Ungermann (2000). Proteins needed for vesicle budding from the Golgi complex are also required for the docking step of homotypic vacuole fusion. . *The Journal of Cell Biology*, 148(6):1223–1229.

Ramalingam, L., S. M. Yoder, E. Oh, and D. C. Thurmond (2014). Munc18c: a controversial regulator of peripheral insulin action. *Trends in Endocrinology and Metabolism*, Pp. 1–8.

Rehman, A., R. J. Jarrott, A. E. Whitten, G. J. King, S.-H. Hu, M. P. Christie, B. M. Collins, and J. L. Martin (2013). Milligram Quantities of Homogeneous Recombinant Full-Length Mouse Munc18c from Escherichia coli Cultures. *PLoS ONE*, 8(12):e83499.

Riento, K. (2000). Munc18-2, a Functional Partner of Syntaxin 3, Controls Apical Membrane Trafficking in Epithelial Cells. *Journal of Biological Chemistry*, 275(18):13476–13483.

Rizo, J. and J. Xu (2015). The Synaptic Vesicle Release Machinery. *Annual Review of Biophysics*, 44(1):339–367.

Rodriguez-Boulan, E., G. Kreitzer, and A. Müsch (2005). Organization of vesicular trafficking in epithelia. *Nature Reviews Molecular Cell Biology*, 6(3):233–247.

Roth, D. and R. D. Burgoyne (1994). SNAP-25 is present in a SNARE complex in adrenal chromaffin cells. *FEBS Letters*, 351:207–210.

Rothman, J. E., R. W. Schekman, and T. C. Südhof (2013). The Nobel Prize in Physiology or Medicine 2013.

Sadoul, K., J. Lang, C. Montecucco, U. Weller, R. Regazzi, S. Catsicas, C. B. Wollheim, and P. A. Halban (1995). SNAP-25 Is Expressed in Islets of Langerhans and Is Involved in Insulin Release. *The Journal of Cell Biology*, 128(6):1019–1028.

Saitsu, H., M. Kato, T. Mizuguchi, K. Hamada, H. Osaka, J. Tohyama, K. Uruno, S. Kumada, K. Nishiyama, A. Nishimura, I. Okada, Y. Yoshimura, S.-i. Hirai, T. Kumada, K. Hayasaka, A. Fukuda, K. Ogata, and N. Matsumoto (2008). De novo mutations in the gene encoding STXBP1 (MUNC18-1) cause early infantile epileptic encephalopathy. *Nature genetics*, 40(6):782–788.

Schmelzle, K. (2006). Temporal Dynamics of Tyrosine Phosphorylation in Insulin Signaling. *Diabetes*, 55(8):2171–2179.

Schollmeier, Y., J. M. Krause, S. Kreye, J. Malsam, and T. H. Söllner (2011). Resolving the function of distinct Munc18-1/SNARE protein interaction modes in a reconstituted membrane fusion assay. *The Journal of Biological Chemistry*, 286(35):30582–30590.

Shen, J., D. C. Tareste, F. Paumet, J. E. Rothman, and T. J. Melia (2007). Selective Activation of Cognate SNAREpins by Sec1/Munc18 Proteins. *Cell*, 128(1):183–195.

Shin, Y. K. (2013). Two gigs of Munc18 in membrane fusion. *Proceedings of the National Academy of Sciences, USA*, 110(35):14116–14117.

Stockli, J., D. J. Fazakerley, and D. E. James (2012). GLUT4 exocytosis. *Journal of Cell Science*, 124(24):4147–4159.

Stroupe, C., K. M. Collins, R. A. Fratti, and W. Wickner (2006). Purification of active HOPS complex reveals its affinities for phosphoinositides and the SNARE Vam7p. *The EMBO Journal*, 25(8):1579–1589.

Struthers, M. S., S. G. Shanks, C. MacDonald, L. N. Carpp, A. M. Drozdowska, D. Kioumourtzoglou, M. L. M. Furgason, M. Munson, and N. J. Bryant (2009). Functional homology of mammalian syntaxin 16 and yeast Tlg2p reveals a conserved regulatory mechanism. *Journal of Cell Science*, 122(13):2292–2299.

Südhof, T. C. and J. E. Rothman (2009). Membrane Fusion: Grappling with SNARE and SM Proteins. *Science*, 323(5913):474–477.

Sutton, R. B., D. Fasshauer, R. Jahn, and A. T. Brünger (1998). Crystal structure of a SNARE complex involved in synaptic exocytosis at 2.4 Å resolution. *Nature*, 395:347–353.

Tamori, Y., M. Kawanishi, T. Niki, H. Shinoda, S. Araki, H. Okazawa, and M. Kasuga (1998). Inhibition of Insulin-induced GLUT4 Translocation by Munc18c through Interaction with Syntaxin4 in 3T3-L1 Adipocytes. *Journal of Biological Chemistry*, 273(31):19740–19746.

Tellam, J. T., S. L. Macaulay, S. McIntosh, D. R. Hewish, C. W. Ward, and D. E. James (1997). Characterization of Munc-18c and Syntaxin-4 in 3T3-L1 Adipocytes. *Journal of Biological Chemistry*, 272(10):6179–6186.

Tellam, J. T., S. McIntosh, and D. E. James (1995). Molecular identification of two novel Munc-18 isoforms expressed in non-neuronal tissues. *Journal of Biological Chemistry*, 11:5857–5863.

Thurmond, D. C., B. P. Ceresa, S. Okada, J. S. Elmendorf, K. Coker, and J. E. Pessin (1998). Regulation of Insulin-stimulated GLUT4 Translocation by Munc18c in 3T3L1 Adipocytes. *Journal of Biological Chemistry*, 273(50):33876–33883.

Thurmond, D. C., M. Kanzaki, A. H. Khan, and J. E. Pessin (2000). Munc18c Function Is Required for Insulin-Stimulated Plasma Membrane Fusion of GLUT4 and Insulin-Responsive Amino Peptidase Storage Vesicles. *Molecular and Cellular Biology*, 20(1):379–388.

Thurmond, D. C. and J. E. Pessin (2000). Discrimination of GLUT4 vesicle trafficking from fusion using a temperature-sensitive Munc18c mutant. *The EMBO Journal*, 19(14):3565–3575.

Togneri, J., Y. S. Cheng, M. Munson, F. M. Hughson, and C. M. Carr (2006). Specific SNARE complex binding mode of the Sec1/Munc-18 protein, Sec1p. *Proceedings of the National Academy of Sciences, USA*, 103(47):17730–17735.

Tomas, A., P. Meda, R. Regazzi, J. E. Pessin, and P. A. Halban (2008). Munc 18-1 and Granuphilin Collaborate During Insulin Granule Exocytosis. *Traffic*, 9(5):813–832.

Toonen, R. F. G. and M. Verhage (2003). Vesicle trafficking: pleasure and pain from SM genes. *TRENDS in Cell Biology*, 13(4):177–186.

Toonen, R. F. G. and M. Verhage (2007). Munc18-1 in secretion: lonely Munc joins SNARE team and takes control. *Trends in Neurosciences*, 30(11):564–572.

Umahara, M., S. Okada, E. Yamada, T. Saito, K. Ohshima, K. Hashimoto, M. Yamada, H. Shimizu, J. E. Pessin, and M. Mori (2007). Tyrosine Phosphorylation of Munc18c Regulates Platelet-Derived Growth Factor-Stimulated Glucose Transporter 4 Translocation in 3T3L1 Adipocytes. *Endocrinology*, 149(1):40–49.

Verhage, M., A. S. Maia, J. J. Plomp, A. B. Brussaard, J. H. Heeroma, H. Vermeer, R. F. Toonen, R. E. Hammer, T. K. van den, Berg, M. Missler, H. J. Geuze, and T. C. Südhof (2000). Synaptic Assembly of the Brain in the Absence of Neurotransmitter Secretion. *Science*, 287(5454):864–869.

Volchuk, A., Q. Wang, H. S. Ewart, Z. Liu, L. He, M. K. Bennett, and A. Klip (1996). Syntaxin 4 in 3T3-L1 Adipocytes: Regulation by Insulin and Participation in Insulin-dependent Glucose Transport. *Molecular Biology of the Cell*, 7:1075–1082.

Weber, T., B. V. Zemelman, J. A. McNew, B. Westermann, M. Gmachl, F. Parlati, T. H. Söllner, and J. E. Rothman (1998). SNAREpins: Minimal Machinery for Membrane Fusion. *Cell*, 92(6):759–772.

Wiederhold, K. and D. Fasshauer (2009). Is Assembly of the SNARE Complex Enough to Fuel Membrane Fusion? *The Journal of Biological Chemistry*, 284(19):13143–13152.

Wong, P. P. C., N. Daneman, A. Volchuk, N. Lassam, M. C. Wilson, A. Klip, and W. S. Trimble (1997). Tissue Distribution of SNAP-23 and Its Subcellular Localization in 3T3-L1 Cells. *Biochemical and Biophysical Research Communications*, 230:64–68.

Wu, M. N., T. Fergestad, T. E. Lloyd, Y. He, K. Broadie, and H. J. Bellen (1999). Syntaxin 1A interacts with multiple exocytic proteins to regulate neurotransmitter release in vivo. *Neuron*, 23(3):593–605.

Wu, M. N., K. L. Schulze, T. E. Lloyd, and H. J. Bellen (2001). The ROP-Syntaxin interaction inhibits neurotransmitter release. *European Journal of Cell Biology*, 80(2):196–199.

Xu, Y., A. B. Seven, L. Su, Q.-X. Jiang, and J. Rizo (2011). Membrane bridging and hemifusion by denaturated Munc18. *PLoS ONE*, 6(7):e22012.

Xu, Y., L. Su, and J. Rizo (2010). Binding of Munc18-1 to Synaptobrevin and to the SNARE Four-Helix Bundle. *Biochemistry*, 49(8):1568–1576.

Yamaguchi, T., I. Dulubova, S.-W. Min, X. Chen, J. Rizo, and T. C. Südhof (2002). Sly1 Binds to Golgi and ER Syntaxins via a Conserved N-Terminal Peptide Motif. *Developmental Cell*, 2(3):295–305.

Yang, B., M. Steegmaier, L. C. Gonzalez, Jr, and R. H. Scheller (2000). nSec1 Binds a Closed Conformation of Syntaxin1A. *The Journal of Cell Biology*, 148(2):247–252.

Yang, C., K. J. Coker, J. K. Kim, S. Mora, D. C. Thurmond, A. C. Davis, B. Yang, R. A. Williamson, G. I. Shulman, and J. E. Pessin (2001). Syntaxin 4 heterozygous knockout mice develop muscle insulin resistance. *The Journal of Clinical Investigation*, 107(10):1311–1318.

Yang, X., S. Wang, Y. Sheng, M. Zhang, W. Zou, L. Wu, L. Kang, J. Rizo, R. Zhang, T. Xu, and C. Ma (2015). Syntaxin opening by the MUN domain underlies the function of Munc13 in synaptic-vesicle priming. *Nature Publishing Group*, 22(7):547–554.

Yechoor, V. K. (2004). Distinct pathways of insulin-regulated versus diabetes-regulated gene expression: An in vivo analysis in MIRKO mice. *Proceedings of the National Academy of Sciences, USA*, 101(47):16525–16530.

Yu, H., S. S. Rathore, J. A. Lopez, E. M. Davis, D. E. James, J. L. Martin, and J. Shen (2013). Comparative studies of Munc18c and Munc18-1 reveal conserved and divergent mechanisms of Sec1/Munc18 proteins. *Proceedings of the National Academy of Sciences, USA*, 110(35):E3271–E3280.

Zhang, W., A. Efanov, S. N. Yang, G. Fried, S. Kolare, H. Brown, S. Zaitsev, P. O. Berggren, and B. Meister (2000). Munc-18 associates with syntaxin and serves as a negative regulator of exocytosis in the pancreatic beta -cell. *The Journal of Biological Chemistry*, 275(52):41521–41527.

Zhou, P., T. Bacaj, X. Yang, Z. P. Pang, and T. C. Südhof (2013). Lipid-Anchored SNAREs Lacking Transmembrane Regions Fully Support Membrane Fusionduring Neurotransmitter Release. *Neuron*, 80(2):470–483.

Ms. Czuee Morey

Ph.D. student, UNIL

Avenue d'Echallens 102,
1005 Lausanne.

Czuee.Morey@unil.ch
Ph: +41 (0)78 686 6921
DOB:18th November, 1985

Education

Year	Degree	Institute/University	Grades
2008	M.Sc. Biotechnology	Indian Institute of Technology Bombay	8.9/10
2006	B.Sc. Biotechnology	Mumbai University	71%

Research Experience

- **Role of Munc18c in SNARE-mediated exocytosis**
  Ph.D. Studies, Supervisor: Dr. Dirk Fasshauer, UNIL, Switzerland *Jan '11–present*
  - Studying the mode of binding and mechanism of action for Munc18c in SNARE-mediated vesicle fusion, using sensitive biochemical and biophysical methods.
- ***In silico* promoter prediction based on DNA structural cues**
  Project Assistant, Supervisor: Prof. Manju Bansal, IISc-Monsanto, Bangalore *Apr '09–Sep '10*
  - Predicted *cis*-regulatory regions in *Arabidopsis* and rice genomes on the basis of DNA structural properties such as free energy, bendability and curvature. Performed statistical and qualitative analysis on predicted regions for application in gene regulation studies.
  - Submitted an online database of ≈20,000 categorized genomic predictions per genome to Monsanto, which could be used for testing.
  - Wrote a publication in an international journal, that has been cited several times; Morey et al. Plant Physiology (2011) 156: 1300-1315.
- **Active site determination of CstII protein by docking analysis**
  Master's Thesis, Supervisor: Prof. P.V. Balaji, IIT Bombay, India *Jan – May '08*
  - Identified donor and acceptor binding site on a glycosyltransferase enzyme by docking the donor-acceptor hybrid based on the Lamarckian Genetic Algorithm. The docking analysis provided putative mutational sites for experimental testing.

Industry Experience

- **Senior Research Associate**, *Evalueserve Pvt. Ltd.*, Gurgaon, India *2008–2009*
  - Job profile included studying and analyzing technology to determine patentability through literature searches, tracking patents, analyzing patents for infringement. Attended intensive training sessions in drafting patent applications and gained in-depth knowledge of IP laws.
  - Received a rating of 3 (on a scale of 5) during the bi-annual appraisal of employees.
  - Certification by WIPO for a Course on Intellectual Property Rights.
- **Summer Internship**, *Nicholas Piramal India Ltd.*, Mumbai, India *2007*
  - Training at a plant for chemical synthesis of Vitamin A and formulations in Quality control and Microbiology laboratories.
- **Project Trainee**, *Haffkine Institute*, Mumbai, India *2005*
  - Gained exposure to industrial applications of biology in clinical and therapeutic fields

Awards and Conferences

- Won the Best poster award at the 58th Biophysical Society Meeting at San Francisco, USA in the 'Exocytosis and Endocytosis' category *2014*
- Presented posters at 1st and 2nd DNF Symposiums *2014, 2015*
- Awarded Ph.D. fellowship from the University of Lausanne *2011*
- Attended the Eighth Asia Pacific Bioinformatics Conference at Bangalore, India *2010*
- Received the prestigious 'Institute Academic Prize' for securing highest grades in the first year of Masters at Indian Institute of Technology Bombay *2007*
- Ranked 11th among 6500 candidates in the nationwide JAM exam conducted by the IITs *2006*

Teaching & Publications

- Taught a practical course on protein produciton and biochemical & biophysical methods to undergraduate students each year (2011-2015).
- Morey C, Mookherjee S, Rajasekaran G, Bansal M. (2011) DNA Free Energy-Based Promoter Prediction and Comparative Analysis of Arabidopsis and Rice Genomes. *Plant Physiology.* 156(3):1300-1315. doi:10.1104/pp.110.167809.

*Year :*2015

Role of Munc18c in SNARE-mediated exocytosis

Czuee Morey